

2006

Microarchitecture of the canine zona pellucida: a scanning electron microscopy study

Matthew O'Brien Lunn
University of Dayton

Follow this and additional works at: https://ecommons.udayton.edu/graduate_theses

Recommended Citation

Lunn, Matthew O'Brien, "Microarchitecture of the canine zona pellucida: a scanning electron microscopy study" (2006). *Graduate Theses and Dissertations*. 4088.
https://ecommons.udayton.edu/graduate_theses/4088

This Thesis is brought to you for free and open access by the Theses and Dissertations at eCommons. It has been accepted for inclusion in Graduate Theses and Dissertations by an authorized administrator of eCommons. For more information, please contact mschlangen1@udayton.edu, ecommons@udayton.edu.

**MICROARCHITECTURE OF THE CANINE ZONA PELLUCIDA:
A SCANNING ELECTRON MICROSCOPY STUDY**

Thesis

Submitted to

The College of Arts and Sciences of the
University of Dayton

In Partial Fulfillment of the Requirements for

The Degree

Masters of Science in Biology

By

Matthew O'Brien Lunn

University of Dayton

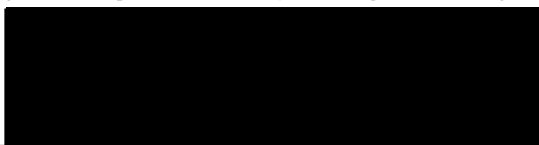
Dayton, Ohio

April 2006

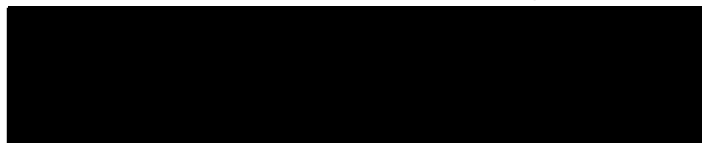
APPROVED BY:



Shirley J. Wright, Ph.D. (Faculty Advisor)



Marie-Claude C. Hofmann, Ph.D. (Committee Member)



Mark G. Nielsen, Ph.D. (Committee Member)

ABSTRACT

MICROARCHITECTURE OF THE CANINE ZONA PELLUCIDA: A SCANNING ELECTRON MICROSCOPY STUDY

Name: Matthew O Lunn

University of Dayton, 2006

Advisor: Shirley J. Wright, Ph.D.

The zona pellucida (an extracellular matrix surrounding the oocyte) has been used as a target for immunocontraception in over-populated wild animals. It would be useful to have a similar immunocontraceptive for feral dog populations. The structure of the zona pellucida is highly variable depending on the species. In most mammals, the zona pellucida is punctuated by small fenestrations or pores. Companion animals have an unusual reproduction, making the typical laboratory animal models (e.g., mouse) unsuitable. Few studies have analyzed the zona pellucida in the canine. We hypothesized that the canine zona pellucida has pores and a heterogeneous structure. The focus of our study was two fold. The first objective was to develop and optimize a process to view the surface of the canine zona pellucida using a scanning electron microscope (SEM). This was established by concurrent fixation and

affixation of oocytes to a glass surface, and viewing gold-coated specimens under high vacuum with a low spot size. The second objective was to analyze the microarchitecture of the canine zona pellucida. Over 300 zona-intact oocytes were isolated from ovaries, denuded of cumulus cells, fixed, critical point dried and viewed at 800 – 35,000X with a conventional and low vacuum SEM. Four different zona pellucida types were observed. The type I zona pellucida had a smooth compact surface with only a few small pores ($<0.5\ \mu\text{m}$). The type II zona pellucida had many elliptical or spherical pores that were often conical and/or bifurcated going deeper into the zona pellucida. The type III zona pellucida had a rough surface with pores that were less spherical and more irregular in shape. The type IV zona pellucida had a rough surface, but was covered in small fibers that clogged the pores making them hard to discern. The breed of the canine oocyte donor significantly affected the zona pellucida type; however there was no significant effect of the canine donor size, age or reproductive maturity on zona pellucida morphology. Donor characteristics significantly effected oocyte diameter. Larger dogs and the older mature dogs had larger oocytes than small dogs or younger immature dogs. Oocytes with the type III zona pellucida were significantly smaller than oocytes with the type II and IV zona pellucida. We established SEM techniques specifically for canine oocytes, which should be applicable to endangered canids. We analyzed the surface morphology of the canine zona pellucida, and show it is heterogeneous. This has implications in immunocontraception. This will aid future studies with *in vitro* maturation and fertilization of canine oocytes.

ACKNOWLEDGMENTS

My special thanks are to Dr. Shirley Wright, my advisor, for providing her time and expertise in the development of the techniques, in the use of the scanning electron microscope and for aiding and directing the development of this thesis. I would like to thank my graduate committee members Dr. Marie-Claude Hofmann and Dr. Mark Nielsen for their guidance in committee meetings and in the time taken to review this text. I would like to show my extreme gratitude to Dr. Christy and all of the staff at Northridge Veterinary Clinic, without which none of my research would have been possible as well as their warm and welcoming greetings everyday I was there.

I would also like to express my gratitude for the help others have given me. Dr. Sudhindra Gadagkar for his invaluable aid and suggestions in using statistics; Jay Lee for his time spent helping me learn to critical point dry, sputter coat, and view my samples; and my cousin Eric, who washed the giant pile of glassware in the lab. I would also like to thank the entire Biology Department for the help they gave, especially Karen, who usually knew what I wanted and where to get it, even if I did not.

This research was funded by the AKC Canine Health Foundation Grant 369 and the University of Dayton Graduate School Summer Fellowships in 2004 and 2005.

TABLE OF CONTENTS

ABSTRACT.....	iii
ACKNOWLEDGMENTS.....	v
LIST OF FIGURES.....	vii
LIST OF TABLES.....	ix
LIST OF ABBREVIATIONS.....	x
CHAPTER	
I. LITERATURE REVIEW.....	1
II. DEVELOPMENT OF TECHNIQUES FOR PREPARING THE CANINE ZONA PELLUCIDA FOR SCANNING ELECTRON MICROSCOPY.....	28
III. THE HETEROGENEITY OF THE CANINE ZONA PELLUCIDA.....	85
IV. CONCLUSIONS AND FUTURE DIRECTIONS.....	156
V. LITERATURE CITED	163

LIST OF FIGURES

1.1.	Diagram of a longitudinal section through a mammalian ovary.....	26
2.1.	Freshly-collected canine ovary.....	55
2.2.	Cleaned and washed canine ovaries.....	57
2.3.	Ovarian mincing procedure	59
2.4.	Freshly-isolated cumulus-oocyte complex from a Shih Tzu ovary.....	61
2.5.	Zona-intact oocyte from a Shih Tzu ovary	63
2.6.	Critical point-dried canine oocytes	65
2.7.	Sputter-coated canine oocytes	67
2.8.	Imaging modes	69
2.9.	Effect of spot size on resolution	71
2.10.	Surface morphology of the canine zona pellucida	73
2.11.	Montage of the canine zona pellucida at high resolution	75
2.12.	High magnification montage of the canine zona pellucida	77
2.13.	Pores of the zona pellucida are conical and bifurcated	79
2.14.	Stereo pair of the outer surface of the canine zona pellucida.....	81
2.15.	Surface characteristics of canine cumulus cells	83
3.1.	Oocyte distribution by canine donor breed	112
3.2.	Oocyte distribution by AKC donor breed type	114

3.3.	Oocyte distribution by canine donor size	116
3.4.	Oocyte distribution by canine donor age	118
3.5.	Oocyte distribution by canine reproductive maturity	120
3.6.	Effect of canine donor breed on oocyte diameter	122
3.7.	Effect of AKC donor breed type on oocyte diameter	124
3.8.	Effect of canine donor size on oocyte diameter	126
3.9.	Effect of canine donor age on oocyte diameter	128
3.10.	Effect of canine reproductive maturity on oocyte diameter	130
3.11.	Canine oocyte with a type I zona pellucida	132
3.12.	Canine oocyte with a type II zona pellucida	134
3.13.	Canine oocyte with a type III zona pellucida	136
3.14.	Canine oocyte with a type IV zona pellucida	138
3.15.	Four canine zona pellucida types	140
3.16.	Oocyte distribution of zona pellucida types	142
3.17.	Effect of canine donor breed on zona pellucida morphology.....	144
3.18.	Effect of AKC donor breed type on zona pellucida morphology	146
3.19.	Effect of canine donor size on zona pellucida morphology	148
3.20.	Effect of canine donor age on zona pellucida morphology	150
3.21.	Effect of canine reproductive maturity on zona pellucida morphology....	152
3.22.	Effect of oocyte diameter on zona pellucida morphology	154

LIST OF TABLES

1.1. American Kennel Club classification of breed types	23
1.2. Size categories of domestic canines	24
1.3. Follicle and oocyte size and description in the canine.....	25
3.1. Relationship between oocyte diameter and canine breed	107
3.2. Relationship between oocyte diameter and AKC donor breed type	108
3.3. Relationship between oocyte diameter and canine age (all dogs).....	109
3.4. Relationship between oocyte diameter and canine age (young dogs)..	110
3.5. Relationship between oocyte diameter and canine reproductive maturity.....	111

LIST OF ABBREVIATIONS

ABBREVIATION	DEFINITION
AKC	American Kennel Club
AMH	Anti-Müllerian hormone
CB	Sodium cacodylate buffer, pH 7.4
COC	Cumulus-oocyte complex
cSEM	Conventional scanning electron microscope
eSEM	Environmental scanning electron microscope
FSH	Follicle stimulating hormone
IVF	<i>In vitro</i> fertilization
LH	Luteinizing hormone
LVSEM	Low vacuum scanning electron microscope
ma	Milliamps
mtDNA	Mitochondrial DNA
Pa	Pascals
PBS	Phosphate-buffered saline, pH 7.2
PZP	Porcine zona pellucida protein
SE	Standard Error
SEM	Scanning electron microscope

CHAPTER I

Literature Review

A. INTRODUCTION

The Dog as a Model

The dog (*Canis familiaris*, *Canis domesticus*) is the most thoroughly studied companion animal in medical practice (Patterson, 2000). Currently the canine is at the front of many research projects. The genome of the dog has recently been sequenced and microsatellite comparison has been done between some of the many dog breeds (Lindblad *et al.*, 2005; Ostrander *et al.*, 2000; Parker *et al.*, 2004; Wayne and Ostrander, 1999). In addition, the first dog was recently cloned producing an Afghan hound named Snuppy. Snuppy was cloned from the nucleus of a somatic skin cell of a male Afghan hound (Lee *et al.*, 2005). Because of the dogs' close companionship with humans, they are one of the most useful models of human genetic disease. Over 215 canine genetic diseases have similarities to human genetic diseases, and 41 have the same gene product (enzyme etc.) being abnormally produced (Ostrander *et al.*, 2000).

The domestication of the modern dog occurred approximately 15,000 – 75,000 years ago (Ostrander *et al.*, 2000; Verginelli *et al.*, 2005). It was bred from the gray wolf (*Canis lupus*) and is considered by most to be the first companion animal domesticated (Verginelli *et al.*, 2005). Although there is much phenotypic variation in the current dog breeds, they can be compared to the gray wolf using mitochondrial DNA (mtDNA), which shows there are only 0.2% differences within the two species' mtDNA (Wayne, 1993). In fact, the wolf and the canine are so closely related genetically they can interbreed, which has been checked using mtDNA (Vila *et al.*, 2003). It is argued that the behavioral and phenotypic differences between the two species (dog and gray wolf) are no more different than between two dog breeds and probably have arisen from rare alleles in the gray wolf populations, bred by humans to become more pronounced phenotypically (Ostrander *et al.*, 2000; Saetre *et al.*, 2004). Although the dog was not domesticated in the recent past, most of the current dog breeds have only been bred into existence in the past two to four hundred years (Wayne and Ostrander, 1999).

The American Kennel Club (AKC) has categorized dog breeds into eight groups based on their common characteristics: Sporting Dogs, Hounds, Working Dogs, Terriers, Toys, Non-Sporting Dogs, Herding Dogs, and Miscellaneous as shown in Table 1.1 (AKC, 1992). The Sporting Dogs are an active group that has very good instincts in the water and woods. Many of the breeds in this group (e.g., pointers, retrievers, spaniels) still actively take place in hunting or other field exercises. The Hounds usually share an ancestral hunting background

using either their sense of smell or ability to run down the quarry; however, the Hound group is a very diverse group (e.g., Afghans, Beagles, Irish Wolfhounds). The Working Dogs (e.g., Doberman Pinscher, Mastiff, St. Bernard) have been bred for jobs such as rescues, guard duty, and pulling sleds. They usually are very intelligent and have strong muscular bodies. The Terriers (e.g., Airedale, Parsons Russell Terrier, Cairn Terrier) are an energetic group of dogs bred to hunt and kill vermin. This has led them to have little tolerance for other animals including other dogs. The Toys (e.g., Chihuahua, Shih Tzu, Pug) are dogs bred mainly for their diminutive size and to give the owner joy. Non-Sporting Dogs (e.g., Chinese Shar-Pei, Poodle, Chow Chow) are a very diverse class with a wide variety of look and function. The Herding Dogs (e.g., Blue Heeler, Collie, Shetland Sheepdog) were, as the name entails, bred to herd farm animals. They are usually fast and intelligent dogs. The Miscellaneous group includes dogs that do not fit the other groups. These AKC groupings (Table 1.1) along with known canine size (Table 1.2) and specific genealogies (Parker *et al.*, 2004) allow for the canine to be used to study developmental defects as well as other medical problems common to humans. The domestic dog can also be used as a model organism for endangered canids, to improve reproductive technology and aid in the possible repopulation of certain species struggling for survival (Durrant *et al.*, 1998).

The reproductive cycle of the domestic dog is the estrous cycle. The canine estrous cycle is separated into four phases beginning with proestrus. Proestrus lasts approximately 9 days and is marked by bloody discharge and a

swelling of the vulva. Follicle stimulating hormone (FSH) and luteinizing hormone (LH) stimulate growth of the follicles, which in return secrete estrogen which causes behavioral differences in the canine (Correa, 2001; Eilts and Davidson, 2005; England, 1998). The next phase is estrus, which lasts approximately 9 days and is marked by a lighter discharge. Estrogen secretion is decreased and progesterone secretion is increased. In estrus, the ovulation of all of the mature oocytes occurs within 3 days of a surge in LH. Usually larger dogs ovulate more oocytes than smaller dogs (Correa, 2001; Eilts and Davidson, 2005; England, 1998). Diestrus is the third phase in the estrous cycle and its duration is about two months. It is regulated by progesterone and lasts until the corpora lutea deteriorate (Correa, 2001; Eilts and Davidson, 2005; England, 1998). If the dog had mated, this marks the beginning of pregnancy and will last about 63 days, if not, then anestrus follows. Anestrus will last two to five months depending on the breed, age and health of the canine. The canine develops first estrous usually around 12 months of age, but it can occur anywhere from 6 to 24 months. Smaller dogs tend to begin estrous sooner than the larger dogs (Correa, 2002; England, 1998). The estrous cycle can occur once every four months (e.g., German Shepard) to once a year (e.g., Basenji). Older females cycle less frequently than those that are younger (Correa, 2001; Eilts and Davidson, 2005; England, 1998).

The canine has unusual reproduction compared to other mammals. The canine oocyte is ovulated as an immature oocyte, containing a germinal vesicle that will mature within the oviduct (see Fayrer-Hosken *et al.*, 2000). The

immature oocyte requires at least 48 hr to completely mature, but can remain viable in the oviduct for up to 108 hr (see Fayrer-Hosken *et al.*, 2000). Sperm require seven hours to capacitate, but can remain viable for up to 268 hrs in the estrous female genital tract. The oocyte may not be completely mature before fertilization (England, 1998; see Fayrer-Hosken *et al.*, 2000). The sperm may be able to penetrate the immature oocyte *in vivo* as shown *in vitro* by Mahi and Yanagimachi (1976); however, Durrant *et al.*, (1998) did not achieve sperm penetration of immature oocytes *in vitro*. Clearly, more research is needed to elucidate the mechanisms of canine reproductive biology.

Introduction to Fertilization

To develop into a healthy mammal, a number of complex steps must be taken. Any of these many steps can be disrupted for the organism to be formed incorrectly or aborted. Even before development of an embryo can start, fertilization of an oocyte must occur correctly. For fertilization to take place, the sperm must come into contact and bind with the zona pellucida, the extracellular matrix surrounding the oocyte. If the sperm can not correctly bind to the zona pellucida, fertilization will not take place, which is normally attributed to problems with the sperm. However, it has been shown that defects within the oocyte can also cause similar sperm-oocyte binding problems, specifically the zona pellucida's inability to allow the sperm to bind to it (Prasad and Dunbar, 2000). Therefore, it would be expected that the zona pellucida should be studied

thoroughly, thereby allowing for the knowledge to fix or prevent many reproductive problems.

Research of the zona pellucida may also aid in the production of an immunocontraceptive vaccine that could do away with the invasive surgeries currently used for sterilization. An immunocontraceptive vaccine uses the organism's immune system to raise antibodies to a specific target that would cause infertility. The zona pellucida has been targeted by injecting zona pellucida proteins or chimeric zona pellucida proteins into an organism causing the immune system to make antibodies which bind to the zona pellucida causing a T-cell reaction (Fayrer-Hosken *et al.*, 2000). This may result in the deterioration of the oocyte and possibly the entire ovary (Fayrer-Hosken *et al.*, 2000). A porcine zona pellucida protein (PZP) immunocontraceptive vaccine was effective in reducing a suburban population of white-tailed deer (Rutberg *et al.*, 2004). By treating females with a vaccine and a booster shot containing the PZP, the treated females' fertility rate dropped significantly compared to untreated females as well as allowing for a 7.9% reduction per year of the deer population (Rutberg *et al.*, 2004).

Although much is known about the zona pellucida for many commonly used lab animals such as the mouse, hamster and rabbit, there is very little known about the zona pellucida in companion animals. The thorough investigation of the canine as a medical model needs to encompass the studying of the canine zona pellucida as well. More information about the canine zona pellucida could allow for the increased success of *in vitro* fertilization (IVF), as

well as aid in the development of a vaccine to sterilize female dogs without the invasive surgery of spaying, the recovery time and the sometimes harmful and fatal errors or complications that are possible with almost any surgery.

Focus of Thesis

My thesis investigates the three-dimensional structure of the canine zona pellucida, viewed with scanning electron microscopy. To provide background information for my thesis, first a literature review of the histology of mammalian ovaries and folliculogenesis will be presented. Next a summary of the zona pellucida detailing its function, biochemistry, molecular biology, biosynthesis, and structure will be discussed. Lastly, the statement of research objectives for the thesis will be presented.

B. THE OVARY

Ovarian Anatomy

The mammalian ovaries are paired organs of approximately equal size in most species. They are found in the abdominal cavity surrounded by a bursa of fatty tissue that greatly varies in size depending on the species (Zuckerman *et al.*, 1962). The ovaries are supplied with blood mainly by the ovarian artery at the mesovarian border. The ovoid ovaries are generally smooth organs. They swell at the onset of breeding season due to the growth of follicles, which usually can be seen on the surface of the ovary as bumps. Each bump represents one

developing follicle containing a developing oocyte, or a corpus luteum. In some species in which multiple oocytes are ovulated at a time (e.g., sow), the ovary becomes very bumpy similar to a bunch of grapes. However, in species which only ovulate one oocyte at a time (e.g., human), the ovary size and shape is not significantly changed (Silverthorn *et al.*, 2004; Zuckerman *et al.*, 1962). In the dog, anestrus ovaries have a very smooth surface due to a lack of growing follicles or corpora lutea (England, 1998).

The mammalian ovary can be divided into two main regions: the medulla and the surrounding cortex (Fig 1.1). The medulla (internal region) of large mammals including the dog contains mainly loose connective tissue and strands of smooth muscle (Fayrer-Hosken *et al.*, 2000). Blood vessels, lymph vessels and nerves are also embedded in the medulla. Surrounding the medulla is the cortex containing developing oocytes within follicles at various developmental stages (Fayrer-Hosken *et al.*, 2000; Silverthorn *et al.*, 2004; Wright, 2005; Zuckerman *et al.*, 1962). A thick connective tissue layer called the tunica albuginea surrounds the cortex. Overlying this layer is a thin cuboidal epithelium.

Oogenesis

Oogenesis is the process by which a mitotic germ stem cell or primordial germ cell undergoes meiosis to form a mature female gamete (oocyte). Unlike sperm which are continually produced in the male's testis throughout life, all of the oocytes that a female will have are thought to be produced before birth and are arrested in the diplotene stage of prophase I (dictyate stage; Epifano and

Dean, 1994). In the dog, proliferating germ stem cells are present for at least two months after birth (Fayrer-Hosken *et al.*, 2000; McDougall *et al.*, 1997). The oocytes stay at rest until the beginning of sexual maturity, at which time one to twelve oocytes may become receptive to the hormonal milieu (and other signaling molecules), and progress through oogenesis (Miller and Shur, 1994). In the mouse, oogenesis takes about a week to reach the preovulatory stage (Telfer *et al.*, 2000, 2005).

An ovarian follicle is composed of an oocyte surrounded by a layer or layers of somatic cells called follicle cells depending on what stage of development the follicle is in. The follicle cells supply nutrients and other necessary metabolites to the oocytes (Eppig, 1994). The oocyte and follicle cells comprise the follicles that grow throughout folliculogenesis. The cortex of a sexually mature mammal contains many follicles with oocytes in different stages of oogenesis, and corpora lutea (see Fayrer-Hosken *et al.*, 2000). After an oocyte is ovulated, the follicle cells that remain in the ovary become the corpus luteum, and secrete progesterone and estrogen to keep the endometrium intact for pregnancy. The corpus luteum either enlarges as in the case of pregnancy, or dissolves leaving the corpus albicans as scar tissue (Wright, 2005). Also visible in the cortex are atretic follicles that contain a degenerating oocyte and follicle cells. The atretic follicles are thought to be more common in new born to young animals and occur less frequently in older animals, but they degenerate slower in the older animals. This makes the atretic oocytes of older animals appear equally as common as in younger animals (Zuckerman *et al.*, 1962).

C. FOLLICULOGENESIS

Folliculogenesis is the specific temporal sequence of morphological and functional changes of both germ cells and somatic cells working in unison (Epifano and Dean, 1994). Folliculogenesis can vary significantly in length depending on the animal being observed. Folliculogenesis in the mouse takes only 17 - 19 days (Hoage and Cameron, 1976), whereas it can take 4 - 5 months in ruminant species (Lussier *et al.* 1987, Gosden *et al.* 1994). In the dog, folliculogenesis begins two to twelve weeks postnatally (Blackmore *et al.*, 2004). Primordial follicles are first visible three weeks after birth (McDougall *et al.*, 1997). Follicles are classified generally based on follicle size, oocyte size, and number of layers of follicle cells, and appearance of the zona pellucida and antrum (see Fayrer-Hosken *et al.*, 2000; Tesoriero, 1981). Dog follicles are additionally classified by the presence of dark lipid yolk material in the oocyte (see Fayrer-Hosken *et al.*, 2000; Tesoriero, 1981).

Stages of Folliculogenesis

The oocyte is derived from primordial germ cells which migrate into the developing ovary during fetal development (Gilbert, 2000). The primordial germ cells undergo mitotic division to form all of the oogonia before birth (Snustad and Simons, 2000). Interestingly, Johnson *et al.* (2004) have recently shown that primordial germ cells in juvenile and adult mouse ovaries undergo mitosis after birth. Upon completion of mitosis, oogonia undergo DNA synthesis and eventually arrest development at the diplotene (dictyate) stage of prophase I of

meiosis. These oogonia are now considered primary oocytes, which have an average diameter of 12 μm in the mouse (Table 1.3). Soon each oocyte is surrounded by a single layer of flattened follicle cells called granulosa cells to form a primordial follicle (Fig. 1.1), which has an average diameter of 17 μm in the mouse and 25 μm in the dog (Epifano and Dean, 1994; Fair, 1993; Luvoni *et al.*, 2005). These primordial follicles can stay at rest for the entire life of the functioning ovary. Alternatively, they may be stimulated to develop by a signal's increase or decrease, which will be discussed in detail below (Epifano and Dean, 1994).

During early folliculogenesis, the granulosa cells become cuboidal and undergo mitosis to form several layers that are surrounded by a basal lamina in the preantral follicle or primary follicle. Another type of follicle cell, called the theca cell, surrounds the outer side of the basement membrane and becomes a multi-tiered outer layer of the follicle. The preantral follicle also begins to grow increasing in size to 78 μm in the canine. The follicle then matures into an advanced preantral follicle, which is 211 μm in the canine (Durrant *et al.*, 1998; Epifano and Dean, 1994; Luvoni *et al.*, 2005). For an overview of follicular size of the mouse and dog during folliculogenesis see Table 1.3.

The next stage in folliculogenesis is the secondary follicle or early antral follicle, which is about 360 μm in the canine. It has a small cavity or antrum forming in the thecal cell layers (Durrant *et al.*, 1998; Epifano and Dean, 1994; Luvoni *et al.*, 2005). The antrum becomes filled with fluid (Fayrer-Hosken *et al.*, 2000). By this time, the primary oocyte is now surrounded by an extracellular

matrix called the zona pellucida, which will be discussed in depth later (Epifano and Dean, 1994; Tulsiani, 2003).

The early antral follicle then develops into a large preovulatory follicle, Graffian follicle or tertiary follicle (2 – 3 mm, Fig. 1.1) that has a larger antrum, many follicular cell layers and a large (120 μ m) oocyte in the dog (Table 1.3). In the preovulatory follicle, many layers of cumulus cells (granulosa cells) surround the oocyte. The theca cells have now differentiated into two layers, an inner theca interna and an outer theca externa. During the preovulatory follicle stage, the oocyte resumes meiosis up to metaphase II in the mouse, whereas it remains in the dictyate stage of prophase I in the dog until fertilization (Gilbert, 2000). The preovulatory follicle is the most mature follicle and will move to the outer most region of the ovarian cortex. During ovulation, the preovulatory follicle ruptures, releasing the oocyte surrounded by cumulus cells. This is referred to as a cumulus-oocyte complex (COC). The growing follicle in the canine can not be seen on the outer surface of the ovary until about 1 – 2 hr before ovulation (Durrant *et al.*, 1998), making the collection of canine oocytes for studies almost impossible without mincing or enzymatically digesting the entire ovary.

Meiotic Competence

During folliculogenesis, the oocyte grows as it becomes transcriptionally and translationally active (Epifano and Dean, 1994). The granulosa cells, also known as the cumulus cells, also synthesize mRNAs and proteins which become deposited in the oocyte via trans-zonal projections which are granulosa cell

extensions that traverse the zona pellucida terminating at the oolemma (Rankin *et al.*, 2000; Thomas *et al.*, 2003). Gap junctions between cumulus cells also facilitate nutrient exchange and transfer of small molecules. These cytoplasmic extensions have been observed in several species including the pig (Suzuki *et al.*, 1994) and bovine (de Paz *et al.*, 2001).

Several studies have shown that oocyte diameter is related to age of the follicle, and that meiotic competence increases with oocyte diameter (Luvoni *et al.*, 2005). Otoi *et al.* (2000) reported that the larger a canine oocyte was, the higher the probability that the oocyte had progressed further through meiosis. The same was shown to be true with immature, mature and inseminated bovine oocytes. The immature oocytes were the smallest on average, and then mature oocytes were larger than the immature oocytes, and the inseminated oocytes were the largest on average (Suzuki *et al.*, 1994). Thus one can conclude that small oocytes are immature and that larger oocytes are more mature. Also larger ($>100\text{ }\mu\text{m}$) oocytes have been seen to resume meiotic maturation significantly more often than smaller ($<100\text{ }\mu\text{m}$) oocytes (Hewitt and England, 1998).

Regulation of Folliculogenesis

Many factors affect the regulation of folliculogenesis, both from surrounding cells and also from the other oocytes causing them to either stay at rest as a primordial follicle or develop further (Thomas *et al.*, 2003). *Steel*, a paracrine factor involved in the Kit-signaling pathway, will cause the primordial follicles to begin development (Hutt *et al.*, 2006; Motro and Bernstein, 1993).

Anti-Müllerian Hormone (AMH) is believed to inhibit follicular growth, because AMH knockout mice show increased follicle growth (Durlinger *et al.*, 2002). In addition, ovaries of two day old mice that have been incubated in AMH show a decrease in primordial follicle growth when compared to control ovaries (Durlinger *et al.*, 1999). AMH is expressed by both by preantral and early antral follicles, which is thought to inhibit the growth of surrounding follicles and allow for the preantral and small antral follicles to further develop without competition (Durlinger *et al.*, 1999). However, AMH does not cause apoptosis as it does in the Müllerin ducts (Baarends *et al.*, 1995; Hirobe *et al.*, 1992; McGee *et al.*, 2001). Once follicles have developed into antral follicles they are reliant on FSH, which will allow them to develop further. Without FSH present in the following stages the follicles will not develop further. More immature follicles have been shown to express the FSH receptor; however FSH is not necessary for their development into an antral follicle (Thomas *et al.*, 2003).

Some factors are stage-specific regulators, in that at certain times of development they will stimulate growth and at other times they will inhibit it. An example of this is activin. When in the presence of early follicles, activin acts as a growth inhibitor halting development (Mizunuma *et al.*, 1999), but when in the presence of late preantral follicles it stimulates the growth of the follicle (McGee *et al.*, 2001). BMP-15 and growth/differentiation factor-9 are expressed specifically in oocytes and effect folliculogenesis by increasing the growth and differentiation of the granulosa cells. The progression of folliculogenesis from a primordial follicle to a Graffian follicle ready to release healthy mature oocytes is

a very complex process requiring the participation of both the surrounding follicular cells, as well as the oocyte (Thomas *et al.*, 2003). Without the surrounding granulosa cells, the oocyte will not develop properly. Without the oocyte and an intact zona pellucida, the cumulus cells can not proliferate and differentiate properly to form the proper COC (Dunbar *et al.*, 2002).

D. ZONA PELLUCIDA

Function

The zona pellucida is the extracellular matrix surrounding the mammalian oocyte and early embryo. It is a "shell" around the oocyte that is made of glycoproteins. It serves in species-specific sperm-oocyte binding in the fertilization process, prevention of polyspermy, physical protection from damage, prevention of improper and early implantation in the female reproductive tract, protection against the female immune system, and proper COC and follicle formation (Dunbar *et al.*, 1994, 2002; Epifano and Dean, 1990; Garside *et al.*, 1997; Green, 1997; Jovine *et al.*, 2005; Sinowatz *et al.*, 2001; Tulsiani, 2003; Wassarman, 1990). Most research on the zona pellucida has been done using well-characterized animal models such as the rodent (e.g., mouse, hamster) and domestic species (e.g., rabbit, pig, cow) as well as the human. Therefore most of my discussion will refer to these species.

Since the zona pellucida surrounds the entire oocyte, it is able to control what can enter or exit the oocyte. Therefore the zona pellucida is also responsible in part for the osmotic regulation of the oocyte (Shivers and Dunbar,

1977). The zona pellucida is a semi-permeable layer that will allow certain molecules such as immunoglobulins and ferritin to penetrate it; however, other molecules such as heparin, which is smaller than the other two molecules, were not able to penetrate the zona pellucida. This shows that the zona pellucida does not selectively allow things to pass through on size alone, but other factors affect a molecule's passage, such as charge and other biochemical and physiological properties (Prasad *et al.*, 2000).

Biochemistry and Molecular Biology

The zona pellucida is made up of three glycoproteins commonly called ZP proteins: ZP1, ZP2 and ZP3 (mouse nomenclature). These proteins can be given other names depending on the species being studied, due to the heterogeneity of the ZP proteins amongst species (Dunbar *et al.*, 1994; Prasad *et al.*, 2000). At the nucleic acid level, the ZP genes from different mammals share 50 – 98% homology. At the amino acid level, mouse ZP1 is 39 – 67% identical to the human, ZP2 is 60% identical, and ZP3 is 67% identical (Prasad *et al.*, 2000). In the mouse, ZP1 has a molecular weight of 200 kD, ZP2 is 120 kD, and ZP3 is 83 kD (Greve and Wassarman, 1985). The ZP proteins are all thought to be important structural proteins with ZP2 and ZP3 forming heterodimers to assemble long strands that are connected to other strands through ZP1 homodimers (Greve and Wassarman, 1985). Studies show that the ZP3 protein is the most highly conserved ZP protein in mammals and is thought to be the primary sperm receptor of a variety of mammals. ZP3 triggers the acrosome

reaction after the sperm has bound to the zona pellucida (Florman and First, 1988; Moller *et al.*, 1990; Wassarman, 1990). ZP2 is thought to aid in secondary sperm binding with a much weaker attraction to the sperm, possibly allowing for a loose connection as the sperm penetrates the zona pellucida to reach the oocyte (Wassarman, 1990).

In mice the genes for the zona pellucida proteins can be knocked out. Mice that have any of the three zona pellucida proteins knocked out exhibit abnormal folliculogenesis and a varying level of infertility (Rankin *et al.*, 2000). In ZP1 knockout mice, a similar number of oocytes can be collected as compared to wild type mice; however, the zona pellucida of the ZP1 knockout mice appears much thinner and looser than the zona pellucida of wild type mice (Rankin *et al.*, 2000). When mated, the litter size is decreased by approximately 50%. The sperm are still able to fertilize the oocytes from the ZP1 knockout mice; however, it is thought that since the ZP1 is responsible for cross-linking the ZP2-ZP3 strands, the embryos are able to hatch out of the zona pellucida earlier, reducing fecundity (Rankin *et al.*, 2000).

In ZP3 knockout mice, the COCs are unorganized and the oocyte lacks a zona pellucida entirely (Liu *et al.*, 1996; Rankin *et al.*, 1996). The ZP3 knockout mice produce a lower number of oocytes and do not become visibly pregnant (Rankin *et al.*, 2000). In ZP2 knockout mice, the zona pellucida is produced in early follicles; however, the zona pellucida is significantly thinner than that of wild type mice and significantly fewer antral follicles develop (Rankin *et al.*, 2001). When oocytes from either ZP2 or ZP3 knockout mice are fertilized *in vitro*, they

can develop to the blastocyst stage. However, when transferred to foster mice, no live births were recorded (Rankin *et al.*, 2001)

Biosynthesis

Even though the functions of the specific ZP proteins are known, the site(s) of biosynthesis of the ZP proteins is highly debated (Eberspaecher *et al.*, 2001). Was the zona pellucida secreted by the oocyte itself, or are the surrounding granulosa cells responsible for synthesizing the zona pellucida? Another possibility is that the zona pellucida is synthesized by both the oocyte and the granulosa cells, which could be why there are layers in the zona pellucida that can be seen with a light microscope (Dunbar *et al.*, 1994; Hinsch *et al.*, 1999). Both the cumulus cells and the oocyte express ZP mRNA and/or protein and are the site of zona pellucida biosynthesis in the mouse, rabbit, pig, cow, marmoset, rhesus monkey and human (Dunbar *et al.*, 2002; Prasad *et al.*, 1996, 2000; Sinowatz *et al.*, 1995). However, Eberspaecher *et al.* (2001) and others (Epifano *et al.*, 1995; Wassarman and Kinloch, 1992) published that only the oocyte itself synthesizes the zona pellucida in the mouse, cynomolgus monkey and human. So there are differences between studies as to what makes the zona pellucida of both the mouse and human. Eberspaecher *et al.* (2001) also said that previous work implicating both the oocyte and the cumulus cells in zona pellucida biosynthesis was erroneous, because it used a fixative that broke up the zona pellucida and dispersed it throughout the cumulus cells as well. However, Hinsch *et al.* (1999) showed that different species possibly have

different ways to synthesize the zona pellucida. In the mouse, it appeared that the ZP3 proteins might be produced by both the cumulus cells and the oocyte, but human ZP3 appeared only to be produced by the oocyte (Hinsch *et al.*, 1999). In the dog, ZP proteins are expressed and synthesized from different sources: ZP1 and ZP3 being produced by the cumulus cells, and ZP2 is synthesized in the oocyte (Blackmore *et al.*, 2004). It is possible that the previous reports conflict due to antibody specificity, fixation methods, and possible degradation of samples. However, it is also possible that the zona pellucida might be produced by differing sources depending on what mammal is being studied. Currently the consensus is that the zona pellucida is synthesized by both the oocyte and granulosa cells for most mammals. Northern analysis of *in vitro*-cultured granulosa cells has revealed ZP1 mRNA in the rabbit, indicating that the granulosa cells actively produce ZP1 (Lee and Dunbar, 1993).

Structure

The ZP proteins entwine to form a heterogeneous meshwork around the oocyte with a varying thickness depending on the species. The thickness of the zona pellucida ranges from 0.5 – 1 μm in the opossum, 5 μm in the mouse, 8 μm in the horse, 9 μm in the dog, 10 – 12 μm in the rabbit, 13 μm in the human, 14 μm in the cat, 16 μm in the pig and elephant, and up to as large as 27 μm in the cow (Barber *et al.*, 2001; Dudkiewicz and Williams, 1977; Dunbar and O'Rand, 1991; Dunbar and Wolgemuth, 1984). The outer meshwork of the zona pellucida is heterogeneous in different mammals as well. Pores in the zona

pellucida can make it look like "Swiss cheese" and can vary to a certain degree as well. For example, of the mammals examined, the rabbit and the feline have the largest pore size and the bovine has the smallest pore size (Dudkiewicz and Williams, 1977; Nikas *et al.*, 1994). In some cases, the ultrastructure of the outer surface of the zona pellucida can be heterogeneous within a given species as well. In the human, for example, there can be as many as four different zona pellucida types: smooth, rough, small pores, and larger meshwork with small pores (Magerkurth *et al.*, 1999). In the mouse, five different types of zona pellucida were reported (Calafell *et al.*, 1992). In the cow, the pores in the zona pellucida varied in size and frequency depending on the embryonic stage of development (Vanroose *et al.*, 2000). On the other hand, studies using rodent and human oocytes showed only one type of zona pellucida with a surface that was covered with a meshwork of fibers (Familiari *et al.*, 1988; Phillips and Shalgi, 1980).

It has not been determined whether the canine zona pellucida is heterogeneous. Only two studies have examined the canine zona pellucida with the scanning electron microscope (SEM). Ström Holst *et al.* (2000) viewed the zona pellucida of canine oocytes that were stored using different methods (frozen, salt-stored and frozen salt-stored) and compared them to fresh oocytes. They saw slightly different zona pellucida types between the storage methods and fresh oocytes. The second study used oocytes from prepubertal dogs, and focused more on the COC (Haenisch-Woehl *et al.*, 2003). They did not mention how many oocytes they viewed, or if all of the zona pellucida looked the same.

Therefore, more research on the canine zona pellucida needs to be performed to determine its ultrastructure. It would also be interesting to see if prepubertal dogs have a similar zona pellucida as mature dogs.

E. RESEARCH OBJECTIVES

It is not understood what factors affect the ultrastructure of the zona pellucida. In some species, it has been reported that the maturity of the oocytes and fertilization affect it (Calafell *et al.*, 1992; Vanroose *et al.*, 2000). It could be possible that other characteristics such as the sexual maturity, age, or genetic background of the organism could affect zona pellucida morphology as well. The overall goal of my thesis was to determine the ultrastructure of the canine zona pellucida and identify factors that may influence it. I hypothesize that the canine zona pellucida's structure is heterogeneous.

The first objective was to determine an effective method for preparing canine oocytes for scanning electron microscopy. This includes methods for isolating, cleaning, affixing, fixing and viewing the canine oocytes under the JEOL JSM-5800LV SEM on the campus of the University of Dayton. Chapter II shows how the methods for this aim were established and optimized.

The second objective was to determine whether the ultrastructure of the canine zona pellucida is heterogeneous. This will be discussed in the first part of the results in Chapter III.

The third objective was to determine whether there was any correlation between the size of dog breed, type of AKC breed, age of oocyte donor, or

maturity of the oocyte (reflected by oocyte size) with the type of zona pellucida that the oocytes had surrounding them. This will be addressed in the second part of Chapter III.

Chapter IV discusses the results of this thesis and addresses future work on the canine zona pellucida that should be continued along the lines of this research.

F. SIGNIFICANCE

This research is significant because it can aid in improving the knowledge of the canine reproductive system, which will help explain and solve the unique problem of maturing and fertilizing canine oocytes *in vitro*. That knowledge could aid in the rescue of struggling populations of endangered caninids around the world. This research could also be applied to developing an immunocontraceptive vaccine to limit and reduce feral dog populations that are not only a nuisance, but also a threat to spread diseases and harm people as well as livestock that they come into contact with. An immunocontraceptive vaccine would also be a luxury for regular dog owners as well as the family dog, because the vaccine could do away with the invasive surgery that currently is required for sterilization of female dogs.

Table 1.1. American Kennel Club classification of breed types.

Dog Breed Type*	Dog Breeds
Sporting Dogs	American Water Spaniel, Cocker Spaniel Mix, English Setter, English Springer Spaniel, Golden Retriever, Irish Setter, Labrador Retriever Mix, Sussex Spaniel, Weimaraner
Hound Dogs	Afghan Hound, American Foxhound, Basset Hound, Beagle, Dachshund, Irish Wolfhound, Otterhound, Rhodesian Ridgeback, Pharaoh Hound, Saluki, Whippet
Working Dogs	Akita, Bernese Mountain Dog, Boxer, Bullmastiff, Doberman Pinscher, Great Dane, Great Pyrenees, Komondor, Newfoundland, Rottweiler, Schnauzer, Siberian Husky Mix
Terriers	Airedale Terrier, Bedlington Terrier, Bull Terrier, Cairn Terrier, Jack Russell Terrier, Kelly Blue Terrier, Scottish Terrier, Staffordshire Terrier, Welsh Terrier
Toys	Affenpinscher, Chihuahua, English Toy Spaniel, Havanese, Maltese, Miniature Pinscher, Pekingese, Pomeranian, Pug, Shih Tzu, Toy Fox Terrier, Yorkshire Terrier
Non-Sporting Dogs	American Bulldog, Bichon Frise Mix, Chinese Shar-Pei, Chow Chow, Dalmatian, Finnish Spitz, Poodle, Schipperke, Shiba Inus Mix, Tibetan Spaniel, Tibetan Terrier
Herding Dogs	Belgian Sheepdog, Blue Healer, Border Collie, German Shepard, Shetland Sheepdog, Shepard-Collie Mix, Pembroke Welsh Corgi, Polish Lowland Sheepdog, Puli
Miscellaneous**	Beauceron, Labrador-St. Bernard Mix, Medium Mix, Pitbull, Plott, Wolf Mix

*American Kennel Club classification.

**Includes dogs classified by the AKC, and also dogs that are not classified by the AKC.

Table 1.2. Size categories of domestic canines.

Dog Breed Size (Weight)	Dog Breeds Used in this Thesis
Small Dogs <13 kg (<30 lb)	Beagle, Bichon Frise Mix, Chihuahua, Cocker Spaniel Mix, Jack Russell Terrier, Maltese, Shetland Sheepdog Mix, Shiba Inus Mix, Shih Tzu, Yorkshire Terrier
Medium Dogs 13 – 23 kg (30 – 50 lb)	Blue Healer, Medium Mix, Schnauzer, Siberian Husky Mix
Large Dogs >23 kg (>50 lb)	American Bulldog, Bernese Mountain Dog, Boxer, Chow Chow, Doberman Pinscher, German Shepard, Golden Retriever, Labrador Retriever, Labrador-St. Bernard Mix, Pitbull, Rhodesian Ridgeback, Rottweiler, Shepard-Collie Mix, Wolf Mix*

*The wolf mix was a mating between a domestic dog and a wolf.

Table 1.3. Follicle and oocyte size and description in the canine.

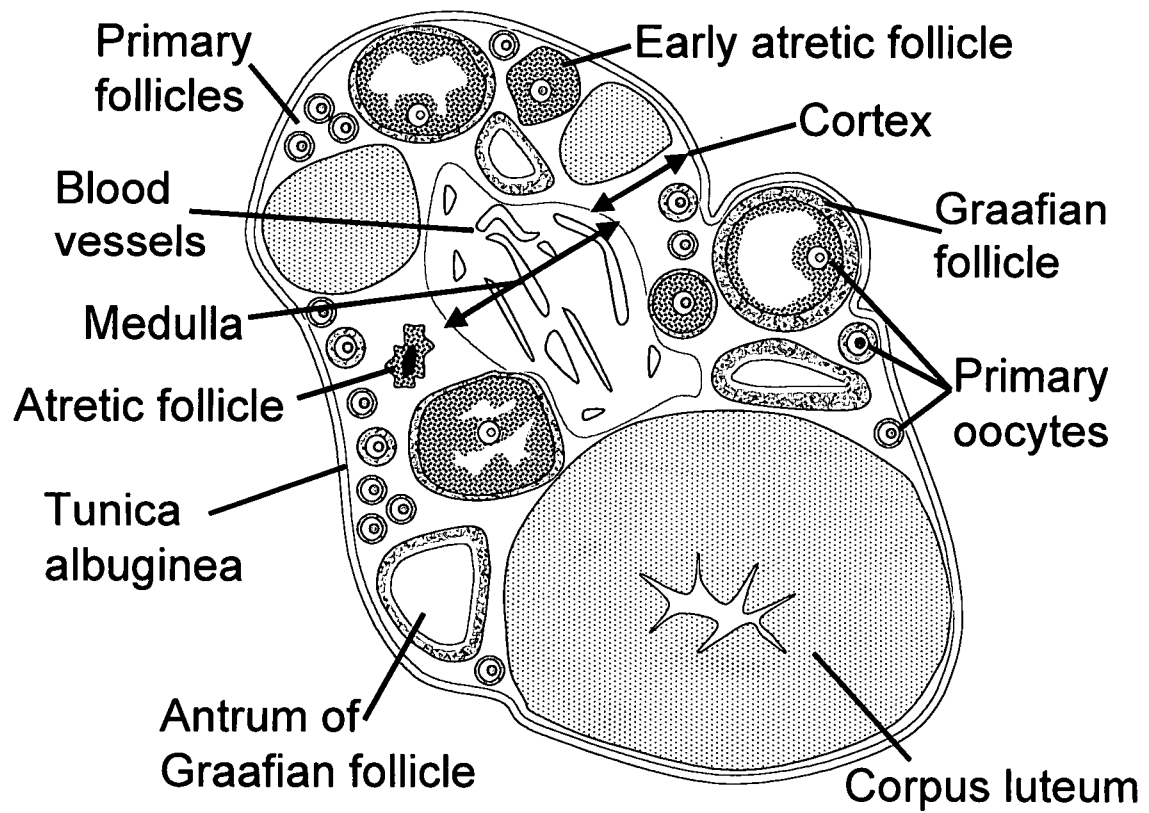
Follicle Name	Canine Follicle Description	Follicle Size (μm) (Oocyte Size; μm)	
		Dog*	Mouse**
Primordial	Small pale oocytes, with single layer of flattened pre-granulosa cells	25 (20)	17 (12)
Preantral	Pale oocyte, with incomplete granulosa layers	78 (--)	28 (20)
Advanced Preantral	Dark lipid filled oocyte, with multiple granulosa layers	211 (115)	150 (60)
Early Antral	Dark lipid filled oocyte, with multiple granulosa layers and small antrum and vesicles	360 (---)	200 (80)
Antral Preovulatory	Dark lipid filled oocyte, with multiple granulosa layers and large antrum and cumulus-oocyte complex	2-3 mm (120 μm)	400-550 (80)

* From Durrant *et al.*, 1998; Luvoni *et al.*, 2005.

** From Epifano and Dean, 1994.

Fig. 1.1. Diagram of a longitudinal section through a mammalian ovary. The ovarian cortex, which surrounds the medulla, contains follicles, while the medulla does not. All follicles contain one oocyte, which may or may not be present in the plane of the section seen here. The follicles are at different stages of development. Cells surrounding follicles and corpora lutea are stroma cells and interstitial gland cells. Adapted from Wright, S. (2005).

Fig. 1.1.



CHAPTER II

Development of Techniques for Preparing the Canine Zona Pellucida for Scanning Electron Microscopy

A. INTRODUCTION

The zona pellucida has been studied in many model organisms; however, it has not been well characterized in the canine (Dunbar *et al.*, 1994; Epifano and Dean, 1994; Prasad *et al.*, 2000). In many species, the zona pellucida has fenestrations or pores on its surface when viewed by scanning electron microscopy (Dudkiewicz and Williams, 1977; Nikas *et al.*, 1994). Very little is known about the appearance and structure of the canine zona pellucida. The chapter focuses on the development of techniques for preparing and viewing canine oocytes with scanning electron microscopy.

In the mid 1930's to the mid 1960's, the SEM was developed (reviewed in Flegler *et al.*, 1993). The SEM allows the surface of a specimen to be scanned by a beam of electrons to produce a three-dimensional surface image of the

object. By using electrons as the "light source," the resolution of the image from a SEM is up to 1,000X better than conventional light microscopy.

The SEM functions by scanning a steady stream of electrons over the sample line- by-line, which is known as a raster (reviewed in Flegler *et al.*, 1993). When using a conventional SEM, the sample chamber must be at high vacuum during viewing because the electrons are so small that any gas in the chamber can cause the electron beam to be disrupted giving an image with a large amount of background noise or static. Therefore, for conventional scanning electron microscopy, most biological samples must be dried before viewing so that they do not interfere with imaging by releasing gases into the sample chamber. Also as the vacuum in the chamber is being created, a biological sample can shrivel up if it is not properly dried. To eliminate the gases in the chamber and preserve the sample's three-dimensional structure, a biological sample is typically dehydrated and critical point dried. The sample can be dehydrated through a graded series of increasing concentrations of ethanol (or acetone), or it can be dehydrated with a chemical such as 2, 2-dimethoxypropane. According to Dudkiewicz and Williams (1977), when critical point drying mouse oocytes, ethanol dehydration and chemical dehydration work equally well to preserve the three-dimensional structure of the oocyte and zona pellucida.

The SEM produces an image by scanning the electron beam across the sample in a raster pattern (reviewed in Flegler *et al.*, 1993). The electrons that are reflected (secondary or backscattered electrons) are detected and computed

to produce a micrograph image. The width of the electron beam is known as the spot size. As the spot size is increased, the resolution of an image is decreased because the resolution is limited by the width of the electron beam. The resolution can not be less than the width of the electron beam. Therefore, the smaller the spot size, the better the image resolution. However, a smaller spot size yields more background noise that can affect image quality. So there is a balance between resolution and background noise that must be determined to optimize spot size for the sample to be viewed.

As the scanning beam of electrons hits the sample, it can interact in a number of ways to produce heat, light, and electrons of different energy (reviewed in Flegler *et al.*, 1993). The electron beam interacts with an area of the sample beneath the surface of where the beam hits. The size of this tear-drop shaped "subterranean area" will change depending on the voltage of the electron beam and atomic number of the atoms in the sample. For example, the higher the voltage of the electron beam, the deeper and wider into the sample the electrons will penetrate. Moreover, the lower the atomic number of the atoms of a sample, the deeper and wider into the sample the electrons will penetrate. When viewing a biological sample, the electron beam can deteriorate the sample because of the heat generated. The area where the raster has been will be "burnt" on the sample, creating artifacts. "Charging" is a build up of electrons that occur because the biological sample does not conduct well. Charging creates static in the image and the resulting bright spots ruin the image and obscure details. Both of the conditions cause SEM images to be of poor quality.

To prevent artifacts and image destruction during conventional scanning electron microscopy, delicate samples can be coated with a layer of metal such as gold or platinum (reviewed in Flegler *et al.*, 1993). Thus, samples can be viewed three major ways in a conventional SEM (cSEM): without metal coating (for samples that are electrically conductive), with metal coating, or the sample can be stained to make it conductive.

Another way to view samples is with an SEM that allows gas in the sample chamber. This permits viewing of samples that are soft, moist and/or electrically nonconductive in their native form without drying and coating. This is important when the sample is precious and should not be altered, such as in old artifacts or crime scene investigations (Stokes, 2003). Two SEMs permit viewing with gas in the specimen chamber: the variable pressure or low vacuum SEM (LVSEM) and environmental SEM (eSEM). The LVSEM can operate with pressure up to 250 Pascal (Pa), whereas the eSEM allows viewing of specimens at atmospheric pressure (101,325 Pa). Thus living tissue or whole organisms (beetle) can be observed without drying out in the eSEM.

Conventional scanning electron microscopy methods have been established for imaging oocytes of many mammalian species including the mouse, hamster, rabbit, cat, sow, goat, cow and even human (Dudkiewicz and Williams, 1977, Schwartz *et al.*, 1996, Tengowski and Schatten, 1997, Vanroose *et al.*, 2000). Specialized SEM techniques have also been used to observe zona pellucida morphology. Tengowski and Schatten (1997) compared two methods to prepare bovine oocytes, which are non-conductive, for scanning electron

microscopy. They concluded that staining the oocytes with 1% osmium tetroxide and 1% thiocarbonylhydrazide, to make them conductive was similar to coating oocytes with gold. However, the conductive staining procedure produced lower resolution images than the metal-coated samples. They also imaged oocytes using a Hitachi S-900 field-emission low voltage SEM, which allowed them to view the oocytes with an ultra-thin layer of platinum (1 – 2 nm thick) that was applied with an argon ion-beam evaporation method. This ultra-thin layer of metal can not withstand a voltage of even 10 kV in a cSEM without specimen damage. This use of the low voltage SEM gave them the best resolution, and the fibril nature of the bovine zona pellucida could be seen at high magnification (100,000X). When bovine oocytes coated with a normal layer of gold (30 nm thick), were viewed in the low voltage SEM, the bulbous nature of the coating could be seen and the fibril nature of the zona pellucida was lost. The low voltage SEM gave an added contrast and resolution that was not possible with the cSEM.

Despite the popularity of the dog in physiological studies, very few studies have analyzed the surface ultrastructure of the canine zona pellucida. Because of the morphological and physiological differences between canine oocytes and those of other mammals, previously established methods do not work well for the canine, and therefore must be significantly modified or abandoned. Only two studies have revealed the canine zona pellucida surface using cSEM. The first study used fresh, frozen and salt-stored samples fixed and stained with heavy metal prior to coating with gold (Ström Holst *et al.*, 2000). To reveal the zona

pellucida, canine oocytes were incubated for 15 min in 75 mM sodium citrate prior to vortexing for 15 min to remove the cumulus cells surrounding the zona pellucida. It is unclear what affect this treatment has on zona pellucida morphology. The second study examined COCs from prepubertal dogs, and did not describe how the cumulus cells were removed to show an image of the zona pellucida (Haenisch-Woehl *et al.*, 2003). Thus, a careful analysis of the ultrastructure of the canine zona pellucida is needed.

To provide detailed information on the morphology of the canine zona pellucida, the objectives of this study were to: 1) optimize methods to prepare canine oocytes for scanning electron microscopy, and 2) to determine the best viewing conditions when comparing a cSEM and a LVSEM. To carry out the objectives, we used a JEOL JSM-5800 LVSEM, which allows samples to be viewed not only under conventional high vacuum conditions, but also under low vacuum, allowing both coated and uncoated oocytes to be imaged on the same instrument.

For low vacuum imaging, oocytes were viewed uncoated or coated with a thin layer of gold. For high vacuum imaging, oocytes were viewed coated with a thin layer of gold only, since uncoated oocytes are very difficult to view under high vacuum because they are not electrically conductive. Since the coating of metal on a biological sample protects the sample from deterioration by the electron beam and prevents charging, we hypothesized that the metal-coated oocytes would produce better images than the oocytes that were uncoated. It was also hypothesized that oocytes viewed under high vacuum will produce

better micrographs due to the lack of gases in the specimen chamber that could interfere with the electron beam. We show that uncoated and coated canine oocytes can be viewed by a LVSEM under low-vacuum conditions, but that a thin metal coating and viewing under high vacuum produces superior results at high magnification.

B. MATERIALS AND METHODS

Chemicals

All chemicals were from Sigma Chemical Co. (St. Louis, MO) and Fisher Scientific Company (Pittsburg, PA) unless otherwise noted.

Animals

Ten mature healthy female dogs of both pure bred and mixed breeds were used for this study.

Collection of Ovaries

Ovaries encased in fat were obtained from ovariectomized dogs from local veterinarians at the Northridge Animal Clinic (5340 N. Dixie Dr., Dayton, OH 45414) or Bigger Road Veterinary Clinic (5655 Bigger Rd., Kettering, OH 45440). Immediately after removal, the ovaries were placed in cold phosphate-buffered saline (PBS; 2.9 mM NaH_2PO_4 , 7.1 mM Na_2HPO_4 , 137 mM

NaCl, pH 7.2). The ovaries were stored at 4 °C and transported to the University of Dayton, where they were stored at 4 °C for less than 24 hr until they were processed.

Collection of the Oocytes

The fat layer must be removed before follicles and COCs can be collected. The ovaries were cut out of the surrounding subcutaneous fat and washed in 4 °C PBS, to remove blood on the surface and improve viewing. The ovaries were repeatedly sliced with a No. 22 scalpel blade at ~5 mm intervals into small pieces (about 2 – 8 mm) in fresh PBS in a 100 x 20 mm culture dish (Falcon 353003) to allow follicles and the COCs to be released into PBS. The COCs were then identified using a stereo microscope (Nikon SMZ-U Stereo Microscope; Fryer Co., Cincinnati, OH) and gently pipetted into a new solution of PBS using a pulled glass pipet with a small bore.

Only COCs of high quality were used for the study. They have a darker color, homogeneous ooplasm, a larger oocyte, and are completely surrounded by a multi-tiered layer of cumulus cells three or more cells thick (Andersen and Simpson, 1973; Durrant *et al.*, 1998). Thus COCs with pale oocytes were not used for the study. Once the better quality COCs were collected, they were placed into fresh PBS. The cumulus cells were removed from the zona pellucida through repeated pipetting (up to thirty times) with THE STRIPPER (MidAtlantic Diagnostic, Inc., Marlton, NJ) using a 150 µm STRIPPER tip (MidAtlantic Diagnostic, Inc., Marlton, NJ). During stripping, the oocytes occasionally broke

open, which could be seen due to a loss of the dark lipids in the ooplasm. These ruptured oocytes were not used for the study. Once oocytes appeared to be completely denuded of cumulus cells, they were washed in fresh PBS. Any COCs that resisted denuding were not used for this study since the cumulus cells obscured the view of the zona pellucida.

Light Microscopy Imaging

Low magnification (7.5X – 75X) light micrographs were taken of ovaries, COCs and living oocytes using a Nikon E950 Coolpix digital camera mounted on a Nikon SMZ-U stereo microscope. Higher magnification (100X) light micrographs using a 10X objective were taken of COCs and oocytes using a Photometrics Cool Snap CF digital camera (Roper Scientific) mounted on a Nikon Eclipse TS100.

Affixation and Fixation

Three methods were used to fix and attach the oocytes to a glass surface (coverslip or slide) in preparation for scanning electron microscopy. In each case, the glass surface was cut with a diamond knife to a size no larger than 6 X 6 mm and was coated with 1 mg/ml poly-L-lysine (Mazia *et al.*, 1975). In the first method, living oocytes were transferred to a depression slide containing cold 2.5% glutaraldehyde in 0.1 M sodium cacodylate buffer, pH 7.4 (CB) for 1 hr on ice (Vanroose *et al.*, 2000). Then the oocytes were washed in cold PBS. In a

fresh solution of PBS, the oocytes were allowed to settle for 1 hr on a small poly-L-lysine-coated fragment of coverslip before dehydration and critical point drying as described below. However, these oocytes stayed affixed to the coverslip only about 50% or less of the time during dehydration and critical point drying. Thus a second method was explored.

In the second method, living oocytes in PBS were affixed for 1 hr to a poly-L-lysine-coated coverslip before the 1 hr fixation in 2.5% glutaraldehyde in CB. The oocytes were not able to be affixed to the coverslip effectively, and about 50% or more of the oocytes were lost during the transfer of the coverslips to fixative. After fixation, dehydration and critical point drying, no oocytes remained affixed to the coverslips. Thus a third fixation method was identified.

The final method was to affix the oocytes to the poly-L-lysine-coated coverslip in 2.5% glutaraldehyde in CB causing the oocytes to be attached to the coverslip while being fixed 1 hr on ice. This method allowed for over 90% of the oocytes to stay on the coverslip during dehydration and critical point drying. During the trial of these three methods, a reoccurring problem was that the coverslips were too thin and they were dropped and flipped over causing all of the oocytes to be crushed and unusable. Therefore the oocytes were affixed to a cut piece of glass slide (0.93 to 1.05 mm thick) no larger than 6 x 6 mm coated with 1 mg/ml poly-L-lysine. This was thicker and easier to work with during transfer. After fixation, the oocytes were subsequently washed twice in fresh CB which lasted 15 min per wash.

Dehydration

The fixed oocytes were dehydrated using a graded series of ethanol from 50%, 60%, 70%, 80%, 90%, 95%, and two 100%. Each immersion in ethanol lasted 15 min, except for the last two 100% immersions which were 1 hour to overnight each. The dehydration steps were performed in six-well tissue culture trays (Falcon # 353046) with approximately 10 ml of ethanol per well per step. For overnight incubations, six-well plates were sealed with parafilm and stored at 4 °C in 100% ethanol. Oocytes were transferred to fresh 100% ethanol in the morning before critical point drying.

Critical Point Drying

The dehydrated oocytes affixed to a fragment of glass slide were placed into a microporous ceramic capsule with size C pores (Ted Pella, Inc., Reading, CA). The ceramic capsule prevents the oocytes from being stripped from the glass slide during the drying process due to the change of liquids. The capsules were placed one at a time into a critical point dryer (AUTOSAMDRI® -814B, from Tousimis Research Corp., Rockville MD). This instrument slowly replaces the 100% ethanol with liquid carbon dioxide (Ris, 1985), which then can be evaporated leaving dried oocytes with an intact three-dimensional structure. The slides were then taped onto an aluminum stub (SEM Specimen Mount Stubs from Electron Microscopy Sciences, Hatfield, PA) using carbon tape (SPI Supplies, West Chester, PA). After critical point drying, oocytes were either

viewed directly in the LVSEM under low vacuum, or sputter coated and viewed under high or low vacuum.

Sputter Coating

Some of the oocytes were sputter coated with gold particles using a Denton Vacuum, LLC Desk II Cold Sputter/ Etch Unit (Denton Vacuum, Moorestown, NJ). According to the manufacturer, when the sputter coater is run for 30 seconds at 45 milliamps (ma), it deposits a layer of gold that is ~100 Ångstroms thick. Thus this setting was used to coat the canine oocytes. According to Tengowski and Schatten (1997), oocytes viewed under high vacuum and a voltage of 15 kV should be sputter coated with heavy metal 1-2 nm thick to allow the electrons to be conducted more easily off the oocytes and to prevent deterioration of the sample due to the electron beam. This will optimize high-resolution imaging. However, sputter coating also can create artifacts and therefore not all samples used in my study were sputter coated with heavy metal for comparison. When viewing uncoated oocytes under low vacuum, the true structure of the zona pellucida should be revealed.

After critical point drying and/or sputter coating, the samples were stored on their aluminum stubs in a four well case (Electron Microscopy Sciences, Ft. Washington, PA) in a dessicator, Frigicator II (Streck Laboratories, Inc., Omaha, NE) at room temperature.

Viewing of Oocytes with the Scanning Electron Microscope

Under low vacuum conditions, cSEMs can not be used. The University of Dayton has a JEOL JSM-5800LV (JEOL Ltd, Tokyo, Japan) LVSEM which allows samples to be viewed under high as well as low vacuum conditions. Under high vacuum conditions, oocytes must be coated with a thin layer of metal. When samples are coated with metal they can develop artifacts (Tengowski and Schatten, 1997). Under low vacuum, samples do not need to be sputter coated, which allows the viewer to see the actual zona pellucida instead of the metal coating on the zona pellucida. This should limit the number of artifacts on the samples.

The oocytes were observed three different ways to optimize viewing conditions. All oocytes were placed in the specimen chamber at a height of approximately 10 – 12 mm. In the first method, oocytes were viewed uncoated with an accelerating voltage of 12 kV under low vacuum (75 Pa) and a spot size of 18. In the second method, the oocytes were coated with a ~ 100 Ångstrom thick coating of gold and viewed with an accelerating voltage of 15 kV under low vacuum (75 Pa). When viewing the coated oocytes under low vacuum, the spot size was manipulated to determine the best image. In the third method, the oocytes were coated with a ~100 Ångstrom thick coating of gold and viewed with an accelerating voltage of 15 kV under high vacuum (0 Pa) with an objective lens aperture of #1 (20 µm in diameter) and a spot size of 6 – 7.

To obtain the optimum amount of information, a consistent method of viewing the oocytes with respect to magnification was needed. Therefore images

were taken at random magnifications to determine the best magnifications for viewing the canine zona pellucida. Stereo pairs were generated by taking two images at the same magnification, with one image tilted seven degrees to the other image.

Image Storage

Micrographs were taken of the oocytes and stored on floppy disks in the form of .tiff, .txt and .sim files. The files were then transferred to a computer hard drive and stored until further analysis. A hard copy of each micrograph was also printed off the JEOL JSM-5800LV with a Sony Video Graphic Printer UP-890MD (Oconomowoc, WI) on Sony Thermal Print Media UPP-110HD (Oconomowoc, WI) and stored in acid-free magnetic photo album pages (Lakeville, MA).

C. RESULTS

Ovary and Oocyte Isolation

Freshly-collected canine ovaries were surrounded by a layer of fat (Fig. 2.1). The ovaries of larger dog breeds (Greyhound) had more fat surrounding them than those from smaller dog breeds such as a Chihuahua or a Toy Poodle. Freshly isolated ovaries were oval in shape (Fig. 2.2). At their longest length, they ranged from ~10 mm to ~20 mm. The ovaries were larger in larger canine breeds than in smaller canine breeds (Fig. 2.2). Once the ovaries were cleaned of fat, they were sliced lengthwise three to four times and sliced

widthwise five to six times to mince the ovary and to release follicles and COCs (Fig. 2.3). Because it is unclear whether completely intact follicles (containing granulosa and complete theca cell layers) were obtained, these structures will be referred to as COCs. Only high quality COCs that looked similar to Fig. 2.4 were used for the study. These COCs had a dark, lipid-filled homogeneous center containing the oocyte and a multi-tiered layer of cumulus cells surrounding the oocyte that was at least 2 - 3 cells thick. The COCs were approximately 180 μm or more in diameter. This corresponds to the early advanced preantral follicle or secondary follicle size reported for the dog (Barber *et al.*, 2001; Durrant *et al.*, 1998)

In the next step of the preparation process, cumulus cells were physically removed from the COCs to leave only an oocyte with an intact zona pellucida (Fig. 2.5). If the oolemma was accidentally ruptured during cumulus cell removal, the dark lipid-filled ooplasm was released and these oocytes were discarded. Also if the cumulus cells resisted stripping, which occurred with the smaller COCs they were not used either. The zona pellucida was approximately 10 μm thick in unfixed oocytes. After fixation with glutaraldehyde and concurrent affixation of the oocytes to the poly-L-lysine coated glass slide, the oocytes were critical point dried (Fig. 2.6) and either viewed under low vacuum, or sputter coated with gold (Fig. 2.7) and viewed under either low or high vacuum (Fig. 2.8).

Conventional and Low Vacuum Scanning Electron Microscopy

To determine optimal viewing conditions, we compared images of the same oocyte prepared for the cSEM and the LVSEM, taken on the same instrument. Figure 2.8 shows the same oocyte viewed three different ways: uncoated under low vacuum (A), coated under low vacuum (B) and coated under high vacuum (C). All three micrographs were taken at relatively low magnifications (900 – 1000X) with an accelerating voltage of 12 kV for uncoated oocytes and 15 kV for coated oocytes. The uncoated oocyte was viewed at a lower accelerating voltage to prevent oocyte deterioration due to the electron beam intensity. Glutaraldehyde fixation provided excellent oocyte preservation. The zona pellucida appeared spongy in each viewing condition; however, fine details were present in the sputter coated oocytes. The uncoated oocyte viewed under low vacuum (A) was blurry, and the top of the oocyte was too light and the bottom too dark. Thus, imaging uncoated oocytes with low vacuum was not desirable. The coated oocyte viewed under low vacuum (B) had more contrast, but the bottom of the oocyte was too dark. The coated oocyte viewed under high vacuum appeared better because the entire oocyte was visible and it was very crisp (Fig. 2.8C). Therefore, high vacuum imaging with metal coating provided the best resolution micrographs at low magnification.

Since spot size affects resolution, we hypothesized that a lower spot size would provide higher resolution images. To test this hypothesis, Fig. 2.9 shows another oocyte that was sputter coated and imaged four different ways: under high vacuum with a spot size of 7 (A, D, G, J) and under low vacuum with a spot

size of 16 (B, E, H, K), spot size of 14 (C, F, I, L), and spot size of 12 (data not shown). Overall the high vacuum images provided better resolution than the low vacuum images. At low magnification (A – C; 1,200X) images of the oocyte viewed under low vacuum with a spot size of 14 or 16 appeared of similar quality to those taken at high vacuum. The low vacuum images have more contrast and the resolution appears to be just as good as the high vacuum image. The low vacuum oocyte image with a spot size of 16 (Fig. 2.9 B) is slightly better than the image with a spot size of 14 (Fig. 2.9 C) which was slightly grainy. The oocyte viewed at spot size 12 under low vacuum was not shown because during imaging it became extremely grainy and could not be focused at higher magnification than 1,000X.

At higher magnification (4,000 – 15,000X), different results were obtained (Fig. 2.9 D – L). Of these images, the high vacuum image series (Fig. 2.9 D, G, J) was the best. At 4,000X the high vacuum image had excellent resolution and was not grainy (Fig. 2.9 D). The low vacuum image with a spot size of 14 also had good resolution and was not grainy (Fig. 2.9 F). The low vacuum image with a spot size of 16 however was already becoming blurry and had low resolution (Fig. 2.9 E). When the magnification was further increased to 8,000X, the resolution of the low vacuum image with a spot size of 16 was even worse (Fig. 2.9 H). The high vacuum image and low vacuum image with a spot size of 14 both have good resolution at 8,000X (Fig. 2.9 G, I), but it is apparent that the high vacuum image had better resolution (Fig. 2.9 G). At 15,000X the resolution difference between the high vacuum image and low vacuum images with a spot

size of 14 was even more pronounced (Fig. 2.9 J – L). The low vacuum images had poor resolution and the high vacuum image still had good resolution. Therefore, the high vacuum images were better overall than the low vacuum images and significantly better than the low vacuum images at the higher magnifications (4,000 – 15,000X).

Imaging the Zona Pellucida

Once it was determined that the zona-intact oocytes were viewed best when coated with a thin layer of gold and viewed under high vacuum at 15 kV with a spot size of 6 – 7, a consistent set of magnifications to view the oocytes was necessary. Since the SEM only takes surface images of samples, the sides of the oocytes adhering to the coverslip were not seen, making the viewing of the zona pellucida random due to how the oocytes fell onto the glass fragments. Since the oocytes are spherical, only the very top center of an oocyte can be viewed because anything else will give a curved image distorting the size and shape of the surface.

To determine the image size that excluded effects of oocyte curvature, images of different magnifications were taken of the oocytes. Figure 2.10 shows that when viewing an oocyte at 4,000X magnification, the largest possible image of the oocyte was obtained without giving much if any of the curvature of the oocyte. Therefore an image of the oocytes was always taken at 4,000X. To obtain consistency of the images, the first image was taken of the whole oocyte, which ranged from 700 – 1,300X depending on oocyte size. If the first image

was taken at a magnification outside the range of 900 – 1,100X, a second image was taken at 1,000X. After that, the 4,000X image was taken and then another higher magnification image was usually taken at 8,000X. Occasionally images were taken at 10,000 – 20,000X or higher magnification.

To obtain a high resolution view of a large region of the zona pellucida, montages were taken of some of the oocytes. The montages consisted of several pictures lined up to make one complete large image: two or three images across, two images across by two down, three images across by two down, three images across by three down, four images across by four down or as many images as necessary to capture structures of interest. Figures 2.11 and 2.12 show montages of two images across by two down, taken at 7,500X (Fig. 2.11) and 20,000X (Fig. 2.12). The spongy and fibrous nature of the zona pellucida can be seen. Figure 2.12 shows that the larger fibers were composed of a much smaller network of microfibrils.

To observe the pores as they penetrated the zona pellucida, Fig. 2.13 shows increasingly higher magnifications of the zona pellucida from a whole view of an oocyte at 1,000X (Fig. 2.13A) to a pore at 35,000X (Fig. 2.13D). At the higher magnifications showing views of the zona pellucida pores (Fig. 2.13 C – D), it is apparent that the pores became smaller as they progressed deeper into the zona pellucida. Moreover, the large pore shown bifurcated into two smaller pores (Fig. 2.13D). Figure 2.14 is a stereo pair showing a three-dimensional view of the zona pellucida with a large pore which was centripetal. Figure 2.14

also shows that the zona pellucida has many layers, and large pores were perforated by smaller pores.

When examining all of the oocytes viewed thus far, it appears that the zona pellucida is not structured exactly the same in all of the oocytes. However, there are many similarities. First, the zona pellucida surface was a spongy fibrous meshwork. Second, the zona pellucida was multilayered. Third, the zona pellucida was punctuated by pores that were usually spherical or elliptical in shape. Fourth, many pores decreased in diameter and/or bifurcated as they penetrated deeper into the zona pellucida

When COCs were partially denuded, the cumulus cells were spherical or elliptical with an approximate diameter of 5 μm (Fig. 2.15). The cumulus cells appeared relatively smooth and were arranged compactly around the zona pellucida. The area of each cumulus cell nearest the zona pellucida narrowed into a single small protrusion that appeared to enter into the zona pellucida. In Fig. 2.12, the protrusions clogging some of the pores may be cumulus cell processes that broke off from the cumulus cells during the stripping process.

D. DISCUSSION

In the present study, ovaries were typically smaller when obtained from donors of small dog breeds. This is consistent with a study by Ström Holst *et al.* (2001) who found a positive correlation between body weight and ovarian weight. They found that ovarian size, however, did not correlate with the numbers of COCs recovered from the ovaries. In contrast Durrant *et al.* (1998) found that

larger ovaries yielded more COCs. We usually recovered fewer COCs from the smaller ovaries.

Several methods have been employed to isolate follicles and COCs from mammalian ovaries (Spears *et al.*, 2002). These include mechanical (slicing) and enzymatic digestion. Enzymatic digestion includes incubation in collagenase and DNase. This technique works well with mouse, rat, hamster and human follicles (Spears *et al.*, 2002). This procedure has also been successfully used with canine ovaries to yield follicles and COCs (Durrant *et al.*, 1998). Because mechanical isolation often leaves the follicles intact, we successfully used mechanical means to isolate canine follicles and COCs, and to denude oocytes of cumulus cells (stripping) to yield cumulus-free zona-intact oocytes.

To remove cumulus cells from the oocytes many studies typically employ hyaluronidase. However, we and others have found this treatment is ineffective with canine oocytes. Mechanically stripping the follicles and COCs with a small bore pipet has been previously used to denude canine oocytes of cumulus cells (Otoi *et al.*, 2004). Vortexing oocytes for 15 min in 75 mM sodium citrate as also been used to remove cumulus cells from canine oocytes (Ström Holst *et al.*, 2001). We have employed mechanical stripping of cumulus cells rather than enzymatic digestion or vortexing treatment which could alter the ultrastructure of the zona pellucida.

The freshly isolated COCs we used for the study were at least 180 μm or larger in size. The oocyte was homogenously dark being full of dark lipid yolk. The oocyte was also centrally located in the COC. Canine COCs within this size

range and characteristic oocyte morphology have been identified as being derived from advanced preantral follicles (Durrant *et al.*, 1998) or secondary follicles (Barber *et al.*, 2001). Typically, these COCs have gone on to resume meiosis when cultured *in vitro* (see Luvoni *et al.*, 2005). Thus, our study has used mature oocytes from preantral and antral follicles. Although we did not test it, these oocytes were most likely functionally competent to resume meiosis.

We found that the zona pellucida of living canine oocytes was approximately 8 – 10 μm thick. This is within the expected range reported for most mammals which can vary in thickness from 0.5 – 27 μm (Dunbar and Wolgemuth, 1984). The canine zona pellucida is reported to be 9.5 μm (Barber *et al.*, 2001) to 13 μm in the canine (Dunbar and O'Rand, 1991). Ström Holst *et al.* (2000) reported that the thickness of the canine zona pellucida ranged from 0.3 to 8 μm : 0.3 – 1.0 μm for salt-stored oocytes, 3 – 6 μm for fresh oocytes, and 6 – 8 μm for frozen oocytes. The variation in thickness maybe due to a number of confounding factors. The source of the canine oocytes they used were from preantral follicles, which according to Barber *et al.* (2000) have a thinner zona pellucida ($3.5 \pm 0.57 \mu\text{m}$). Their method of collecting COCs was the same as this study's (collection of COCs by mincing of the ovaries); however, they removed the cumulus cells from the oocytes using 75 mM sodium citrate. This treatment could have thinned the zona pellucida. In addition, the thin zona pellucida could have been due to dehydration induced by the salt storage treatment and/or SEM preparation they used. Since we only used fresh oocytes to determine zona

pellucida thickness, it is unclear what our fixation protocol may do to the thickness of the zona pellucida when prepared for scanning electron microscopy.

We found that concurrent glutaraldehyde fixation and affixation on poly-L-lysine coated glass slides yielded the highest specimen recovery method for SEM preparation of the canine oocytes. Through a series of scanning electron micrographs, this investigation has shown that the highest resolution was obtained with metal-coated canine oocytes viewed at high vacuum. Coating the oocytes with a thin layer of metal allows the oocytes to be viewed under high vacuum, which produces higher resolution micrographs than viewing the oocytes under low vacuum. However, this is a serious trade off, because when viewing oocytes coated with metal the actual zona pellucida is not seen, but instead the layer of metal above the zona pellucida is viewed. This can cause small discrepancies that require caution to be taken in the interpretation of the results (Vanroose *et al.*, 2000). Uncoated oocytes were not electrically conductive and had to be viewed under low vacuum, which allowed gas in the specimen chamber. The gas interfered with the imaging, producing lower resolution images. The uncoated oocytes also have a good chance to be burnt by the electron beam (although we did not observe this). Therefore it was determined that optimal results were obtained when oocytes were coated and viewed at high vacuum.

Changing the spot size of the electron beam will greatly enhance or reduce the resolution of the micrographs. Therefore spot size was manipulated in this study to optimize micrograph resolution. Theoretically, a smaller spot size

allows for higher resolution; however, eventually the image becomes too grainy due to background noise. The spot size that resulted in an optimized balance of resolution and background noise was 6 – 7 under high vacuum conditions. The fixation methods and the setup of the SEM under high vacuum produced excellent images of the morphology of the zona pellucida. Tengowski and Schatten (1997) used a field emission low voltage SEM to view the zona pellucida of the bovine oocyte. This instrument is capable of producing higher resolution images than the University of Dayton's LVSEM. In our study, it was possible to see the smaller microfibrils that made up the larger structures of the zona pellucida as a whole (Fig. 2.13). This is what Tengowski and Schatten (1997) lost when they viewed bovine oocytes under cSEM with gold coating. By viewing the cSEM samples under the field emission low voltage SEM, they could see the bulbous nature of the gold coating over the zona pellucida. Because we could see the microfibrils that made up the larger network of fibers of the zona pellucida, we concluded that our preparation techniques were optimized and yielded high resolution images.

Our methods to prepare canine oocytes for scanning electron microscopy yielded images of the zona pellucida that are comparable (or better) than previous studies of the mammalian zona pellucida (Calafell *et al.*, 1992; Dudkiewicz and Williams, 1977; Familiari *et al.*, 1988, 1989, 2001; Funahashi *et al.*, 2000; Haenisch-Woehl *et al.*, 2003; Magerkurth *et al.*, 1999; Michelmann *et al.*, 2001; Nikas *et al.*, 1994; Ström Holst *et al.*, 2001; Tengowski and Schatten, 1997; Tengowski *et al.*, 2001; Suzuki *et al.*, 1994, 2000; Vanroose *et al.*, 2000;

Xia *et al.*, 2001). Compared to other mammals, the canine generally had a similar zona pellucida in that it was spongy and porous, often with a net-like structure surrounding the oocyte similar to the mouse, rat, hamster, rabbit, pig, cow and human zonae pellucidae (Calafell *et al.*, 1992; Dudkiewicz and Williams, 1977; Magerkurth *et al.*, 1999; Nikas *et al.*, 1994; Tengowski and Schatten, 1997; Tengowski *et al.*, 2001; Vanroose *et al.*, 2000). Each of the different mammalian zonae pellucidae varied, so it is important to compare our work to other work done in the canine.

Our images of the surface of the canine zona pellucida were consistent with those reported by Ström Holst *et al.* (2000). They were investigating the effects of different storage methods (salt and freezing) on the zona pellucida compared to fresh oocytes. Their study showed that storage of the oocytes caused the zona pellucida to look slightly different. In the freshly-fixed oocytes, the zona pellucida had a sponge-like appearance with a fenestrated meshwork, whereas in the oocytes that were stored (frozen, salt-stored, or frozen and salt-stored) the zona pellucida tended to have larger fenestrations with a thicker meshwork. The zona pellucida in our study also generally looked similar to a study of the zona pellucida of prepubertal canine oocytes (Haenisch-Woehl *et al.*, 2003).

Our results demonstrate that the base of each cumulus cell narrowed into a thin process that appeared to penetrate the zona pellucida, similar to what has been reported for COCs from prepubertal dogs (Haenisch-Woehl *et al.*, 2003), the porcine (Suzuki *et al.*, 2000) and the bovine (Suzuki *et al.*, 1994). These

transzonal projections are thought to supply needed nutrients from the cumulus cells to the oocyte as it develops (Guraya, 1965; Luvoni *et al.*, 2005). When compared to cumulus cells from prepubertal dogs (Haenisch-Woehl *et al.*, 2003), our results using mature dogs indicate that the surface of the cumulus cells does not significantly change during follicular growth. Moreover, our preservation methods do not introduce significant artifacts in cumulus cell morphology or ultrastructure of the zona pellucida. Therefore the techniques used in this study to obtain, fix, dehydrate, critical point dry and coat the oocytes for viewing are excellent techniques that resulted in optimal resolution.

It is not, however, apparent if the pores go through the zona pellucida all the way to the oolemma or if they close up somewhere in the zona pellucida. In the present study, the outer surface of the canine zona pellucida was punctuated by pores that often narrowed as they penetrated the zona pellucida (Figs. 2.13, 2.14). Studies on the porcine zona pellucida have shown that while the outer zona pellucida has large pores, the inner surface has very small orifices (Funahashi *et al.*, 2000; Suzuki *et al.*, 2000). Whether these completely transverse the zona pellucida is unclear, but Vanroose *et al.*, (2000) have shown that viruses are unable to completely penetrate the bovine zona pellucida indicating that the pores are not continuous with the perivitelline space.

We conclude the following. Concurrent affixation and glutaraldehyde fixation to poly-L-lysine-coated glass slides provide the maximum yield of oocytes. Viewing metal-coated oocytes under conventional high vacuum conditions is preferable to low vacuum conditions especially at higher

magnifications. The outer surface of the canine zona pellucida is a spongy meshwork with many spherical or elliptical pores that often narrow as they split into smaller pores deeper in the zona pellucida. Each cumulus cell immediately surrounding the zona pellucida narrows to form a process that appears to penetrate the zona pellucida. The SEM techniques presented here will enable future studies of canine oocytes including endangered canids during oocyte maturation and gamete interactions.

Fig. 2.1. Freshly-collected canine ovary. This ovary is from a Greyhound which was ovariohysterectomized during routine spaying by a local veterinarian. The ovary is surrounded by a layer of adipose tissue (fat). The fat will be removed before mincing the ovary to release follicles and cumulus-oocyte complexes. Scale bar represents 5 mm.

Fig. 2.1.



Fig. 2.2. Cleaned and washed canine ovaries. The ovaries shown in A and B have been removed from the surrounding fat and were washed in PBS. The ovary in A came from a Shih Tzu (small dog) and the ovary in B came from a Greyhound (large dog, from ovary surrounded in fat in Fig. 1). The ovary from the Greyhound is larger than the ovary from the Shih Tzu. The ovaries are now ready to be minced to release cumulus-oocyte complexes. Scale bar represents 5 mm.

Fig. 2.2.

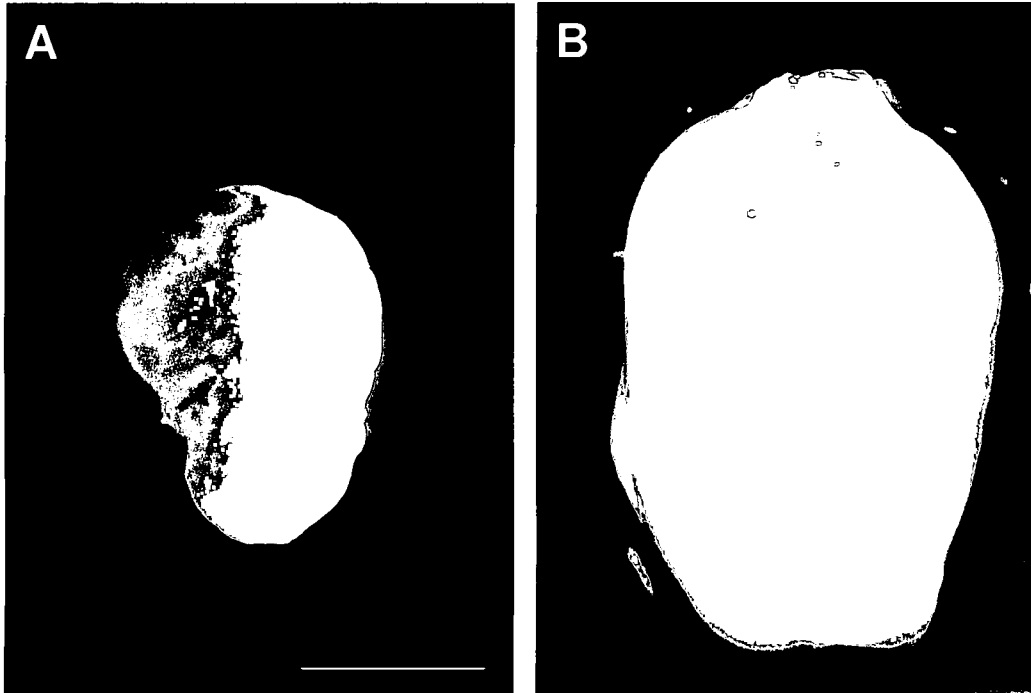


Fig. 2.3. Ovarian mincing procedure. The Greyhound ovary shown in A is overlaid with a grid to show the mincing pattern used to release cumulus-oocyte complexes. The grid is numbered line by line. The first cut was made along line number one, then line two and so on. The resulting pieces in a petri dish shown in B are approximately 2 - 8 mm in length. Scale bar represents 5 mm in A and 10 mm in B.

Fig. 2.3.

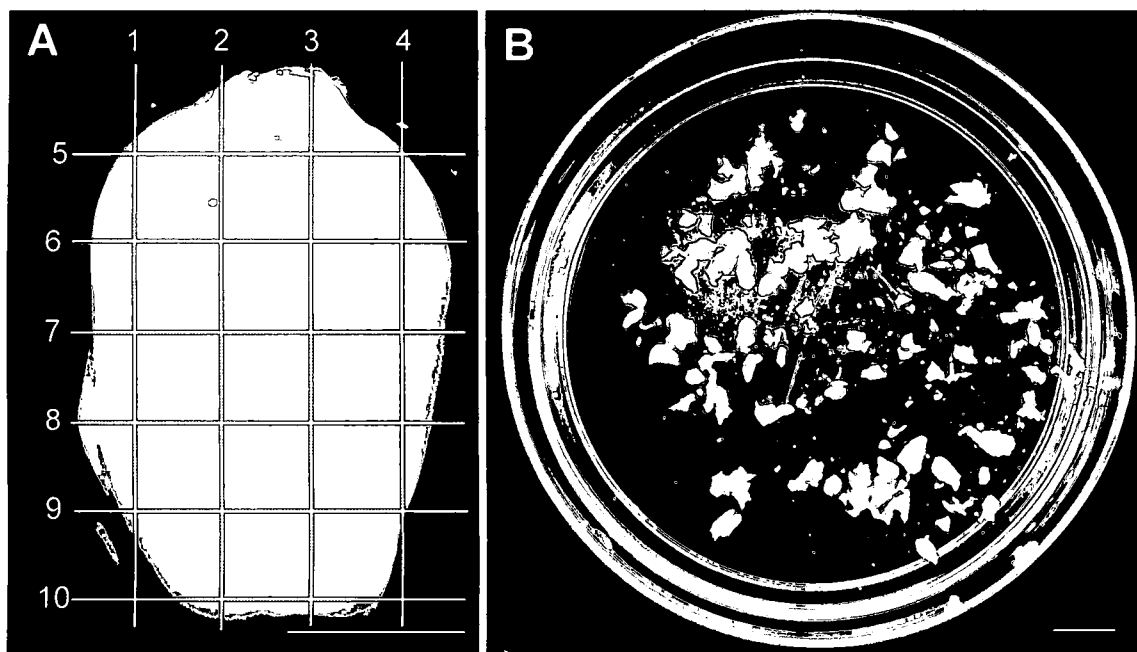


Fig. 2.4. Freshly-isolated cumulus-oocyte complex (COC) from a Shih Tzu ovary. COCs were isolated from minced ovaries and transferred into a solution of fresh PBS. The thick arrow shows the cumulus cells surrounding the oocyte. The thin arrow shows the zona pellucida. The small spots in the background surrounding the COC are individual cumulus cells. Only COCs with a layer of cumulus cells two to three cells thick or more and a dark oocyte were used for this study. This COC is ready to be denuded of cumulus cells in preparation for scanning electron microscopy. Scale bar represents 50 μm .

Fig. 2.4.

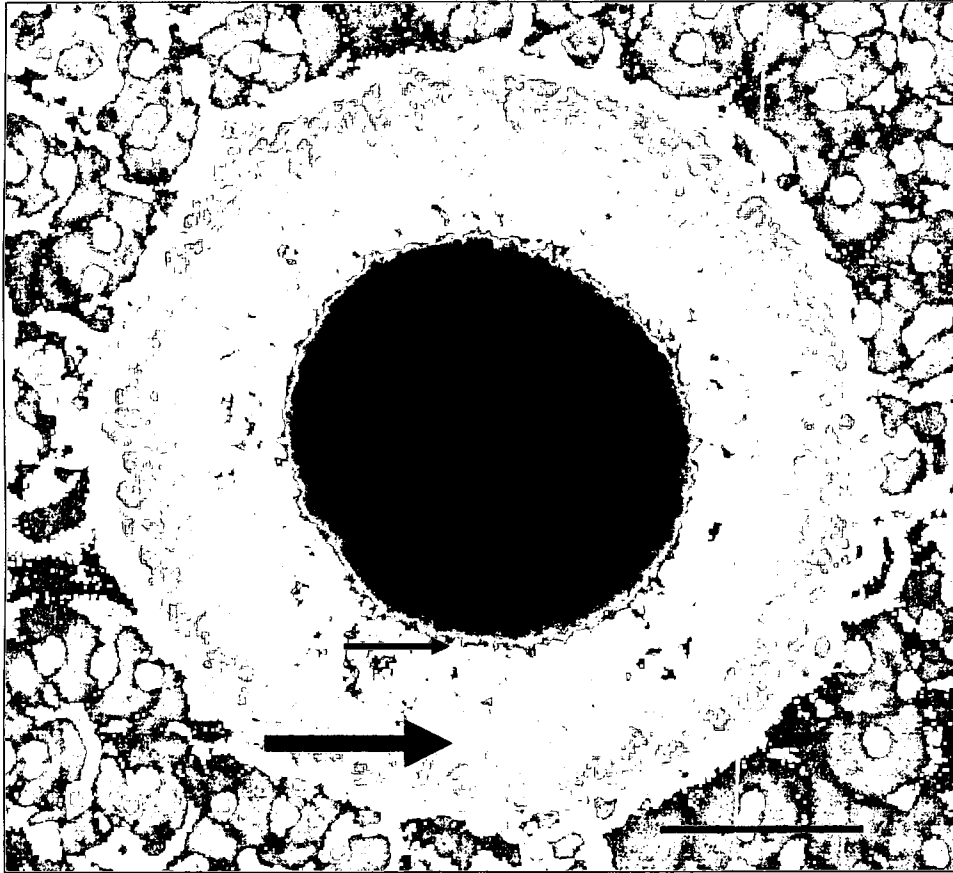


Fig. 2.5. Zona-intact oocyte from a Shih Tzu ovary. The oocyte shown has been denuded of all of its surrounding cumulus cells by repeated pipetting (~20 times). The transparent zona pellucida (arrow) surrounds the dark oocyte. This oocyte is ~110 μm in diameter and the zona pellucida is ~10 μm thick. The small spheres in the background are individual cumulus cells. This oocyte is ready to be attached to a glass slide with other oocytes, fixed and dehydrated for critical point drying. Scale bar represents 50 μm .

Fig. 2.5.

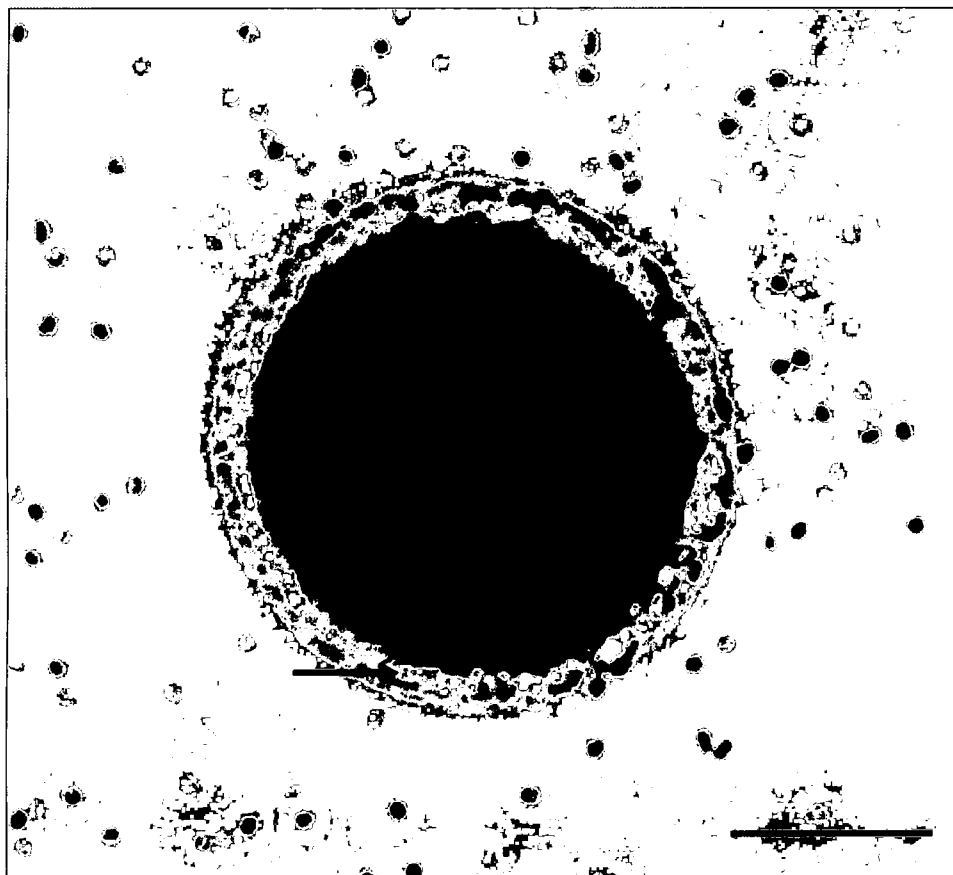


Fig. 2.6. Critical point-dried canine oocytes. These four oocytes isolated from Chihuahua ovaries have been critical point dried to preserve their external structure for viewing in the scanning electron microscope (SEM). If the oocytes were not critical point dried, they would shrivel up as they dried out under even the low vacuum of the SEM. The oocytes were mounted on a glass slide which was affixed to a specimen stub using black carbon tape which shows through the slide. The image was taken using a Nikon E950 Coolpix digital camera mounted on a Nikon SMZ-U stereo microscope. The average diameter (mean \pm SE) of these zona intact oocytes is $85.53 \pm 3.31 \mu\text{m}$ (range 78.95 to 94.74 μm). The oocytes are now ready to be viewed in the SEM under low vacuum, or sputter coated and then viewed in the SEM under high or low vacuum. Scale bar represents 100 μm .

Fig. 2.6.

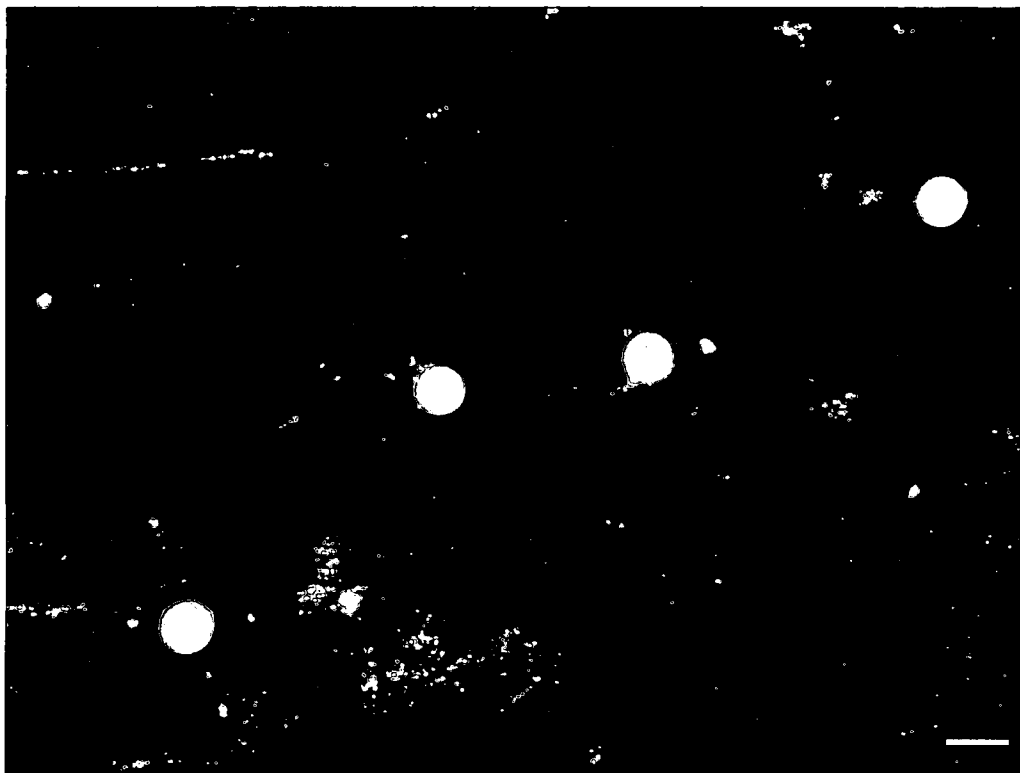


Fig. 2.7. Sputter-coated canine oocytes. These five oocytes isolated from Schnauzer ovaries have been sputter coated with approximately 100 Angstroms of gold to make them electrically conductive to prevent charging and/or deterioration from the electron beam of the scanning electron microscope (SEM). The oocytes were mounted on a glass slide that was affixed to a specimen stub using black carbon tape which shows through the slide. The image was taken using a Nikon E950 Coolpix digital camera mounted on a Nikon SMZ-U stereo microscope. The average diameter (mean \pm SE) of these zona-intact oocytes is $96.47 \pm 1.96 \mu\text{m}$ (93.07 to 100.76 μm). These oocytes are ready to be viewed under high or low vacuum in the SEM. Scale bar represents 250 μm .

Fig. 2.7.

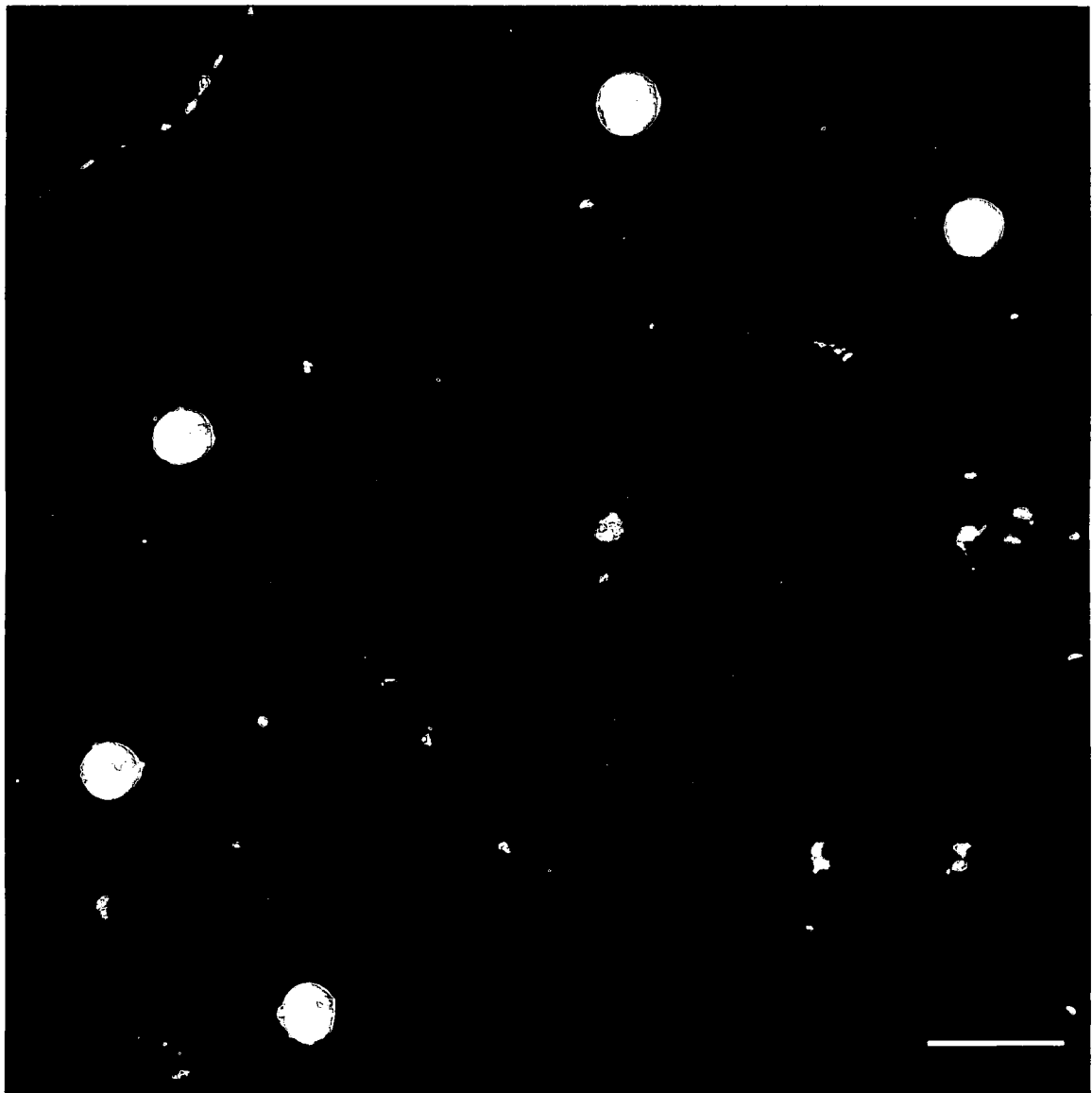


Fig. 2.8. Imaging modes. Scanning electron micrographs showing different imaging modes in the low vacuum scanning electron microscope. The same canine oocyte is viewed three different ways: uncoated (A), or coated and viewed under low vacuum (B), or coated and viewed under high vacuum (C). The oocyte in B is rotated $\sim -30^\circ$ from the oocyte in A. The oocyte in C is rotated approximately 80° from the oocyte in A. Magnification: A, 1000X; B, 900X; C, 950X. Scale bars represent 20 μm . In this low magnification range, sputter coating and viewing at either low or high vacuum provides better resolution than viewing the oocyte uncoated at low vacuum.

Fig. 2.8.

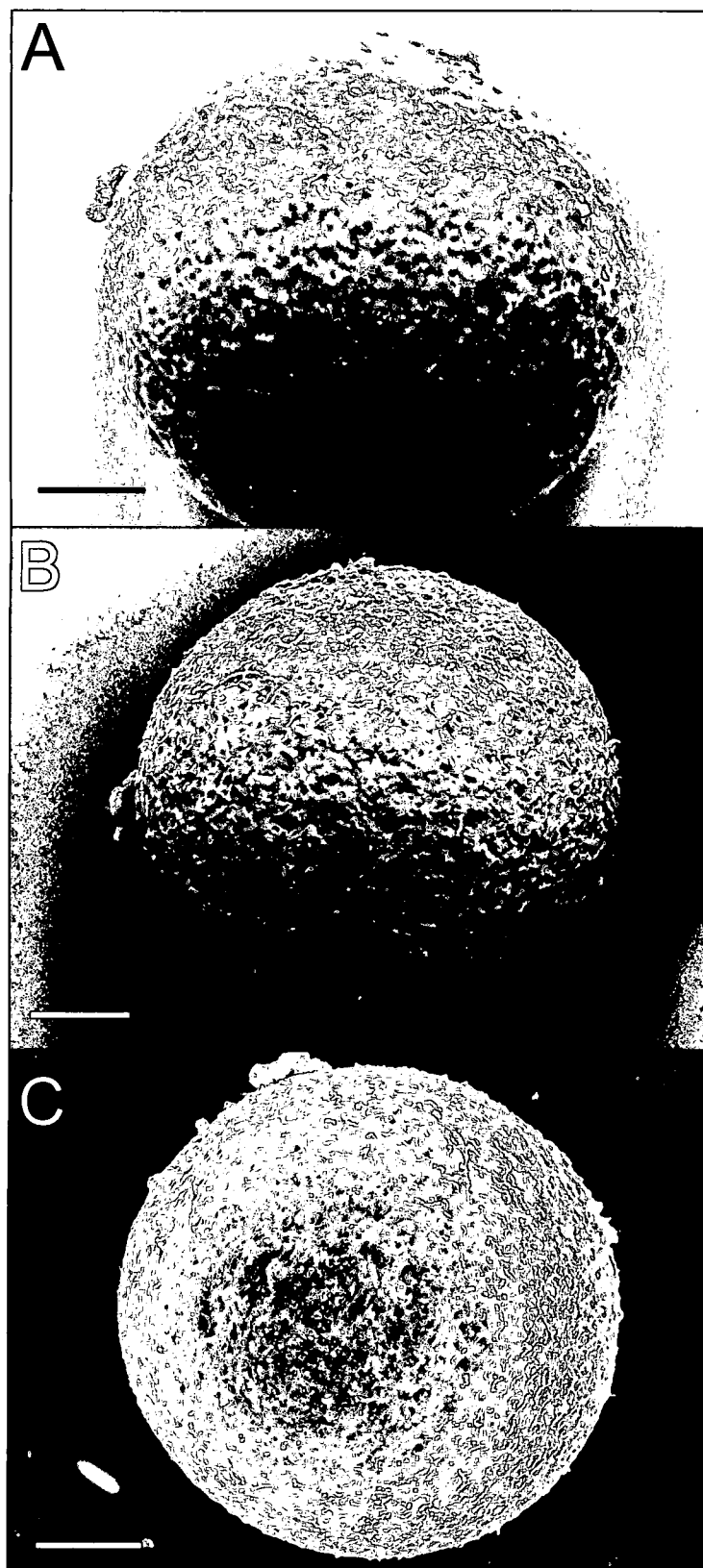


Fig. 2.9. Effect of spot size on resolution. The same canine oocyte was coated and viewed three different ways: under high vacuum with a spot size of 7 (A, D, G, J), under low vacuum with a spot size of 16 (B, E, H, K), and under low vacuum with a spot size of 14 (C, F, I, L). The oocyte in each condition was viewed with an accelerating voltage of 15 kV. The oocyte was isolated from a one year old Siberian Husky mix. Scale bars represent 10 μm (1,200X) in A – C, 5 μm (4,000X) in D – F, 2 μm (8,000X) in G – I, and 1 μm (15,000X) in J – L. Decreasing the spot size under low vacuum improves the images, but they are inferior to the high vacuum images. Therefore, high vacuum imaging gives the best resolution micrographs overall.

Fig. 2.9.

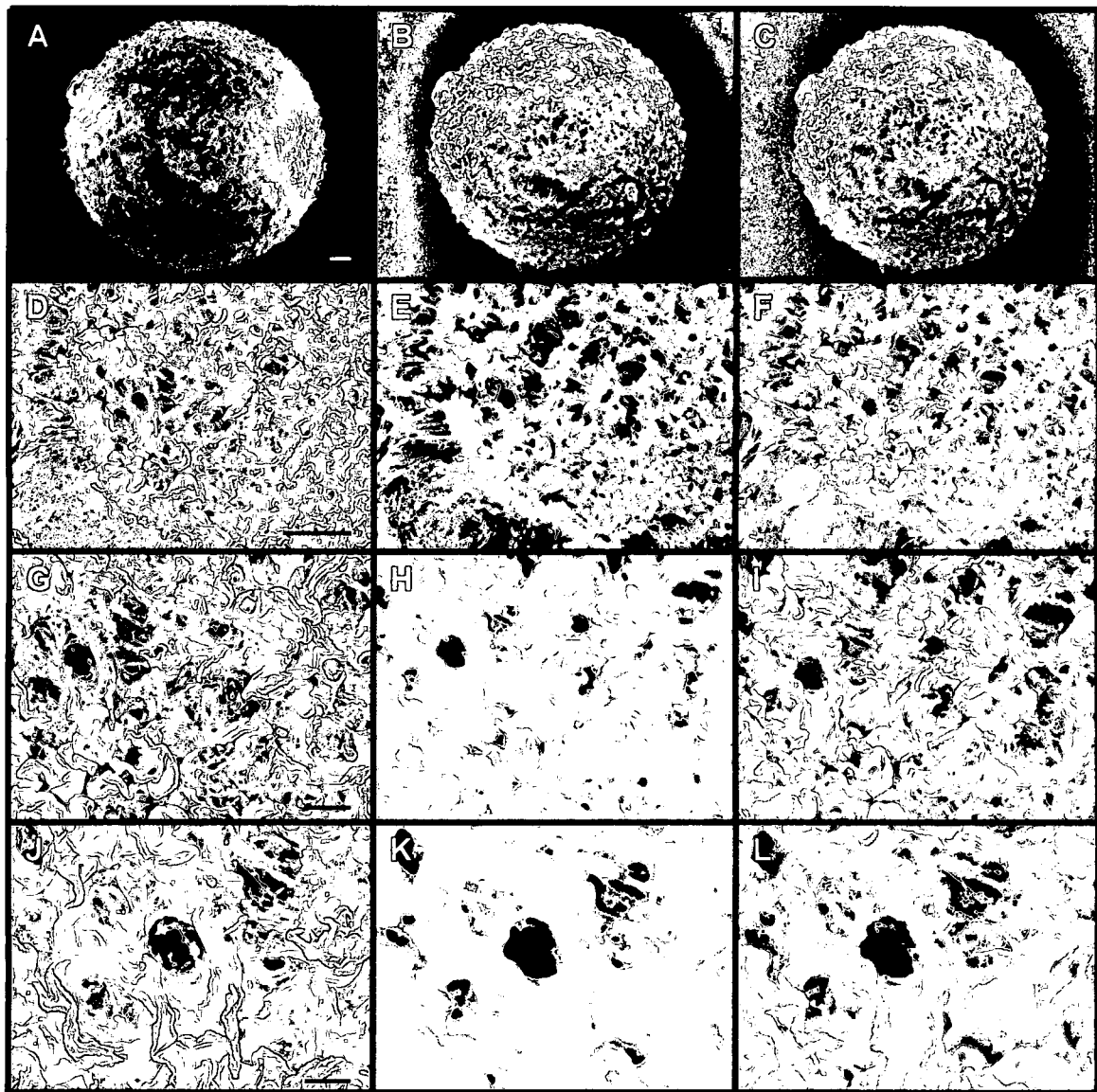


Fig. 2.10. Surface morphology of the canine zona pellucida. A panoramic view of a zona-intact canine oocyte (A) taken at 1,000X shows the fibrous and spongy nature of the zona pellucida over its entire surface. This oocyte was coated with metal and viewed under high vacuum with a spot size of 7 and accelerating voltage of 15 kV. This oocyte is 121.54 μm in diameter. The white box in A shows the same area taken at 4,000X in B. Scale bars represent 20 μm in A and 5 μm in B. Images taken at 4,000X are not distorted by the curvature of the oocyte. Higher magnification reveals numerous spherical pores in a multi-layered, zona pellucida matrix.

Fig. 2.10.

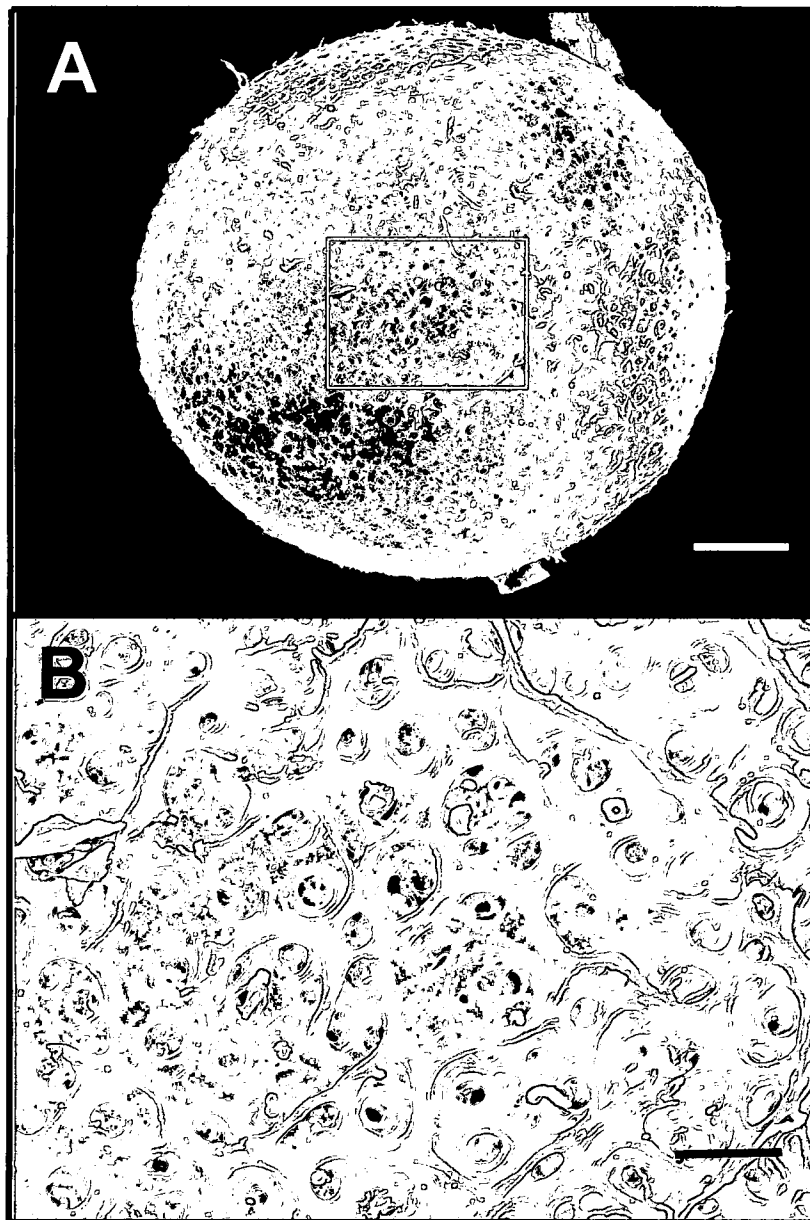


Fig. 2.11. Montage of the canine zona pellucida at high resolution. The image was constructed by placing four slightly overlapping images that were taken at 7,500X to form a larger picture with higher resolution than it would have been if taken at a lower magnification. The montage is two images across by two images down. Scale bar represents 4 μm . The fibrous nature of the zona pellucida is shown.

Fig. 2.11.

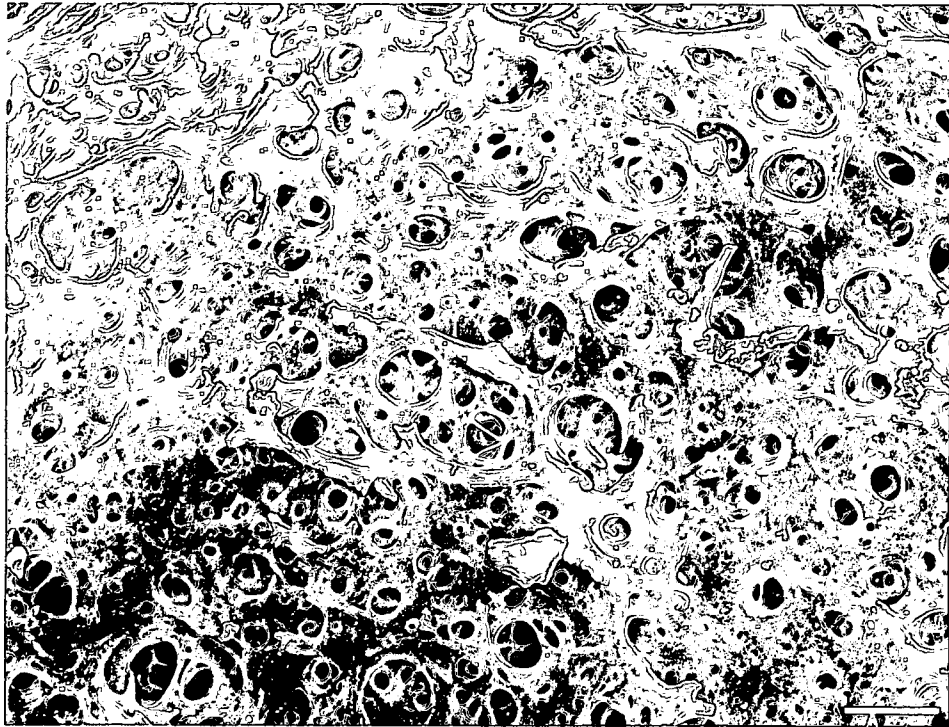


Fig. 2.12. High magnification montage of the canine zona pellucida. The oocyte was isolated from a seven year old Boxer. The image was constructed by placing four slightly overlapping images that were taken at 20,000X magnification to form a larger picture with higher resolution than it would have been if taken at a lower magnification. The montage is two images across by two images down. Scale bar represents 1 μm . The fibrous nature of the zona pellucida is shown along with the microfibrils that make up the thicker areas of the zona pellucida. Some pores split into smaller fenestrations deeper into the zona pellucida.

Fig. 2.12.

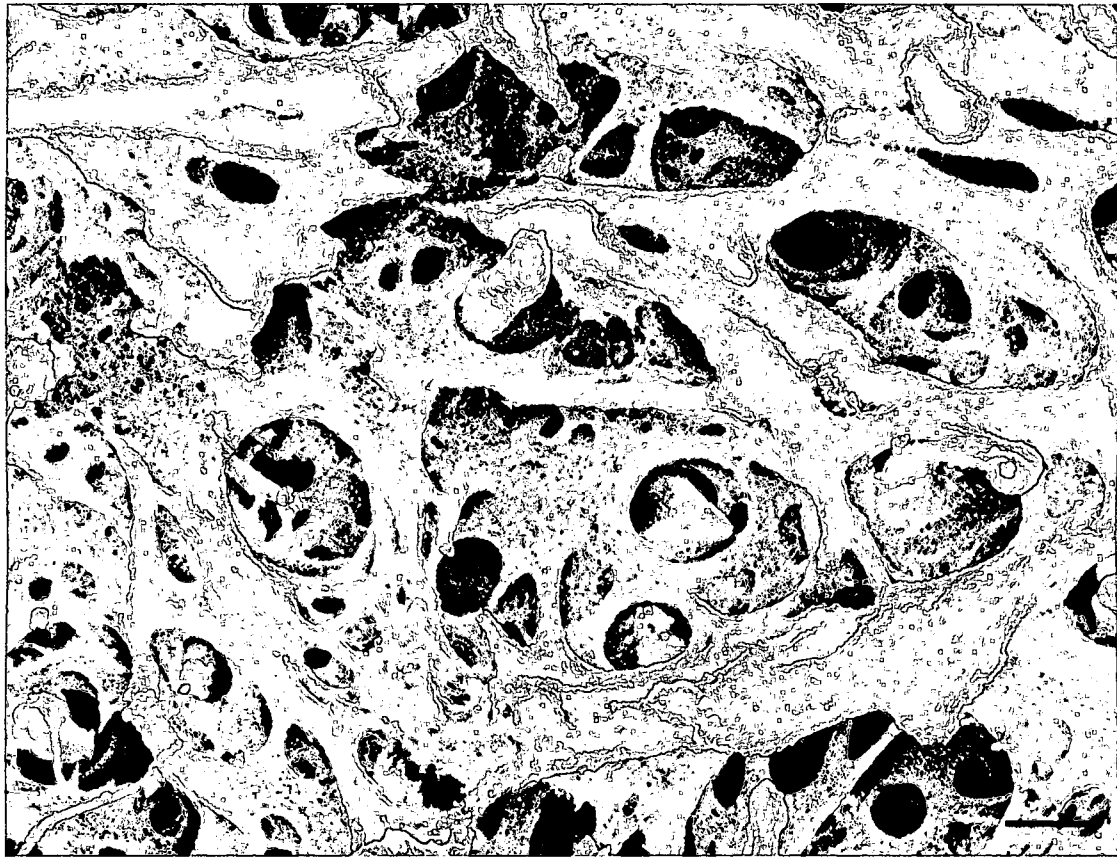


Fig. 2.13. Pores of the zona pellucida are conical and bifurcated. This oocyte was isolated from a nine month old Cocker Spaniel Mix. This figure shows four images of the same oocyte at increasing magnification. A shows the entire oocyte at 1,000X. B shows the area in the box of A magnified to 4,000X. C shows the area in the box of B magnified to 10,000X. This pore is large on the surface of the zona pellucida and narrows as it enters the zona pellucida which appears composed of multiple layers. D shows the area in the box of C magnified to 35,000X. The pore narrows as it progresses deeper into the multi-layered zona pellucida. Moreover, the pore bifurcates into two smaller pores deep into the zona pellucida. Scale bars represent 10 μm in A, 5 μm in B, 1 μm in C, and 0.5 μm in D.

Fig. 2.13

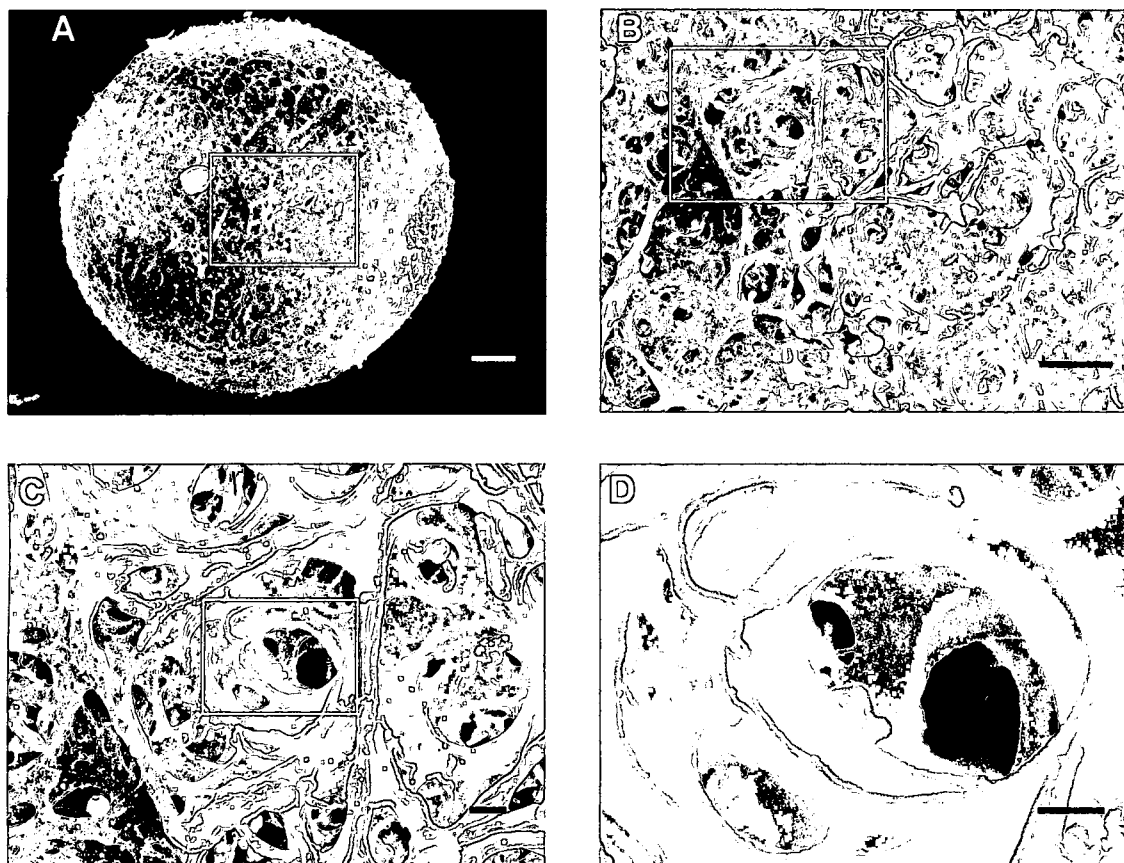


Fig. 2.14. Stereo pair of the outer surface of the canine zona pellucida. This oocyte was isolated from a three year old Shetland Sheepdog Mix. The conical and bifurcated nature of the pores of the canine zona pellucida are visible in three dimensions. This stereo pair was taken at 8,000X with a tilt of seven degrees. A large open pore narrows deeper into the multi-layered zona pellucida, and bifurcates into several smaller pores deep into the zona pellucida. Scale bar represents 2 μm .

Fig. 2.14.

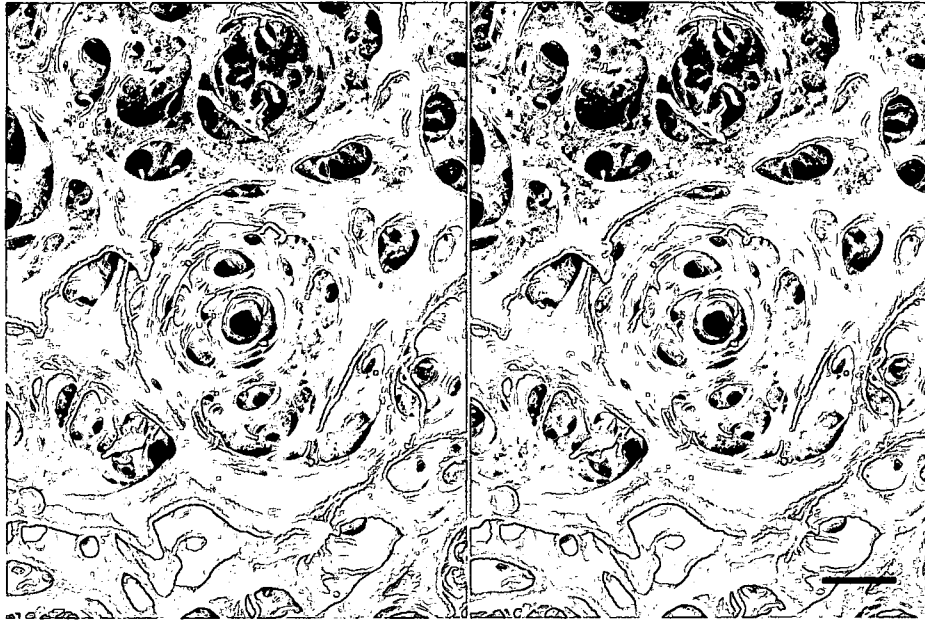
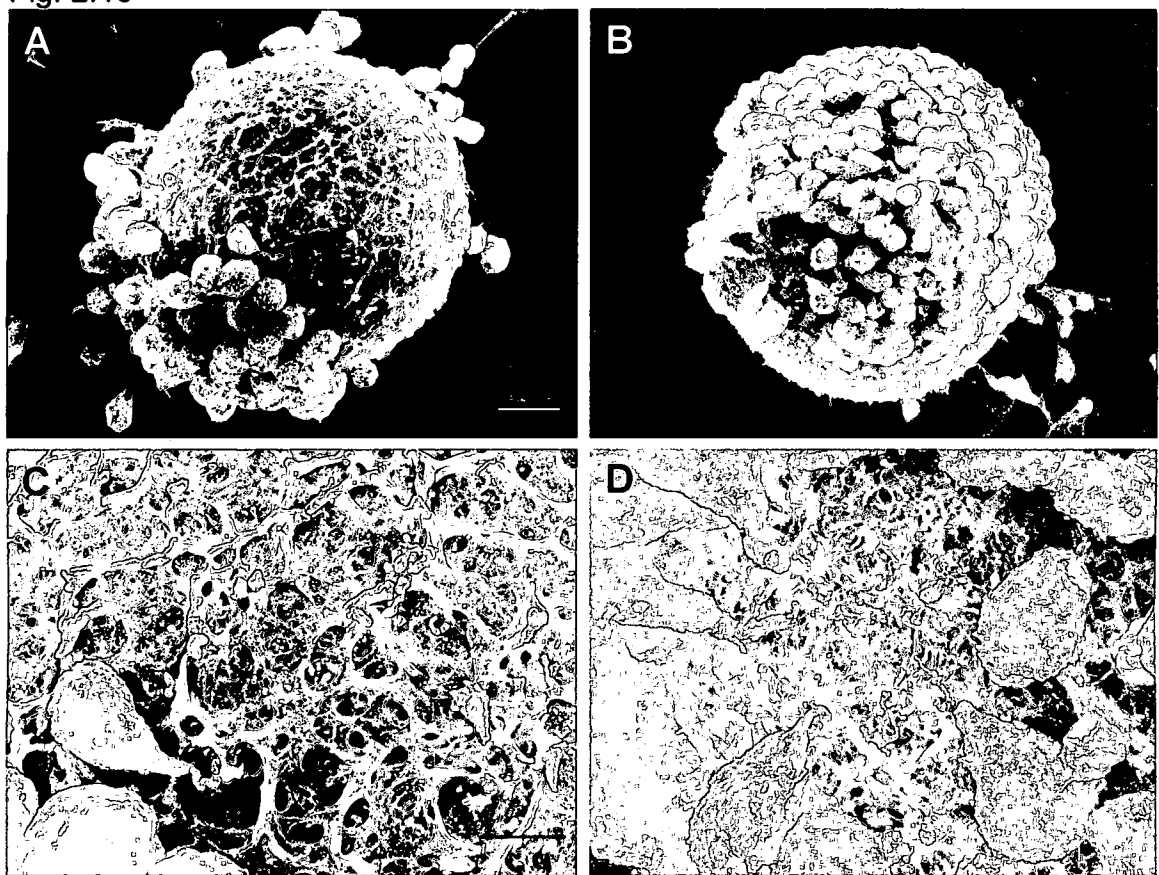


Fig. 2.15. Surface characteristics of canine cumulus cells. The two different oocytes in this figure were isolated from a nine month old Cocker Spaniel mix (A and C) and a two year old Wolf mix (B and D). C magnifies the center of the oocyte in A. D magnifies a portion of the lower left region of the oocyte in B. The spherical cumulus cells are approximately 5 – 7 μm in diameter. Each cumulus cell narrows into a small protrusion that enters the zona pellucida in C and D. The fibrous meshwork and pores of the zona pellucida are also visible in C and D. Scale bars represent 10 μm in A and B (1,000X), and 5 μm in C and D (4,000X).

Fig. 2.15



CHAPTER III

The Heterogeneity of the Canine Zona Pellucida

A. INTRODUCTION

Upon closer examination of the oocytes in Chapter 2, it appears that the ultrastructure of the zona pellucida varies between the different oocytes. For example, Fig. 2.8C is of an oocyte that has a smooth zona pellucida with only a few pores viewed at low magnification. However, the oocyte in Fig. 2.10 is covered with many more pores that are larger. Moreover, the oocytes in Figs. 2.9 and 2.13 have zonae pellucidae that appear to be very rough at low and high magnification and are more "spongy." In addition, the zona pellucida shown in Fig. 2.15D is very stringy at high magnification. Our data are consistent with previous scanning electron microscopy studies of various mammals that show differences in the ultrastructure of the zona pellucida (Dudkiewicz and Williams, 1977).

Studies using murine, porcine and bovine oocytes have shown that the zona pellucida undergoes structural alterations during oocyte maturation and fertilization (Calafell *et al.*, 1992; Funahashi *et al.*, 2000; Jackowski and Dumont,

1979; Suzuki *et al.*, 1994, 2000; Vanroose *et al.*, 2000), but other studies using rodent (mouse and hamster) and human oocytes did not observe any changes (Familiari *et al.*, 1988; Phillips and Shalgi, 1980). This difference may be due to *in vitro* maturation, which has a significant effect on zona pellucida thickness compared to *in vivo* maturation in mouse embryos (Silva *et al.*, 1997). Calafell *et al.* (1992) reported that as the mouse oocyte matured, the zona pellucida appearance changed. The most immature oocytes had an unstructured zona pellucida (Y-type) with the most cellular debris. Slightly more mature oocytes had a more structured zona pellucida with pores that were shallow and small in diameter (Z-type) with less cellular debris than the most immature oocytes. Mature oocytes (A/B type) had a smooth zona pellucida either with (A-type) or without (B-type) a fibrous network. In addition, these mature oocytes lacked cellular debris. Aged oocytes also had a unique structure (C-Type): a rough appearance with only a few random pores. The last type of zona pellucida observed (D-Type) was of a deteriorating or atretic oocyte, which had a flat, unstructured zona surface without pores, cellular debris or cumulus cells.

Vanroose *et al.* (2000) observed two main zona pellucida types in bovine oocytes and embryos. The first zona pellucida type showed a spongy appearance with a network of pores. The second was a zona pellucida that had a more compact structure with larger pores in lower numbers than the first type. The zona pellucida morphology changed as the oocytes were fertilized and developed from a zygote to a morula: matured oocytes were rough and spongy, whereas zygotes had a more compact, "smooth, melted" surface with fewer

pores. This compact nature of the zona pellucida was consistent for most of the bovine embryos; however, the 8-cell stage exhibited both the spongy and compact types. Morulae had a rough-appearing zona pellucida with many smaller pores. Similar results were reported for maturing and mature porcine oocytes which had a zona pellucida with a fibrous, open mesh-like structure that became smoother and less porous after fertilization (Funahashi *et al.*, 2000; Suzuki *et al.*, 2000).

A report by Magerkurth *et al.* (1999) stated that human oocytes collected for *in vitro* fertilization had different zona pellucida morphologies as well, but there was no correlation between the maturity of human oocytes and the type of zona pellucida present. They detected four types of zona pellucida. Type A and type B had a porous net-like structure, with type A having larger and deeper pores than type B. Type C had an uneven and spongy surface with fewer pores and the net-like structure disappeared. Type D had a smooth surface with very few pores. Most of the oocytes they investigated ($n = 359$) were types A and B (61%), with fewer type C (35%) and very few (4%) with a type D zona pellucida.

Using canine oocytes, Ström Holst *et al.* (2000) observed differences in the zona pellucida based on how the oocytes were stored (fresh, frozen, salt-stored, or frozen-salt-stored) before SEM preparation. They also noted that within each storage treatment, the surface morphology of the zona pellucida was heterogeneous. However, they did not identify the zona pellucida types and made no correlation to whether the heterogeneity was due to oocyte maturity or any other characteristic that they observed, other than storage methods.

The focus of this chapter is to determine the extent of the ultrastructural heterogeneity of the canine zona pellucida observed in Chapter 2, and to determine what factors may affect this heterogeneity. In this chapter, the effect of dog donor characteristics {including the breed of the oocyte donors, breed type which is consistent with the AKC standards, breed size (by weight), age of the oocyte donor, and the maturity of the oocytes as reflected in oocyte size (diameter)} on zona pellucida morphology will be examined with scanning electron microscopy to determine whether these characteristics relate to the differing microarchitecture of the canine zona pellucida.

B. MATERIALS AND METHODS

Chemicals

All chemicals were from Sigma Chemical Co. (St. Louis, MO) and Fisher Scientific Company (Pittsburg, PA) unless otherwise noted.

Animals

Thirty-six healthy female dogs from 28 different breeds (both pure bred and mixed breeds) were used for this study. They ranged in age from 3 – 108 mon (9 years) with a mean \pm standard error (SE) of 28 ± 4.56 mon. Mature females were in various stages of the estrous cycle, since ovaries were collected throughout the year as described in Chapter 2. Oocyte donors were classified according to breed type using the AKC standards (Herding, Hound,

Non-Sporting, Sporting, Terrier, Toy, Working, and Miscellaneous). They were also grouped by weight: small (<13 kg or <30 lb), medium (13 – 23 kg or 30 – 50 lb), and large (>23 kg or >50 lb). In addition, the dogs were categorized into four age groups regardless of weight: prepubertal (<6 mon), juvenile (6 – 11 mon), mature (12 – 48 mon), and old (>49 mon).

Collection of Ovaries

Ovaries encased in fat were obtained from a local veterinarian during routine ovariohysterectomy as described in Chapter 2. After surgery, the ovaries were immediately placed in cold PBS and were stored at 4 °C for less than 24 hr until they were processed.

Collection of the Oocytes

Oocytes were collected from COCs as described in Chapter 2. Briefly, subcutaneous fat was removed from the ovaries which were washed in PBS and minced to release COCs. Only COCs with dark ooplasm, a larger-size centrally placed dark oocyte, and three or more complete layers of cumulus cells were used for the study. The cumulus cells were removed from the zona pellucida through repeated pipetting (up to fifty times) using a 150 µm STRIPPER pipet (MidAtlantic Diagnostic, Inc., Marlton, NJ). Any COCs that resisted denuding or had a ruptured oolemma were not used for this study. Denuded COCs were

transferred to fresh PBS. This yielded 306 high-quality oocytes that were used for the study.

Affixation and Fixation

Denuded oocytes were simultaneously affixed and fixed on a ~6 X 6 mm cut glass slide coated with 1 mg/ml poly-L-lysine in a depression slide containing cold 2.5% glutaraldehyde in 0.1 M CB for one hr on ice (Mazia *et al.*, 1975; Vanroose *et al.*, 2000). After fixation, the oocytes were then washed twice in fresh CB which lasted 15 min per wash.

Dehydration

Fixed oocytes were dehydrated using a graded series of ethanol as described in Chapter 2. In an additional step, oocytes were transferred to fresh 100% ethanol just before critical point drying.

Critical Point Drying

After dehydration, the glass slide fragments with adhering oocytes were placed into a Ted Pella size C microporous ceramic capsule and critical point dried in a Tousimis AUTOSAMDRI® -814B critical point dryer. The slides were

then taped onto an aluminum stub (SEM specimen mount stubs from Electron Microscopy Sciences) using carbon tape (SPI Supplies).

Sputter Coating

The oocytes were sputter coated with a ~100 Ångstrom thick layer of gold particles using a Denton Vacuum Desk II Cold Sputter/ Etch Unit for 30 sec at 45 ma. After sputter coating, the samples were stored on their aluminum stubs in a four-well case (Electron Microscopy Sciences) in a dessicator, Frigicator II (Streck Laboratories, Inc.) at room temperature.

Viewing of Oocytes with the Scanning Electron Microscope

Oocytes were viewed in a JEOL JSM-5800LV SEM under high vacuum (0 Pa) with a voltage of 15 kV, a spot size of 6 – 7, objective lens of 20 µm, and a height of 11 mm. Typical micrographs included low (900 – 1,000X) and high magnification (4,000X), with occasional higher magnifications.

Image Storage

Micrographs were stored on floppy disks in the form of .tiff, .txt and .sim files. The files were then transferred on to a computer hard drive and stored until further analysis. A hard copy of each micrograph was also printed off the JEOL

JSM-5800LV with a Sony Video Graphic Printer UP-890MD (Oconomowoc, WI) on Sony Thermal Print Media UPP-110HD (Oconomowoc, WI) and stored in acid free magnetic photo album pages (Lakeville, MA).

Statistical Analysis

Oocyte diameters were measured from scanning electron micrographs and reported as the mean \pm SE. Comparisons between groups were performed using a one-way ANOVA and Tukey-post-hoc analysis. Other values are reported as the mean \pm SE. Oocytes were placed into one of four categories based on zona pellucida surface morphology as described in the Results. Comparisons between groups were performed using a Friedman's test (breed), two-way ANOVA (breed types and age), and a Chi-square test (breed size) with a significance level of $P < 0.05$ (SPSS version 13.0, SPSS, Inc., Chicago, IL).

C. RESULTS

Distribution of Oocytes from Canine Donors

Three hundred and six oocytes from 28 different breeds of pure bred and mixed breed dogs were examined. Figure 3.1 shows the different breeds of oocyte donors used for the study, and the number of oocytes collected from each breed. The average number of oocytes collected per breed was 10.9 ± 1.2 (mean \pm SE). No more than 8.5% of the oocytes came from any one breed; therefore, the data were not skewed towards any specific breed. Oocytes were

also grouped by breed type (AKC classification; Fig. 3.2) and donor size (Fig. 3.3). Less than half of the oocyte donors (42.5%) were herding dogs (20.6%) or working dogs (22%). Over half (53%) of the oocytes came from large dogs, with fewer oocytes from medium (13.7%) and small dogs (33.3%).

The average (mean \pm SE) age of dogs used in the study was 28 ± 4.56 mon. Small dogs ranged from 8 – 84 mon (38.09 ± 9.15 mon). Medium dogs ranged from 6 – 24 mon (10.9 ± 3.47 mon). Large dogs ranged from 3 – 108 mon (26.15 ± 6.09 mon). When oocytes were categorized by donor age (Figs. 3.4 and 3.5) it is important to note that only 0.98% of the oocytes came from prepubertal dogs (<6 mon old), 31.37% came from juvenile dogs (6 – 11 mon old), 52.94% came from mature dogs (12 – 48 mon old), and 14.71% came from old dogs (>49 mon old). By the age of one year, dogs should be mature (i.e., have experienced the estrous cycle). At least two thirds (67.6%) of the oocytes ($n = 207$) used here came from a mature donor (1 – 9 years) capable of producing healthy viable oocytes. It is possible that some or all of the dogs that were 6 – 11 mon old ($n = 96$) were also mature, in that they had experienced the estrous cycle at least once. Therefore we conclude that most of the oocytes used for this study were from mature dogs that had cycled at least once and thus were capable of producing healthy oocytes.

Several conditions affected the oocyte yield. First, when possible, oocytes were collected from multiple donors of the same breed, but this depended on availability from the veterinary clinic. In our study, the multiple donors per breed included a Schnauzer ($n = 2$), a Wolf mix ($n = 2$), a Boxer ($n = 3$), and a German

Shepard ($n = 3$). Second, some canine donors yielded few COCs leaving fewer oocytes after stripping. Third, some COCs could not be stripped, leaving fewer oocytes to examine. Fourth, during fixation, dehydration and critical point drying, some oocytes were occasionally lost. We conclude that the oocytes used for this study are not biased towards any one dog breed or breed type and most are from mature large or small dogs (Figs. 3.1 – 3.4).

Effects of Canine Donor Characteristics on Oocyte Diameter

The diameter of fixed oocytes used in the study ranged from 56.92 – 119.09 μm with an average of $85.82 \pm 0.67 \mu\text{m}$. Oocyte diameter is a general indication of oocyte maturity. Living canine oocytes $<100 \mu\text{m}$ are unable to resume meiosis, while oocytes with larger diameters ($\sim 110 \mu\text{m}$) are capable of resuming meiosis *in vitro* (Hewitt and England 1998; Otoi *et al.*, 2000). Therefore, the effect of oocyte diameter on the various characteristics of the dog donors used in our study was statistically analyzed.

Breed and AKC Breed Type. Some individual dog breeds had a significant effect on oocyte diameter with the Chihuahua ($60.96 \pm 0.88 \mu\text{m}$) having the smallest oocyte diameter, and the Maltese ($105.61 \pm 2.15 \mu\text{m}$) having the largest (Fig. 3.6, Table 3.1). Not all dog breeds or AKC breed types had a significantly different oocyte diameter when compared to all the other breeds or AKC breed types; however, they all significantly differed from at least one breed or breed type (Tables 3.1 and 3.2). As shown in Fig. 3.7 and Table 3.2, the mean \pm SE oocyte diameter of the sporting dogs ($77.71 \pm 1.65 \mu\text{m}$) was

significantly smaller than all the other AKC breed types except the non-sporting dogs ($81.56 \pm 1.93 \mu\text{m}$). In addition, the hound group ($93.63 \pm 2.83 \mu\text{m}$) had a significantly larger oocyte diameter than the non-sporting group ($81.56 \pm 1.93 \mu\text{m}$). Therefore, donor breed can significantly affect oocyte diameter.

Donor Size. When the size (weight) of the donor (see Table 3.1 for grouping) was analyzed with respect to oocyte diameter (Fig. 3.8), it was found that the small dogs ($< 13 \text{ kg}$) had significantly smaller diameter oocytes ($83.00 \pm 1.35 \mu\text{m}$) than the large dogs ($> 23 \text{ kg}$) ($87.56 \pm 0.83 \mu\text{m}$). However, the medium size dogs ($13 - 23 \text{ kg}$) did not have oocytes of a significantly different diameter ($86.25 \pm 1.13 \mu\text{m}$) than either the small or large dogs. Therefore donor size (especially smaller dogs) significantly affected oocyte diameter.

Donor Age. The oocyte diameter for the dog donors of various ages is shown in Fig. 3.9. When donor age was compared to oocyte diameter, there were significant differences between the age groups (Table 3.3). However, there was no consistent pattern as to which oocytes were significantly larger or smaller when younger donors were compared to older donors. When the younger dogs ($\leq 2 \text{ years}$) were grouped into 3 month increments (Table 3.4), an overall trend could be seen that oocytes from older dogs ($16 - 24 \text{ mon}$) were significantly larger in diameter than those from younger dogs ($0 - 9 \text{ mon}$). When the oocyte diameter for the dog donors were grouped into the four categories (Fig. 3.10): prepubertal dogs ($<6 \text{ mon old}$, $73.85 \pm 7.34 \mu\text{m}$), juvenile dogs ($6 - 11 \text{ mon old}$, $79.12 \pm 1.22 \mu\text{m}$), mature dogs ($12 - 48 \text{ mon old}$, $87.79 \pm 0.7 \mu\text{m}$), and old dogs

(>49 months old, $93.79 \pm 1.68 \mu\text{m}$) a more definite trend was observed; the older the dog, the larger the average oocyte diameter. In these groups, there were significant differences (Table 3.5). The oocytes from prepubertal dogs were smaller than those from old dogs. The juvenile dogs' oocytes were smaller than both the mature and old dogs' oocytes. Oocytes from old dogs were significantly larger in diameter than those from the three younger groups. Therefore, donor age significantly affected oocyte diameter.

Surface Morphology of the Canine Zona Pellucida

By increasing the number of collected oocytes to over 300, we found that there were four general types (types I – IV) of ultrastructure of the canine zona pellucida. The type I zona pellucida was very smooth with a melted appearance at low (1,000X) and high (4,000X) magnification and had very few small pores or none at all (Fig. 3.11). The pores that were observed on the type I zona pellucida were usually less than $0.5 \mu\text{m}$ in diameter and were randomly spread out across the zona pellucida at low density. Since cumulus cell morphology was well-preserved (Fig. 3.11), we conclude that this zona pellucida type is not an artifact of preparation.

The type II zona pellucida was relatively smooth or even at low magnification, and at high magnification appeared fenestrated due to many round or elliptical pores (Fig. 3.12). The pores were at high density and often were conical and/or bifurcated as they neared the oolema, similar to Fig. 2.13. In addition, the type II zona pellucida appeared multi-layered (Fig. 3.12A').

At low magnification, the type III zona pellucida had a rough or uneven surface (Fig. 3.13A) as compared to type I and II oocytes (Figs. 3.11A, 3.12A). At high magnification, the type III zona pellucida was very rough and spongy or mesh-like (Fig. 3.13A'). It often had many pores that were less elliptical and more irregularly shaped with raised edges. The type III pores became bifurcated and occasionally conical as they penetrated the zona pellucida.

The zona pellucida of type IV had a rough surface at low magnification (Fig. 3.14A). At high magnification (Fig. 3.14A'), it was similar to the type III zona pellucida, except that it had many stringy filaments that often clogged and transversed the deeper pores, making the pores very difficult to discern. Because of these filaments, the type IV zona pellucida looked less compact than the other three zona pellucida types. A side-by-side comparison of all four zona pellucida types is shown at high and low magnification in Fig. 3.15.

All 306 oocytes used in the study were placed in these four categories of zona pellucida type (Fig. 3.16). Many (36.9%) of the oocytes ($n = 113$) had a type III zona pellucida. A large group (30.7%) were type II ($n = 94$) or type IV (28.8%, $n = 88$). Only 3.6% had a type I zona pellucida ($n = 11$). When type I oocytes are excluded, about one third of the oocytes were found in each category (31.9% type II, 38.3% type III, 29.8% type IV).

Effect of Canine Characteristics on Zona Pellucida Morphology

To determine the effects of canine donor characteristics on zona pellucida surface morphology, statistical comparisons were made for the four zona

pellucida types for each characteristic (dog breed, AKC breed type, dog size and the age of the dog). In addition, we analyzed the effect of oocyte diameter on the four zona pellucida types to determine if the zona pellucida ultrastructure was due in part to oocyte maturity.

Effect of Breed and AKC Breed Type on Zona Pellucida Morphology.

Figure 3.17 shows the effect of dog breed on the four different zona pellucida types identified in this study. Only 3.6% ($n = 1$) of all 28 breeds observed had only one type of zona pellucida (type III, Medium Mix), and 35.7% ($n = 10$) had two types with 50% of type III and IV, and 40% of type II and III. When the effect of the dog breed on the zona pellucida type was analyzed using Friedman's test, it was found that the breed does significantly effect the type of zona pellucida ($P < 0.05$). When the breeds were grouped into the AKC breed types (Fig. 3.18), three or more of the zona pellucida types were observed in 60.7% of the dog breeds: 46.4% have three zona pellucida types ($n = 13$), and 14.3% have all four types of zona pellucida. When the effect of AKC breed type on zona pellucida morphology was analyzed using a two-way ANOVA with age as a covariate, it was found that breed type did not significantly ($P > 0.05$) effect zona pellucida type. However, there was a significant ($P < 0.05$) variation within the breed types. For the analysis, the terrier group was dropped due to no replicates in the group. This indicates that zona pellucida morphology is highly variable within breeds.

Effect of Donor Size on Zona Pellucida Morphology. When the effect of breed size (weight) on zona pellucida structure was analyzed (Fig. 3.19), all four zona pellucida types were found in all weight categories. Chi-square analysis

indicated that breed size had no significant effect ($P > 0.05$) on the zona pellucida type.

Effect of Donor Age on Zona Pellucida Morphology. Figures 3.20 and 3.21 show the effects of canine donor age and reproductive maturity on zona pellucida morphology. All of the age (Fig. 3.20) and maturity (Fig. 3.21) groups had multiple zona pellucida types. Only 18.2% ($n = 2$) of the eleven age groups in Fig. 3.20A have only two types (types III, IV) of zona pellucida, 45.4% ($n = 5$) have at least three zona pellucida types, and 36.4% ($n = 4$) have all four zona pellucida types. When zona pellucida type was analyzed using a Friedman's test to compare the age groups for younger dogs and all dogs, it was found that the age of the donor did not significantly ($P > 0.05$) effect zona pellucida type. Only the prepubertal group (25%) had only two zona pellucida types, and both the juvenile and mature group (50%) had all four types of zona pellucida (Fig. 3.21). When the reproductive maturity groups were analyzed using a Friedman's test, it was found that the maturity of the donor did not significantly ($P > 0.05$) effect zona pellucida type.

Effect of Oocyte Diameter on Zona Pellucida Morphology. To determine whether the maturity of the oocyte (~size) had an effect on the surface morphology of the zona pellucida, Fig. 3.22 shows the average diameter of the canine oocytes grouped into the four zona pellucida types (Type I was $89.35 \pm 2.02 \mu\text{m}$, Type II was $87.40 \pm 1.13 \mu\text{m}$, Type III was $82.75 \pm 1.24 \mu\text{m}$, and Type IV was $87.62 \pm 1.06 \mu\text{m}$). The oocyte diameter had a significant effect ($P < 0.05$) on zona pellucida morphology as determined by a one-way ANOVA.

The Tukey post-hoc test showed that only the Type III oocytes were significantly smaller than the Type II and Type IV oocytes. The Type I oocytes were not significantly different from any of the other mean oocyte diameters. This indicates that smaller oocytes tended to exhibit the type III zona pellucida.

D. DISCUSSION

In our scanning electron microscopic study, four different types of zona pellucida surface morphologies were observed. This is consistent with several studies that have shown at least two or more zona pellucida types in a variety of mammals: a net-like version, and a more compact smooth version (Calafell *et al.*, 1992; Familiari *et al.*, 1989, 2001; Magerkurth *et al.*, 1999; Vanroose *et al.*, 2000). Magerkurth *et al.* (1999) reported four different zona pellucida types for human oocytes: two porous types, a rough type, and a smooth type. Familiari *et al.* (2001) also reported multiple zona pellucida types for human oocytes: a porous netlike zona pellucida, and a smooth compacted zona pellucida. Two types of bovine zona pellucida have also been reported: a spongy surface with many pores, and a more compacted structure with fewer, larger pores (Vanroose *et al.* 2000). Familiari *et al.* (1989) reported that the mouse had two different zona pellucida types: one type had fine structural organization, and the other was a compact structure lacking the detail of the first type. In contrast, Calafell *et al.* (1992) observed six different types of zona pellucida in the mouse: two fibrous and porous types, a smooth type with shallow pores, an unstructured type with a significant amount of cellular debris, a rough type with only a few pores,

and a flat type without any cellular debris. Therefore our findings of four different types of zona pellucida are consistent with that reported for other species.

The changes in zona pellucida morphology have been correlated with oocyte maturation in the mouse, pig and cow (Calafell *et al.*, 1992; Funahashi *et al.*, 2000; Jackowski and Dumont, 1979; Suzuki *et al.*, 1994, 2000; Vanroose *et al.*, 2000), but not in the human (Magerkurth *et al.*, 1999). It is unclear whether the zona pellucida types we observed relate to canine oocyte maturity; however, we used a relatively uniform oocyte size that suggests that most oocytes were at the germinal vesicle stage (although we did not directly test this). Several studies using lectin histochemistry have shown variations in the presence and distribution of carbohydrate residues in the zona pellucida during folliculogenesis in several mammals (hamster, rat, cat, rabbit, boar) including the dog (see Parillo *et al.*, 2005). It is not understood whether these alterations in carbohydrates contribute to the zona pellucida types we have observed.

Different types of canine zona pellucida were also seen by Ström Holst *et al.* (2000); however, the zonae pellucidae shown resemble our type III group only. They attributed the differences to the storage methods of the oocytes, whether they were fresh, salt-stored or frozen. They did not look at any other contributing factors to the zona pellucida types. Because of the great heterogeneity in zona pellucida morphology that we report, we urge strong caution in interpreting any data that examines the effects of treatment(s) on the canine zona pellucida – the heterogeneity is too great before treatment to be assured that the effects seen are due only to the treatment. Thus this reflects

another difference between canine reproductive biology and other mammals (mouse, pig, cow).

It is interesting to note that only about four percent of the oocytes in our study had a Type I zona pellucida, which was smooth with a low density of small pores randomly located around the zona pellucida. In many of the publications on zona pellucida types of other mammals, a smooth, unstructured, compact zona pellucida with or without pores is mentioned. Some of the groups (Calafell *et al.*, 1992; Familiari *et al.*, 1988, 1989) thought that this type of zona pellucida was from atretic or degenerating oocytes. Magerkurth *et al.* (1999) also observed a smooth type zona pellucida that occurred infrequently (3.62%). So in our study, the oocytes with a smooth zona pellucida (type I) might be atretic; however, we tried to avoid atretic oocytes by only using dark oocytes with a homogeneous cytoplasm and at least three complete layers of cumulus cells. If COCs were collected at the beginning of deterioration, these COCs might have looked healthy with the light microscope and this may explain why there were so few canine oocytes with the Type I zona pellucida. This needs to be investigated further.

In our study, we examined several characteristics of the canine ovary donors including breed, AKC breed type, breed size (weight), dog age, and reproductive maturity to determine their possible effects on oocyte diameter and/or zona pellucida morphology. In addition, we compared oocyte diameter to zona pellucida type to determine if zona pellucida morphology was based on maturity of the oocyte.

Effect of Breed and AKC Breed Type. There was a significant effect of breed and breed type on oocyte diameter. The four zona pellucida types were observed in the different dog breeds, and we found that the zona pellucida type is dependent on the breed of dog, but not the type of dog. Durrant *et al.* (1998) reported that purebred dogs have less antral follicles than mixed breed dogs. They explained this was due most likely to inbreeding and lack of genetic variation in pure bred dogs, whereas mixed breed dogs have more genetic variation allowing for more viable and healthy follicles. Specific purebred versus mixed breed dogs were not examined in our study, but it would be interesting to analyze the effect of mixed breed versus specific purebred dogs on zona pellucida characteristics, especially in light of purebred dogs having fewer pups.

Effect of Breed Size. When the donors were grouped into breed size (weight), oocyte diameter was significantly larger in large dogs than in small dogs, but zona pellucida type was independent of breed size. The relationship of donor size to oocyte size and ultrastructure of the zona pellucida has not been reported for other mammals so it is unclear if this is a common occurrence. Durrant *et al.* (1998) and Ström Holst *et al.* (2001) both reported that canine body weight has no effect on the number of follicles collected, and the maturity of those follicles.

Effect of Donor Age. When donors were grouped into categories by age in mon and reproductive maturity, the older and more mature dogs had larger oocytes than younger dogs suggesting that older and more mature dogs are able to produce more mature oocytes (using the oocyte diameter as a general

indicator). When the age of the donors was compared to the zona pellucida type, it appeared that the age of the donor has no significant effect on what type of zona pellucida was produced. Significant age effects have been observed for oocytes and follicles in other studies. Durrant *et al.* (1998) reported that they were able to collect the highest quantity of the most mature follicles and oocytes from their older dogs (>48 mon). In contrast, Ström Holst *et al.*, (2001) reported that they found twice as many oocytes in the young dogs (<7 years) than they did in the old dogs (>7 years). This difference could be do to the age categories they used, because Durrant *et al.* (1998) considered dogs to be old at 4 years, whereas Ström Holst *et al.*, (2001) used 7 years as the distinction for old dogs. It is possible that somewhere from age four to seven that the reproductive health of a dog begins to significantly decline and that is why there were conflicting reports. Hewitt and England (1998) reported that they were able to mature oocytes *in vitro* from old dogs (>7 years), but that their ability to mature was reduced compared to oocytes from younger dogs (<7 years). Several studies have shown that dogs of breeding age (7 – 48 mon) have higher rates of *in vitro* meiotic maturation than older dogs (Bolamba *et al.*, 1992; Durrant *et al.*, 1998; Goodrowe *et al.*, 2000; Hewitt and England, 1998). That we used oocytes from dogs that averaged 28 ± 4.56 mon, suggests that the oocytes were functionally competent to resume meiosis (although we did not test this directly).

Effect of Oocyte Diameter. Oocyte diameter has been used as a general indicator of oocyte maturity (Otoi *et al.*, 2000; Hewitt and England, 1998). In our study, oocytes with the type III zona pellucida were significantly smaller than

those with type II and type IV, but not type I zona pellucida. This suggests that the type III zona pellucida is from more immature oocytes than the type II and type IV oocytes. Interestingly, the type III oocytes do not significantly differ in size from the type I oocytes.

As indicated earlier, several studies have reported that the ultrastructure of the zona pellucida changes as the oocyte undergoes meiotic maturation and fertilization in the mouse (Calafell *et al.*, 1992), cow (Suzuki *et al.*, 1994; Vanroose *et al.*, 2000), pig (Funahashi *et al.*, 2000; Suzuki *et al.*, 2000) and human (Familiari *et al.*, 1988, 2001). In light of these studies, and our results showing canine oocytes with a type III zona pellucida are significantly smaller than type II and IV, we suggest that type III oocytes may be the most immature oocytes, type II and IV the most mature. The type I oocytes are possibly from early atretic follicles due to the "melted" look of the zona pellucida and the fact that they were observed in such low numbers. This would need to be directly tested.

In conclusion, there was a significant effect of the dog breed, AKC breed type, size of the donor, and dog age on oocyte diameter. We report for the first time four zona pellucida surface morphologies (type I – IV) with type III being the most common. There was a significant effect of dog breed on zona pellucida morphology with great heterogeneity between breeds and individuals of the same breed. There was no correlation of AKC breed type, donor size, dog age or reproductive maturity on zona pellucida ultrastructure. Type III oocytes were smaller than the others suggesting they may be the most immature. It is

anticipated that this ultrastructural study allows the three-dimensional surface of the zona pellucida to be investigated during future studies of gamete interactions during fertilization.

Table 3.1. Relationship between oocyte diameter and canine breed.

Breed of Dog	Breed Size*	Significant Mean Difference with Breeds [†]
1. American Bulldog	Large	4, 6, 7, 11, 14, 16, 17, 19, 20, 22, 24, 28
2. Beagle	Small	7, 9, 17, 18
3. Bernese Mountain Dog	Large	4, 6, 11, 16, 17, 19, 20, 28
4. Bichon Frise Mix	Small	1, 3, 5, 7, 8, 9, 15, 18, 21, 23, 25, 26, 27
5. Blue Healer	Medium	4, 7, 9, 11, 16, 17, 19, 20, 28
6. Boxer	Large	1, 3, 7, 8, 9, 15, 17, 18, 25
7. Chihuahua	Small	1, 2, 4-8, 10-17, 19-24, 26-28
8. Chow Chow	Large	4, 6, 7, 11, 16, 17, 19, 20, 28
9. Cocker Spaniel Mix	Small	2, 4-6, 10-17, 19-24, 26-28
10. Doberman Pinscher	Large	7, 9, 16-18
11. German Shepard	Large	1, 3, 5, 7-9, 15, 17, 18, 21, 23, 25, 26
12. Golden Retriever	Large	7, 9, 17, 18
13. Siberian Husky Mix	Medium	7, 9, 16-19
14. Jack Russel Terrier	Small	1, 7, 9, 18, 25
15. Labrador Retriever Mix	Large	4, 6, 7, 9, 11, 16-20, 28
16. Lab-St. Bernard Mix	Large	1, 3, 5, 7-10, 13, 15, 18, 21, 23, 25-27
17. Maltese	Small	1, 2, 3, 5, 6-13, 15, 18, 21-27
18. Medium Mix	Medium	2, 4, 6, 10-20, 22-24, 26-28
19. Pit Bull	Large	1, 3, 5, 7-9, 13, 15, 18, 21, 23, 25-27
20. Rhodesian Ridgeback	Large	1, 3, 5, 7-9, 15, 18, 21, 23, 25-27
21. Rottweiler	Large	4, 7, 9, 11, 16, 17, 19, 20, 28
22. Schanauzer	Medium	1, 7, 9, 17, 18, 25
23. Shetland Sheepdog Mix	Small	4, 7, 9, 11, 16-20
24. Shepard-Collie Mix	Large	1, 7, 9, 17, 18, 25
25. Shiba Inus Mix	Small	4, 6, 11, 14, 16, 17, 19, 20, 22, 24, 28
26. Shih Tzu	Small	4, 7, 9, 11, 16-20, 28
27. Wolf Mix	Large	4, 7, 9, 16-20
28. Yorkshire Terrier	Small	1, 3, 5, 7-9, 15, 18, 21, 25, 26

*Small <13 kg, Medium 13-23 kg, Large >23 kg.

[†]Differences between oocyte diameter from breeds shown were found using a one-way ANOVA and Tukey post-hoc test for individual comparisons at a significance of $P<0.05$.

[†]Breed differences are indicated by only their number.

[†]See Fig. 3.1 for number of oocytes examined for each breed, and Fig. 3.6 for actual average oocyte diameters.

Table 3.2. Relationship between oocyte diameter and AKC donor breed type.

AKC Breed Type	Mean Oocyte Diameter [†]	Significant Mean Difference with Other Breed Types [‡]
1. Herding	88.38 ± 1.18	Sporting
2. Hound	93.63 ± 2.83	Non-Sporting, Sporting
3. Non-Sporting	81.56 ± 1.93	Hound
4. Sporting	77.71 ± 1.65	Herding, Hound, Terrier, Toy, Working, Miscellaneous
5. Terrier	92.03 ± 2.31	Sporting
6. Toy	85.79 ± 2.45	Sporting
7. Working	87.29 ± 0.94	Sporting
8. Miscellaneous	88.94 ± 2.11	Sporting

[†]Mean ± SE (µm).

[‡]Differences between oocyte diameters from the American Kennel Club (AKC) breeds were found using a one-way ANOVA and Tukey post-hoc test at a significance level of $P < 0.05$.

[‡]See Fig. 3.2 for numbers of oocytes per breed type, and Fig. 3.7 for actual average oocyte diameters.

Table 3.3. Relationship between oocyte diameter and canine age (all dogs).

Age Groups of Donors*	Mean Oocyte Diameter [†]	Significant Mean Differences with Donors [‡]
1. 0 – 6 Months	81.13 ± 1.38	3-5, 7, 8, 11
2. 7 – 12 Months	83.36 ± 0.94	3-5, 7, 8, 10, 11
3. 13 – 18 Months	88.79 ± 2.15	1, 2, 8
4. 19 – 24 Months	93.94 ± 1.00	1, 2, 6, 8
5. 25 – 30 Months	91.85 ± 1.81	1, 2, 8
6. 31 – 36 Months	84.12 ± 1.50	4, 7, 8, 11
7. 43 – 48 Months	98.26 ± 3.64	1, 2, 6
8. 49 – 54 Months	105.61 ± 2.62	1-6, 9, 10
9. 67 – 72 Months	88.08 ± 1.01	8
10. 79 – 84 Months	87.29 ± 2.49	2, 8, 11
11. 103 – 108 Months	99.59 ± 0.86	1, 2, 6, 10

*Oocyte donors were not available for analysis for dogs aged 37 – 42, 55 – 66 and 85 – 102 months.

[†]Mean ± SE (µm).

[‡]Age groups differences are indicated by only their number.

[‡]Differences between oocyte diameters from the age groups were found using a one-way ANOVA and Tukey post-hoc test at a significance level of $P < 0.05$.

[‡]See Fig. 3.4A for numbers of oocytes per age group.

Table 3.4. Relationship between oocyte diameter and canine age (young dogs).

Age Groups of Donors*	Mean Oocyte Diameter [†]	Significant Mean Differences with Donors [‡]
1. 0 – 3 Months	73.85 ± 7.34	6, 7
2. 4 – 6 Months	81.13 ± 1.38	3, 5, 6, 7
3. 7 – 9 Months	75.15 ± 1.71	2, 4, 5, 6, 7
4. 8 – 12 Months	83.36 ± 0.94	3, 7
5. 16 – 18 Months	88.79 ± 2.15	2, 3
6. 19 – 21 Months	92.55 ± 1.45	1-3
7. 22 – 24 Months	94.32 ± 1.21	1-4

*Oocyte donors were not available for analysis for dogs aged 13 – 15 months.

[†]Mean ± SE (µm).

[‡]Age groups differences are indicated by only their number.

[‡]Differences between oocyte diameters from the age groups were found using a one-way ANOVA and Tukey post-hoc test at a significance level of $P < 0.05$.

[‡]See Fig. 3.4B for numbers of oocytes per age group.

Table 3.5. Relationship between oocyte diameter and canine reproductive maturity.

Age Group*	Mean Oocyte Diameter [†]	Significant Mean Differences [‡]
Prepubertal	73.85 ± 7.34	Old
Juvenile	79.12 ± 1.22	Mature, Old
Mature	87.79 ± 0.72	Juvenile, Old
Old	93.79 ± 1.68	Prepubertal, Juvenile, Mature

*Prepubertal <6 mon, Juvenile 6 – 11 mon, Mature 12 – 48 mon, Old >48 mon.

[†] Mean ± SE (µm).

[‡]Differences between oocyte diameters from the reproductive maturity groups were found using a one-way ANOVA and Tukey post-hoc test at a significance level of $P < 0.05$.

[‡]See Fig. 3.5 for numbers of oocytes per age group.

Fig. 3.1. Oocyte distribution by canine donor breed. The pie graph shows the number of oocytes collected per given breed. The name of the canine breed is followed by the number of oocytes used in the study from that given breed. Some dogs were pure bred and others were mixed breeds as indicated by "Mix" following the breed name. Some of the breeds had multiple donors contribute oocytes (Schnauzer, $n = 2$; Wolf mix, $n = 2$; Boxer, $n = 3$; German Shepard, $n = 3$). Twenty eight different dog breeds were used in this study, with a mean \pm SE of 10.9 ± 1.2 oocytes per breed. This shows that the oocytes came from a large variety of dog breeds, and the study does not focus on a specific breed.

Fig. 3.1.

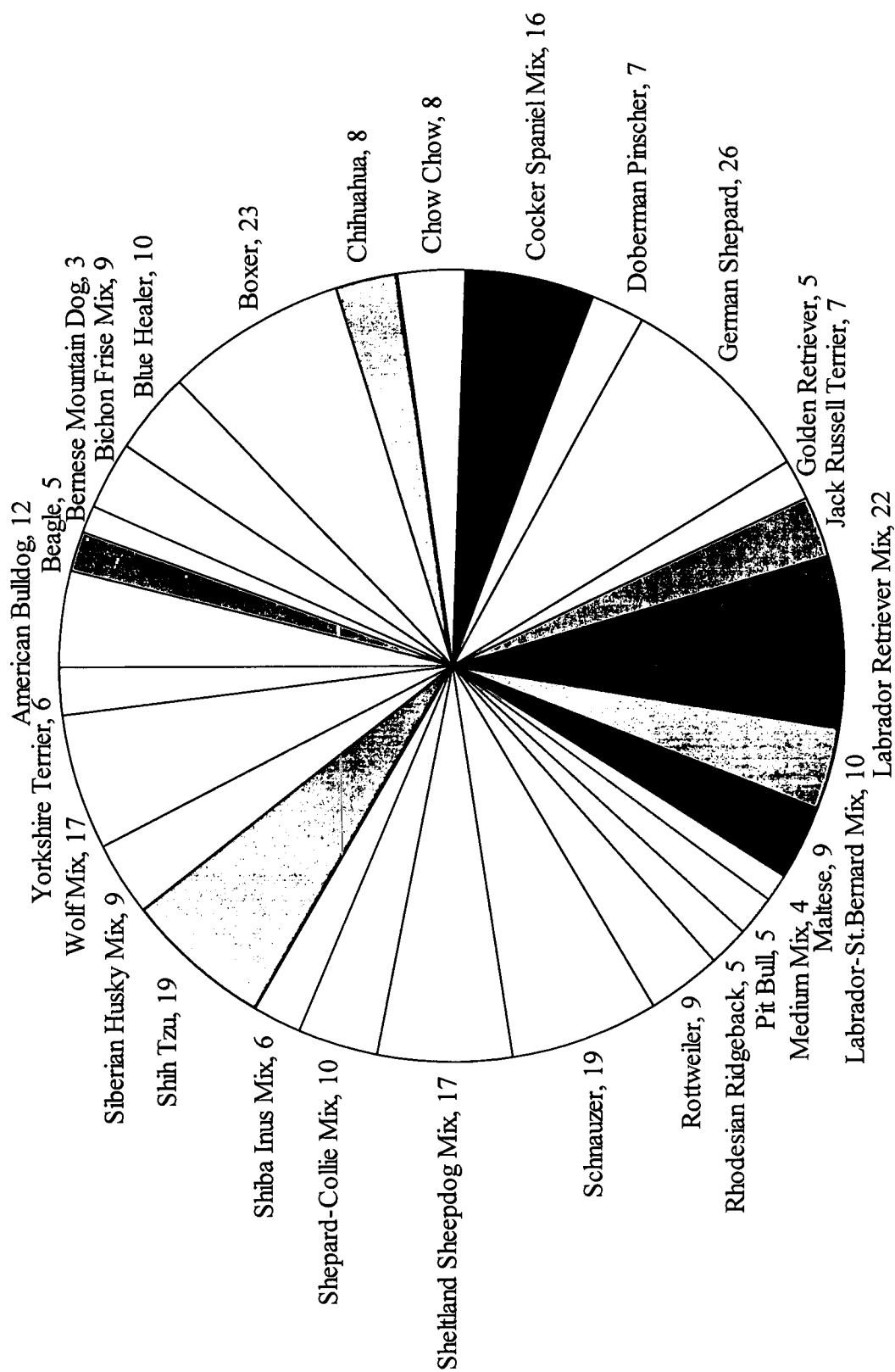


Fig. 3.2. Oocyte distribution by AKC donor breed type. The pie graph shows the number of oocytes per given breed type based on the classification scheme used by the American Kennel Club (AKC). The name of the breed type is followed by the number of oocytes used in the study from that given breed type. Eight different breed types were used in this study, with a mean \pm SE of 36.7 ± 7.8 oocytes examined per breed type. This shows that the oocytes came from a wide variety of dog breed types, and no more than 22% focuses on a dog type bred to do one specific activity (e.g., Working dog).

Fig. 3.2.

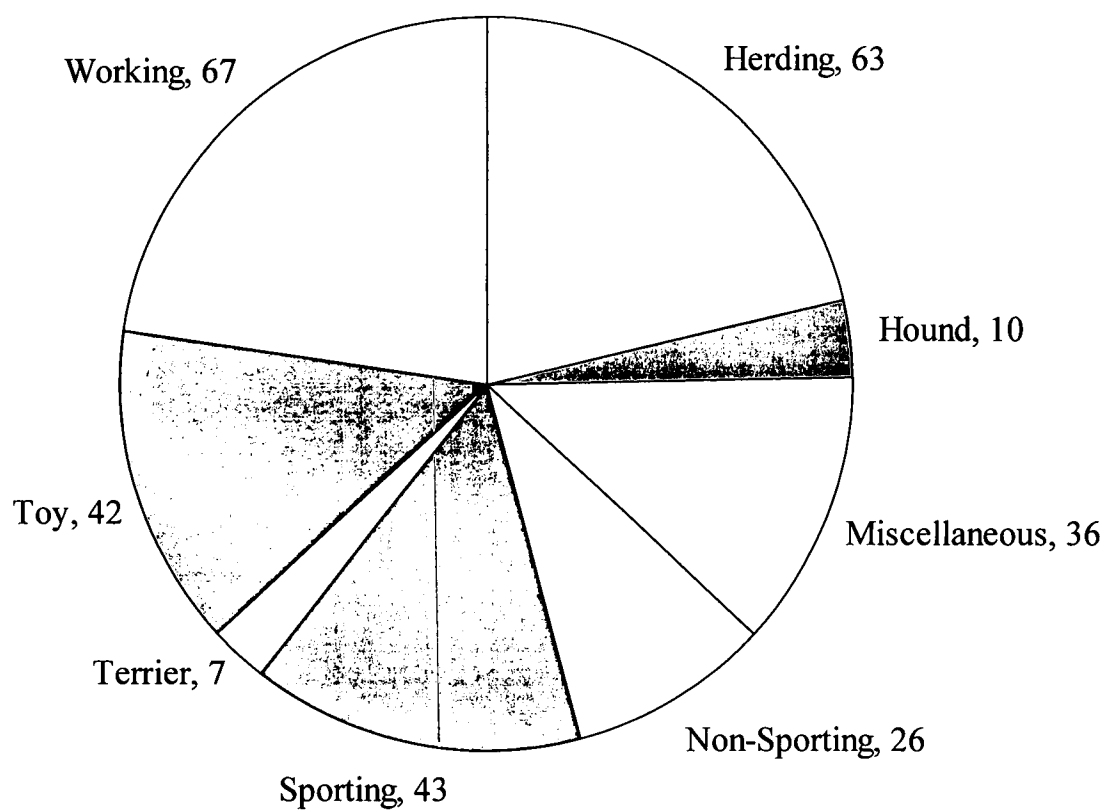


Fig. 3.3. Oocyte distribution by canine donor size. The pie graph shows the number of oocytes collected per donor size. Dog weights were classified as small <13 kg (<30 lb), medium 13 – 23 kg (30 – 50 lb), and large >23 kg (>50 lb). The breed size is followed by the number of oocytes used in the study from that given breed size. Of the three breed sizes, a mean \pm SE of 102 ± 34.6 oocytes were observed per breed size. This shows that the oocytes came from different-sized dogs with a variety of weights.

Fig. 3.3.

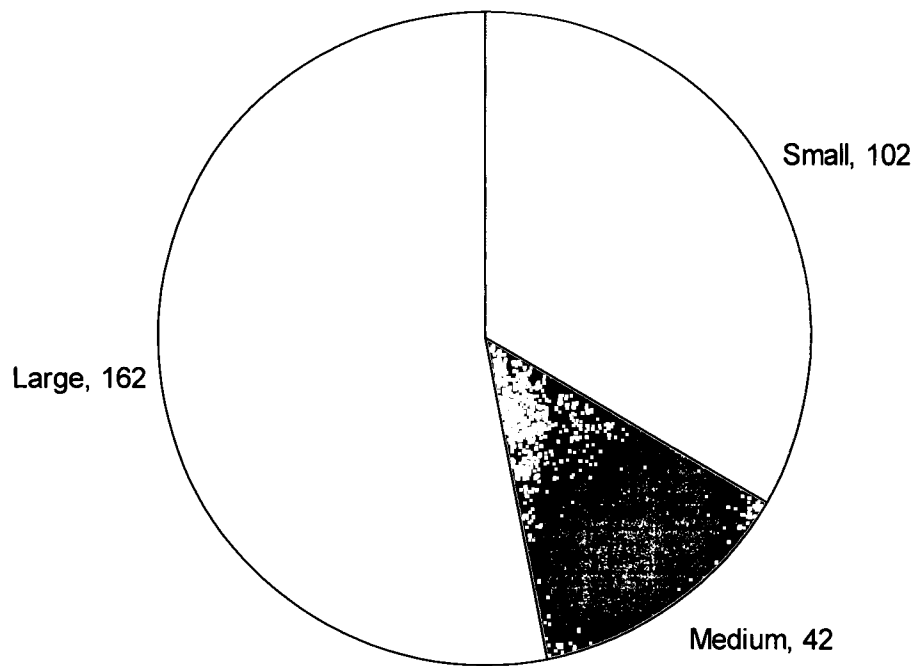


Fig. 3.4. Oocyte distribution by canine donor age. Graph A shows the number of oocytes from each age group of donors categorized by six months. Some of the age groups had multiple donors contribute oocytes, and no donors were available for others. Graph B breaks down the oocyte distribution for the donors that are two years or younger into three months. This shows that the largest group of oocytes in graph A (7 – 12 mon) were collected from mostly older (10 – 12 mon) donors (graph B), which have possibly reached reproductive maturity.

Fig. 3.4.

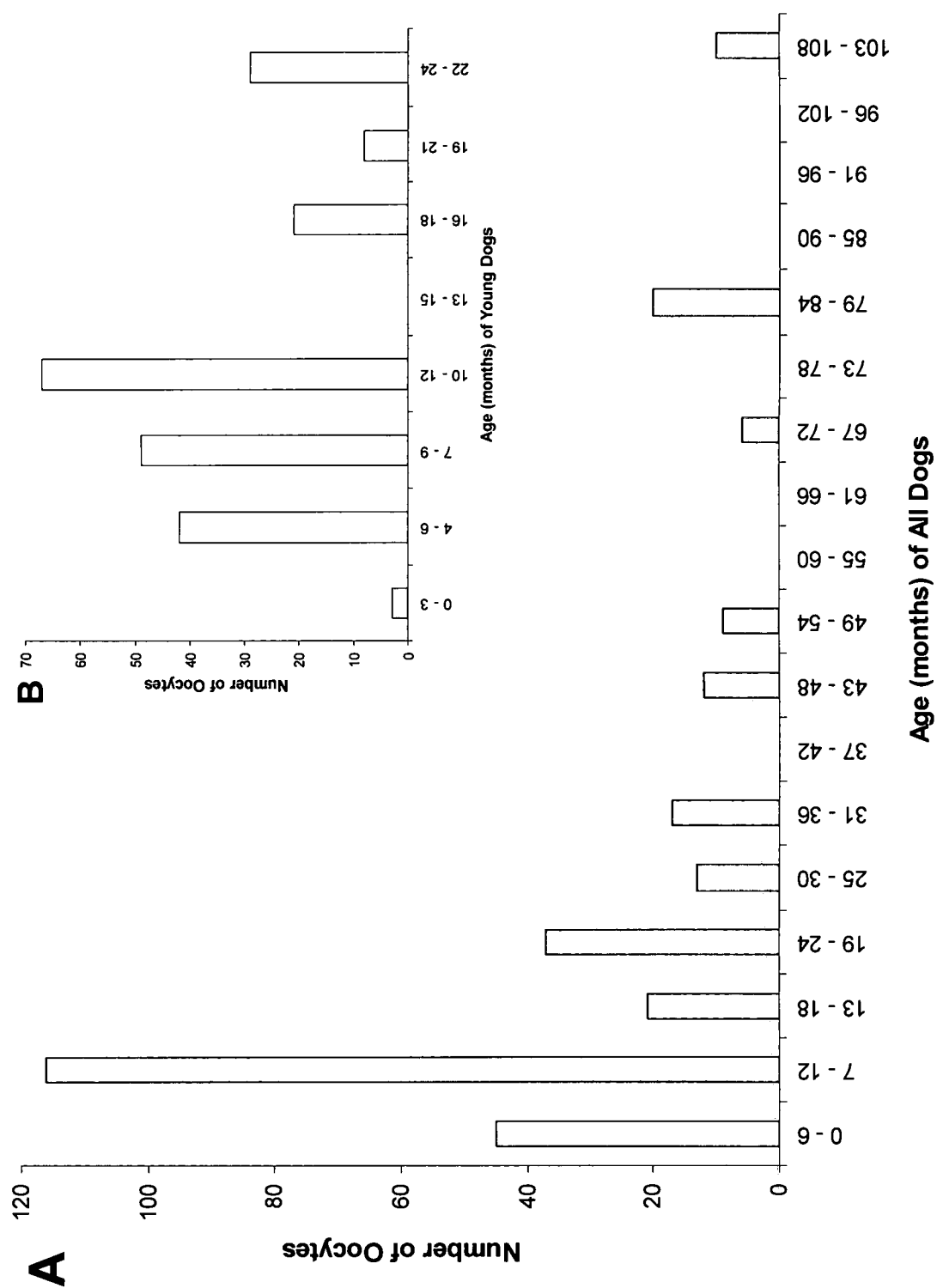


Fig. 3.5. Oocyte distribution by canine reproductive maturity. The pie graph shows the number of oocytes collected from each age group. Dogs were grouped according to their maturity: prepubertal (<6 mon), juvenile (6 – 11 mon), mature (12 – 48 mon), and old (>48 mon). This graph shows that oocytes were collected from donors with a variety of ages and 68% of the oocytes ($n = 207$) came from dogs that have reached maturity (≥ 1 yr) and are capable of producing healthy viable oocytes.

Fig. 3.5.

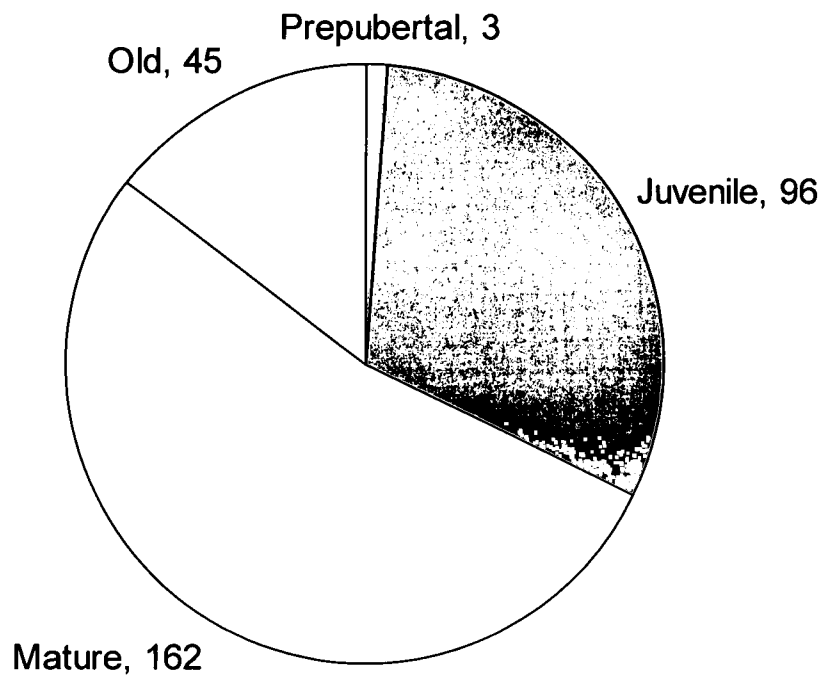


Fig. 3.6. Effect of canine donor breed on oocyte diameter. This graph shows the mean \pm SE of oocyte diameters for each of the dog breeds. The oocytes ranged from 56.92 to 119.09 μm with an average of $85.82 \pm 0.67 \mu\text{m}$ (mean \pm SE). See Fig. 3.1 for the number of oocytes examined in each breed, and Table 3.1 for statistical comparisons.

Fig. 3.6.

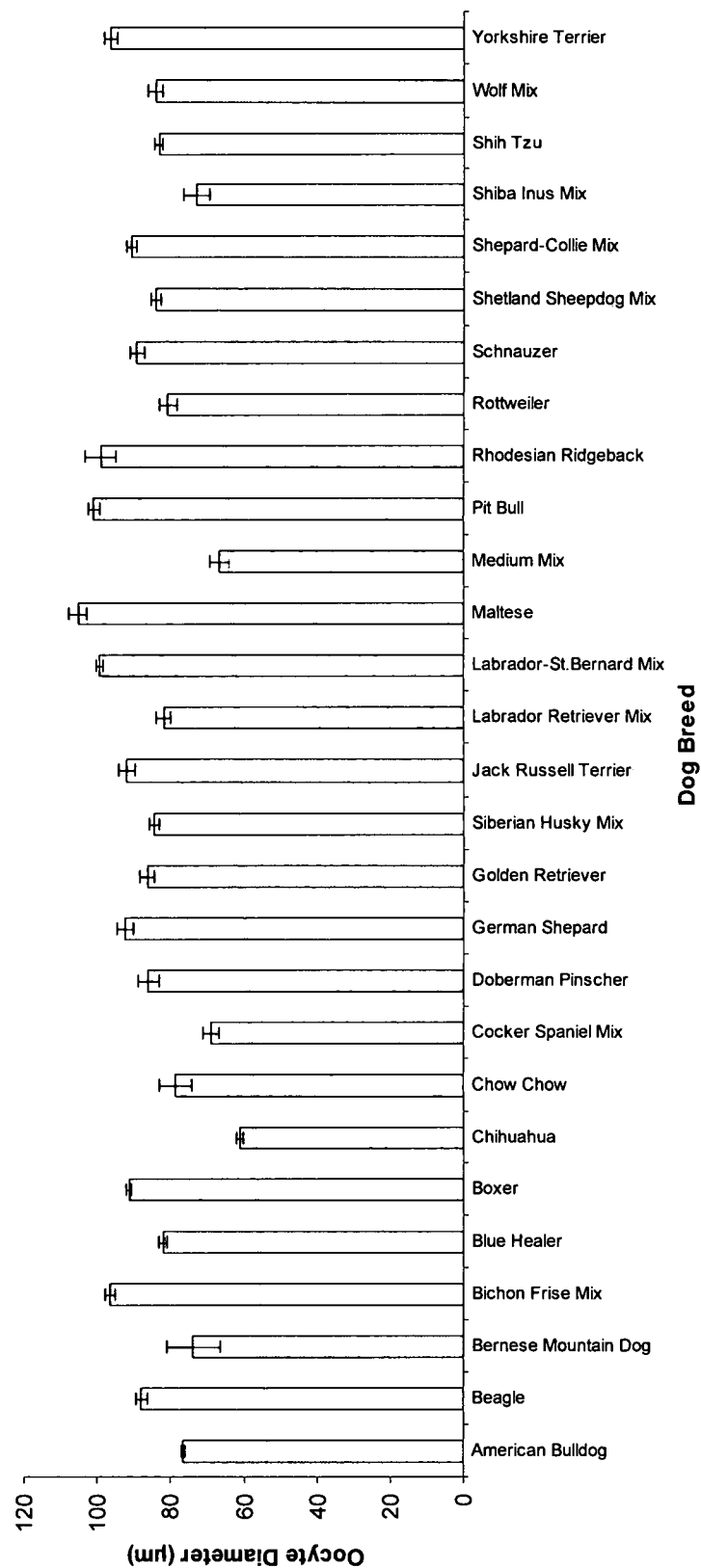


Fig. 3.7. Effect of AKC donor breed type on oocyte diameter. This graph shows the mean \pm SE of the oocyte diameter for each of the dog breed types of the American Kennel Club (AKC). See Fig. 3.2 for numbers of oocytes in each group, and Table 3.2 for statistical comparisons.

Fig. 3.7.

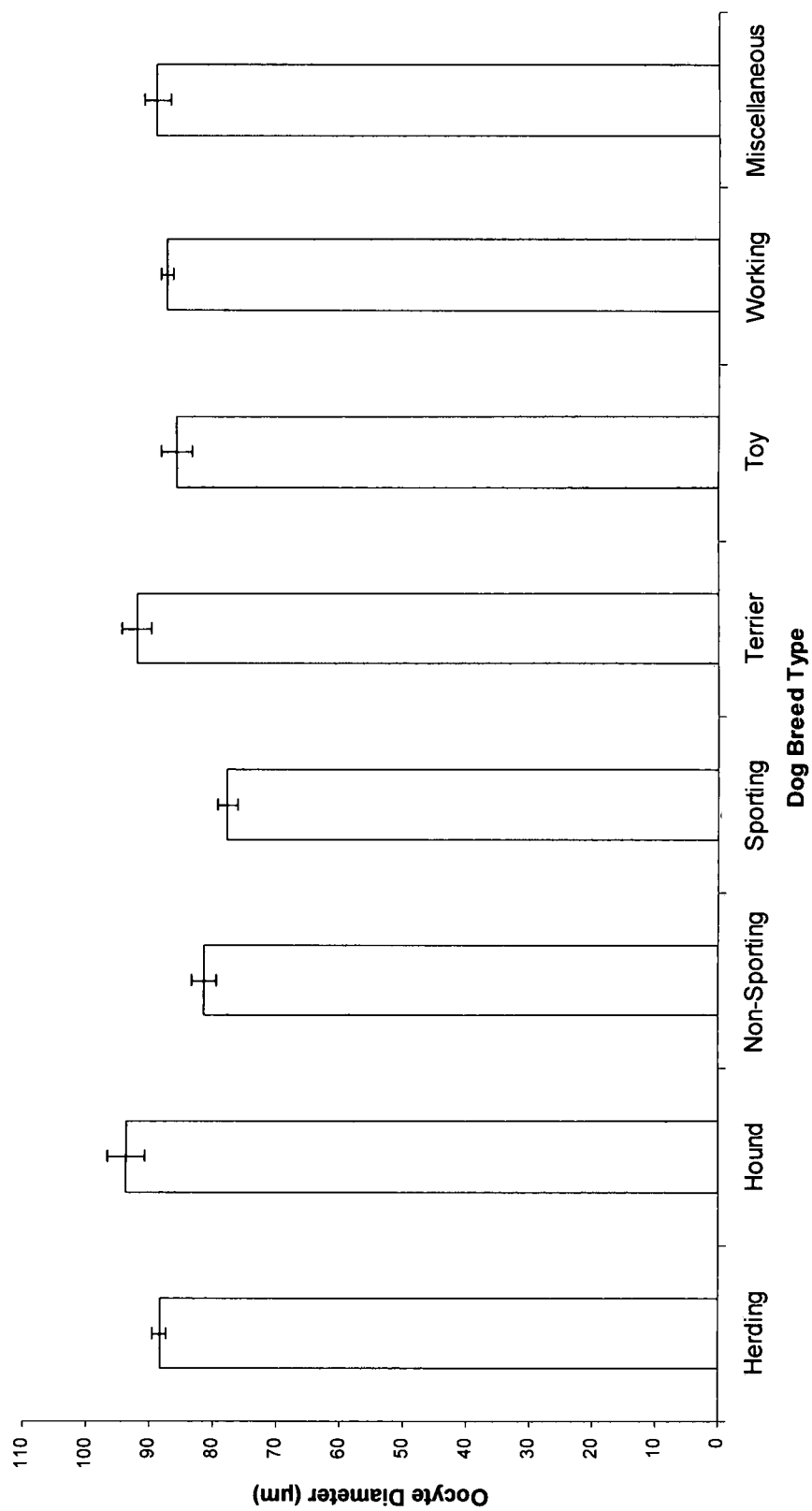


Fig. 3.8. Effect of canine donor size on oocyte diameter. This graph shows the mean \pm SE of the oocyte diameter for each of the dog breed sizes: small <30 lbs, medium 30 – 50 lbs, and large > 50 lbs dogs. See Fig. 3.3 for the number of oocytes examined in each category. The mean diameter of the oocytes for each dog breed size was taken and statistically compared using a one-way ANOVA and Tukey post-hoc test at a significance level of $P < 0.05$. Oocytes from small dogs were significantly smaller than those from large dogs as indicated by the asterisk. Oocytes from medium dogs were not statistically different from either the small or large dog oocytes.

Fig. 3.8.

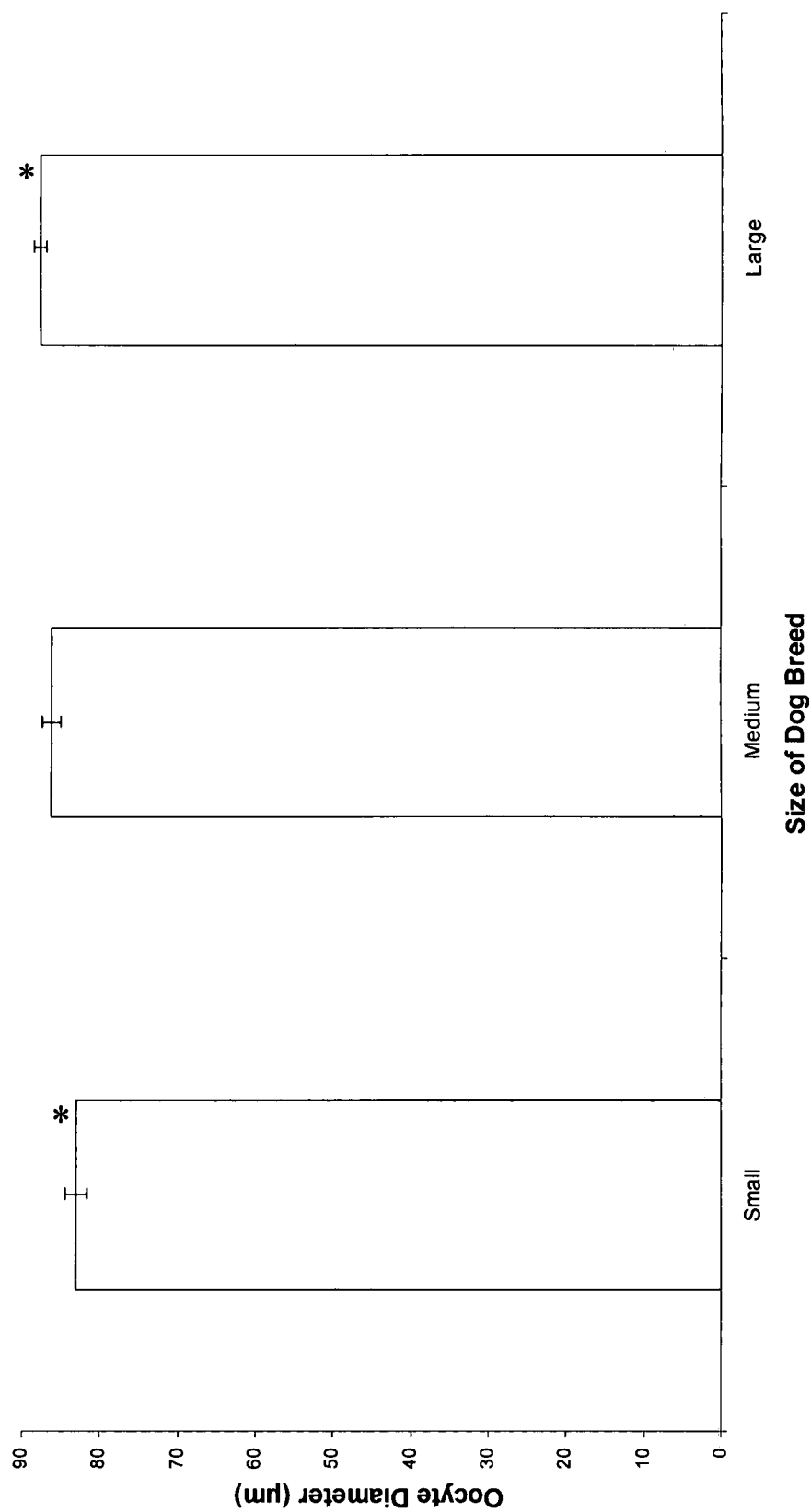


Fig. 3.9. Effect of canine donor age on oocyte diameter. The average diameter (mean \pm SE) of the oocytes for each donor age group is shown. Graph A shows the age distribution every 6 months for all dogs. Graph B shows the age distribution every 3 months for the dogs two years and younger. See Fig. 3.4 for the number of oocytes examined in each category, and Tables 3.3 (all dogs) and 3.4 (young dogs) for statistical comparisons.

Fig. 3.9.

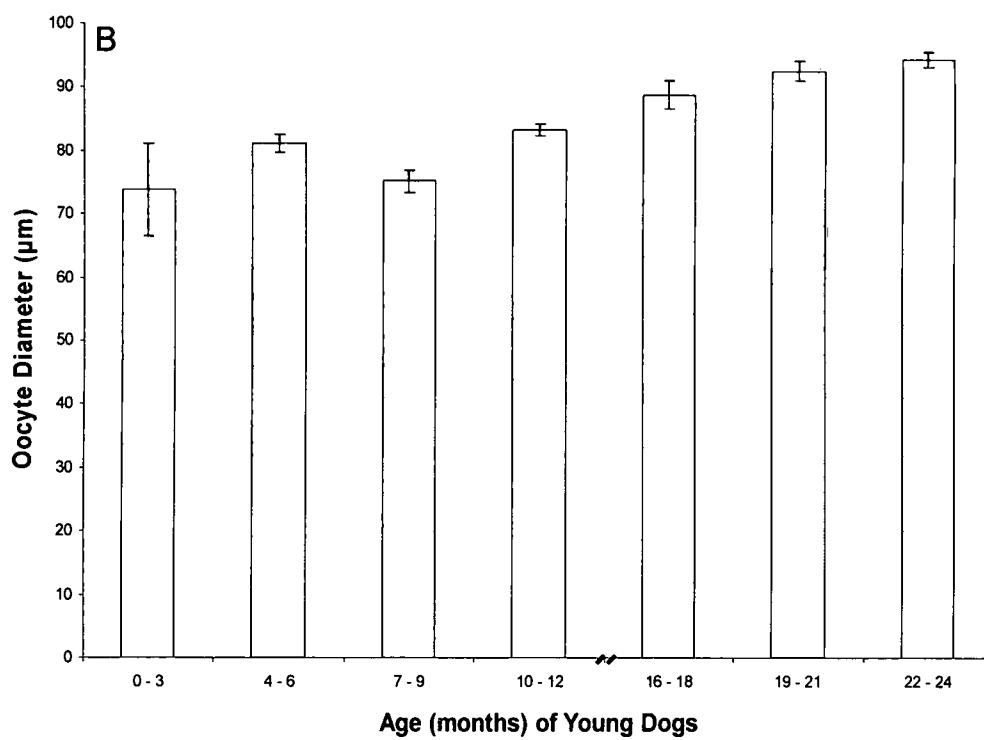
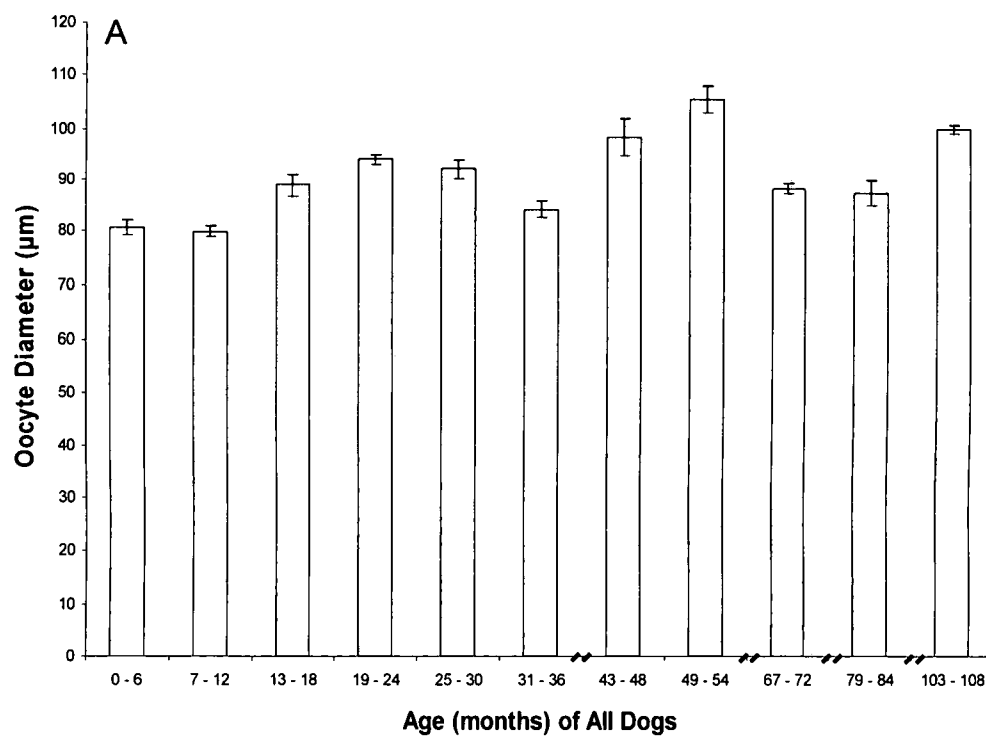


Fig. 3.10. Effect of canine reproductive maturity on oocyte diameter. The average diameter (mean \pm SE) of the oocytes for each donor age group is shown. Dogs were grouped according to their reproductive maturity: prepubertal (<6 mon), juvenile (6 – 11 mon), mature (12 – 48 mon), and old (>48 mon). See Fig. 3.5 for the number of oocytes examined in each category, and Table 3.5 for statistical comparisons.

Fig. 3.10.

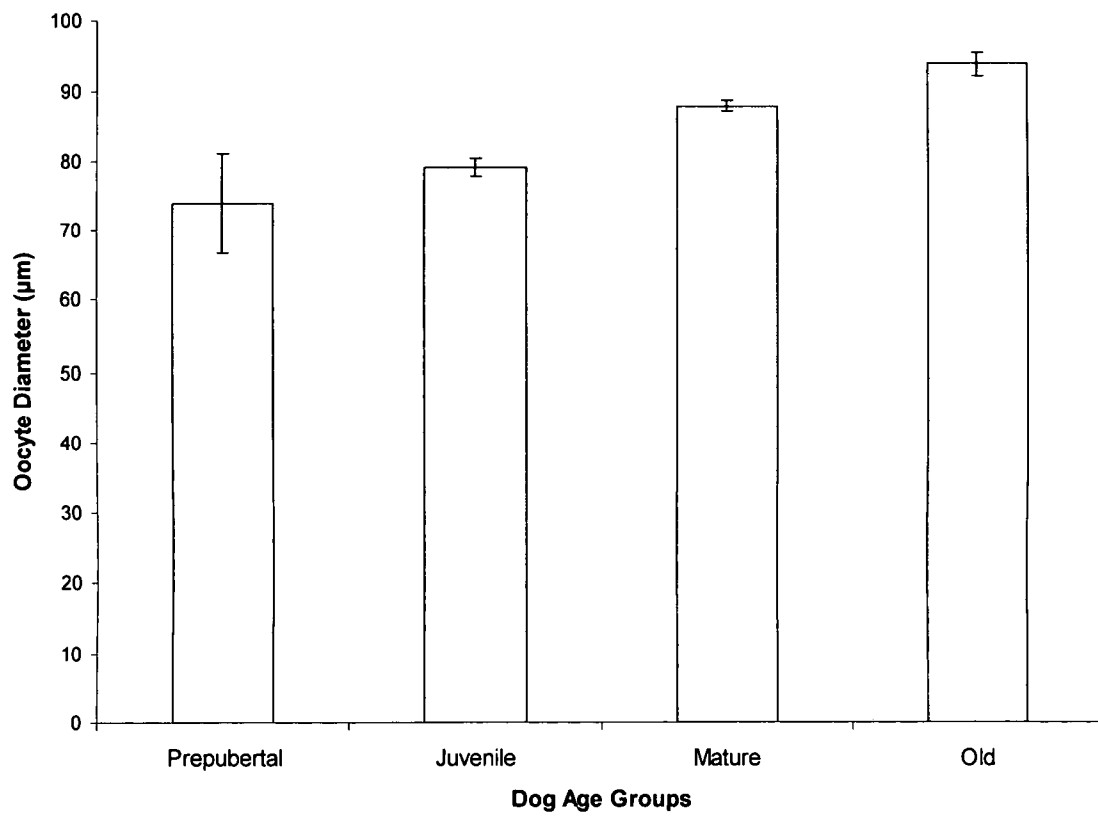


Fig. 3.11. Canine oocyte with a type I zona pellucida. The two images are of the same German Shepard oocyte at low (A, 1,000X) and high (A', 4,000X) magnification showing the Type I zona pellucida, which has a smooth surface at both magnifications. The oocyte is 98 μm in diameter and had cumulus cells still attached to the right side of the oocyte. Pores are barely visible at low magnification and are very small ($<1 \mu\text{m}$) in A'. Scale bar represents 10 μm in A and 5 μm in A'.

Fig. 3.11.

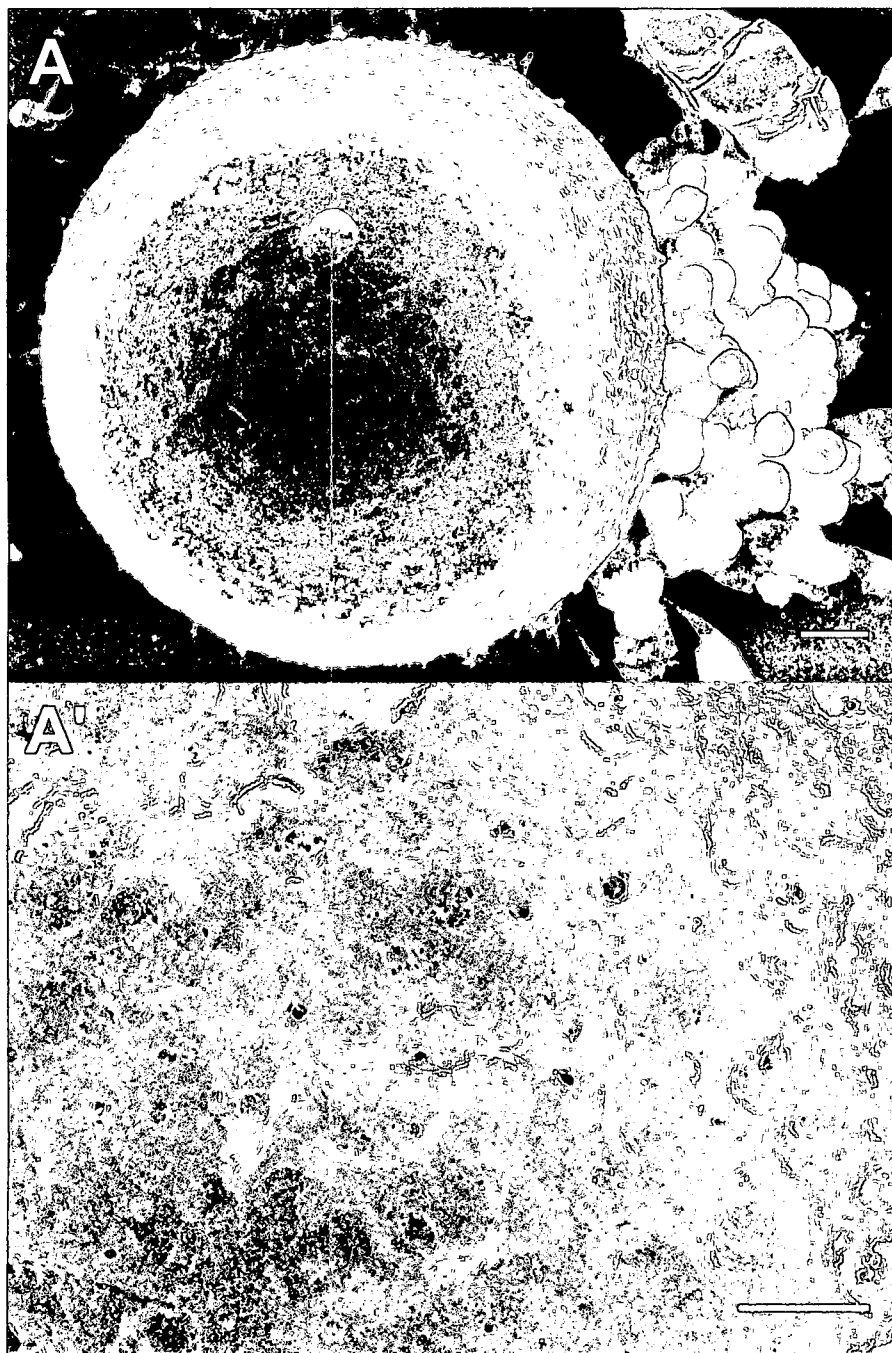


Fig. 3.12. Canine oocyte with a type II zona pellucida. The two images are of the same Boxer oocyte at low (A, 1,000X) and high (A', 4,000X) magnification. The oocyte is 92 μm in diameter. The type II zona pellucida has a relatively smooth surface at low magnification and a rougher appearance at high magnification. The enlargement in A' shows a fenestrated and layered surface which has many round or elliptical pores and hollows. Some pores have smaller pores deeper within them, and other pores bifurcate deep in the zona pellucida. Scale bar represents 10 μm in A and 5 μm in A'.

Fig. 3.12.

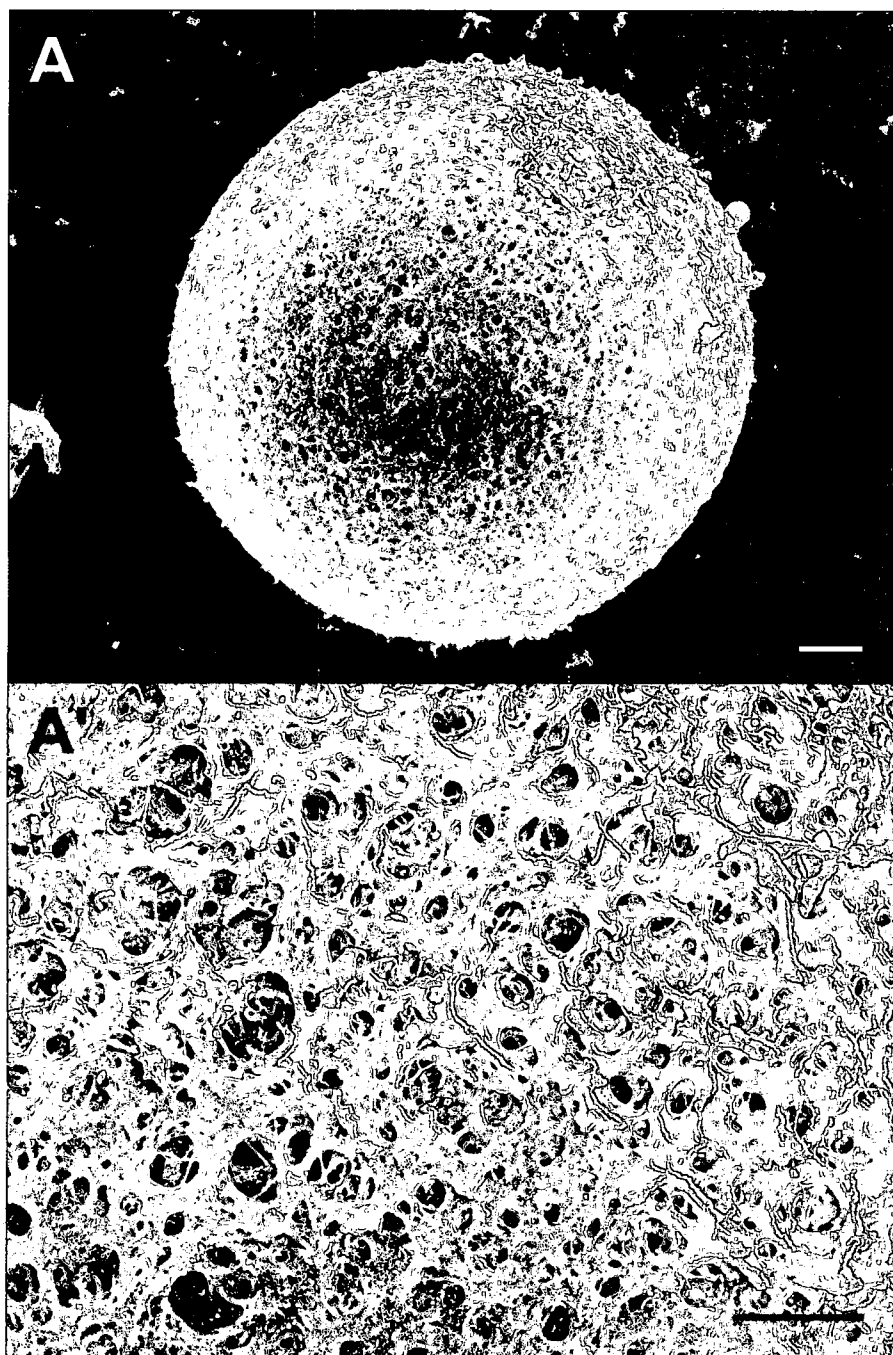


Fig. 3.13. Canine oocyte with a type III zona pellucida. The two images are of the same Golden Retriever oocyte at low (A, 1,000X) and high (A', 4,000X) magnification. The oocyte diameter is 86 μm . The type III zona pellucida has a rough, uneven appearance at both low and high magnification. The enlargement of A' shows a spongy, mesh-like surface with some of the zona pellucida filaments raised to form hollows and pores making the surface irregular. In addition, some pores have smaller pores within them, and other pores bifurcate deeper into the zona pellucida. Scale bar represents 10 μm in A and 5 μm in A'.

Fig. 3.13.

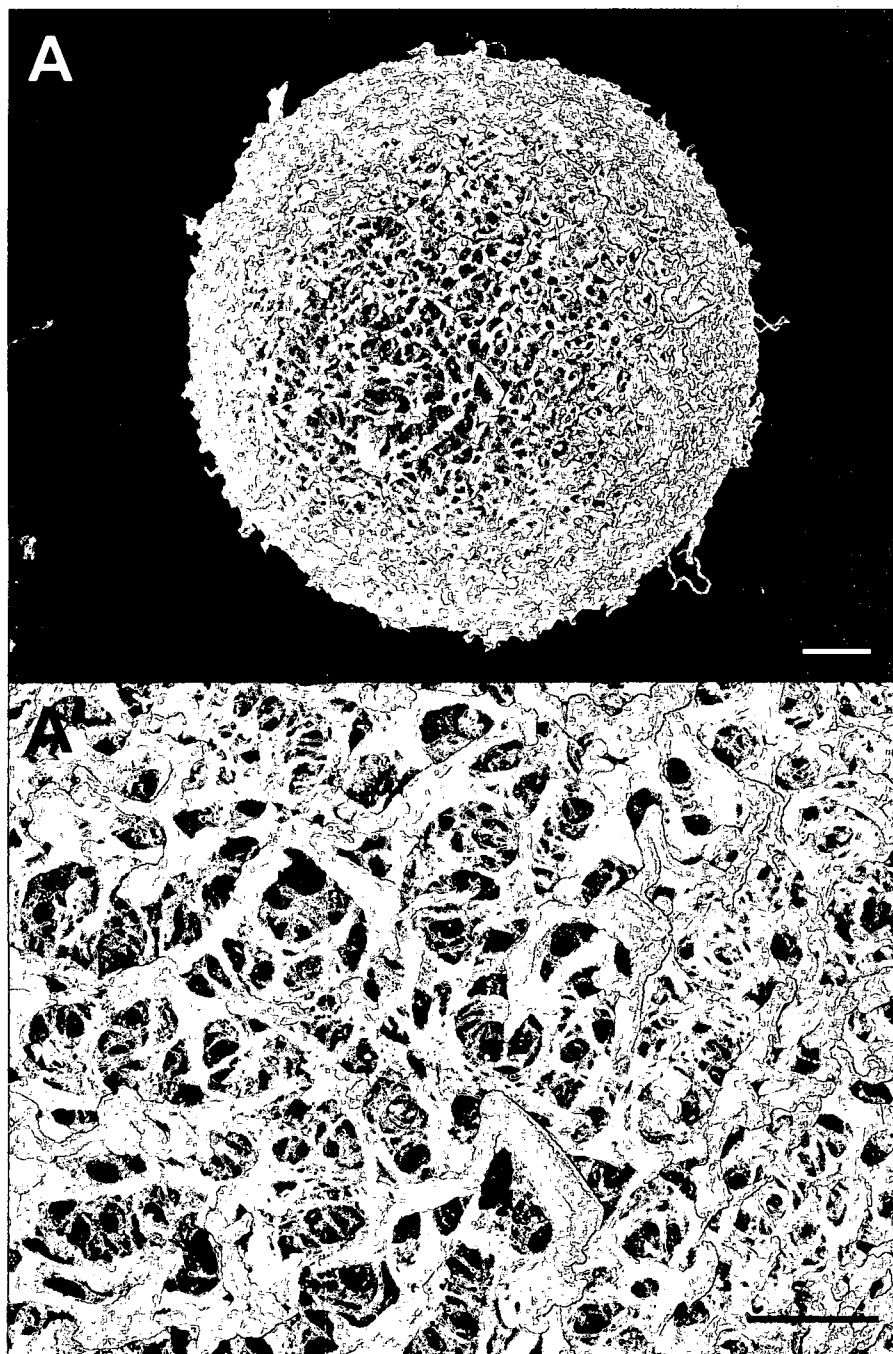


Fig. 3.14. Canine oocyte with a type IV zona pellucida. The two images are of the same Maltese oocyte at low (A, 900X) and high (A', 4,000X) magnification. The oocyte diameter is 111 μm . The type IV zona pellucida has a rough uneven appearance at low and high magnification. The enlargement in A' accentuates the rough appearance and reveals small fibers in between flat plates and raised whorls. The type IV zona pellucida may or may not have visible pores, but often has hollows. Scale bar represents 10 μm in A and 5 μm in A'.

Fig. 3.14.

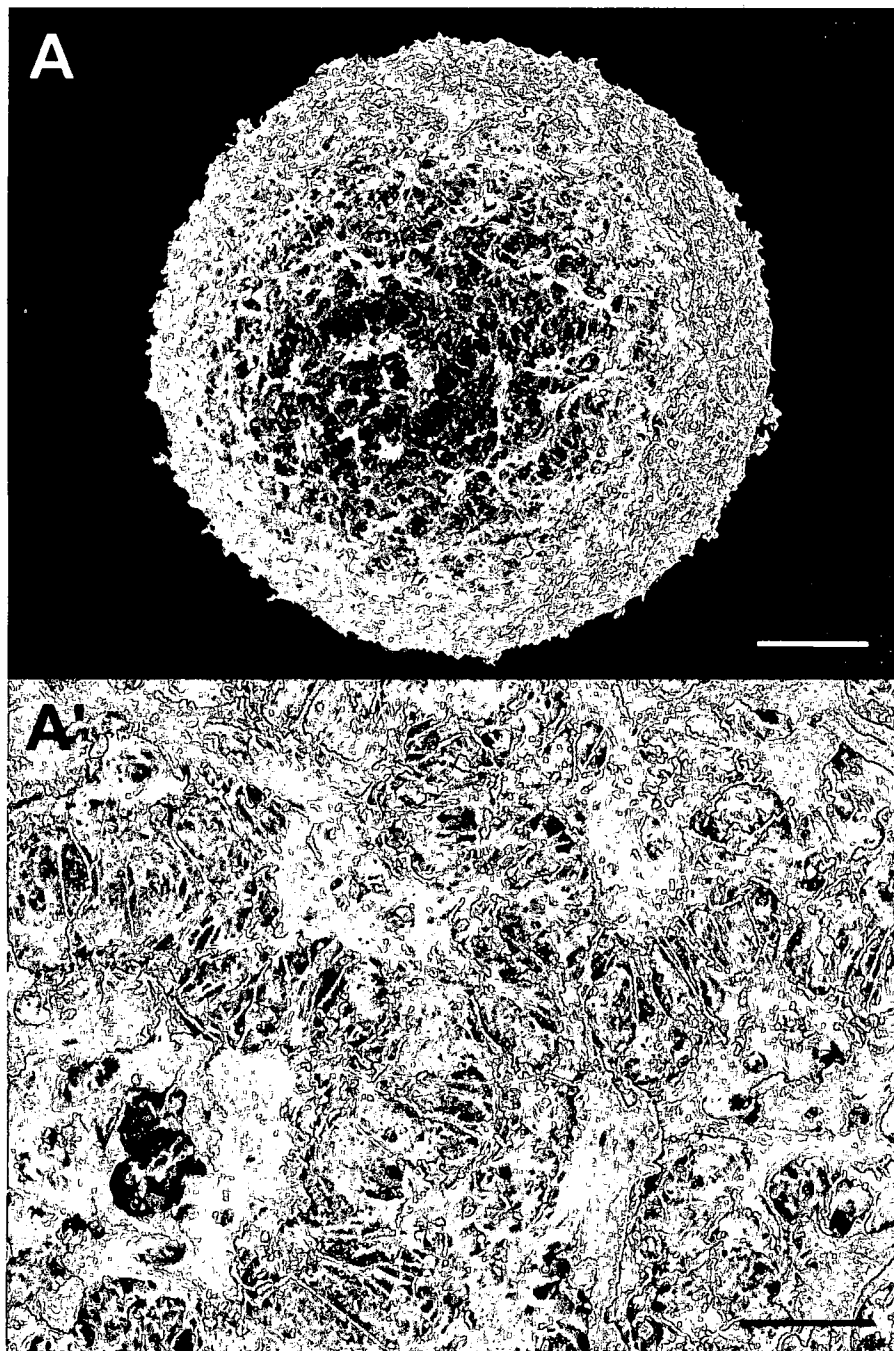


Fig. 3.15. Four canine zona pellucida types. Four canine oocytes showing the four types of canine zona pellucida found in this study. A – D are low magnification images (900 – 1,000X) of the entire canine oocyte. A' – D' are correspondingly higher magnifications (4,000X) showing each type of zona pellucida more clearly. A and A' show a type I zona pellucida which was smooth with only a few small pores or none at all. B and B' show a type II zona pellucida which was relatively smooth with very many round or elliptical shaped pores. C and C' show a type III zona pellucida which has a rough surface, and the pores are less elliptical and more random in shape. D and D' show a type IV zona pellucida which has a rough surface with stringy filaments that make up a zona pellucida that looks less compact than the others. Oocyte diameters are 111 μm in A, 97 μm in B, 90 μm in C, and 89 μm in D. Scale bars represent 20 μm in A – D and 5 μm in A' – D'.

Fig. 3.15.

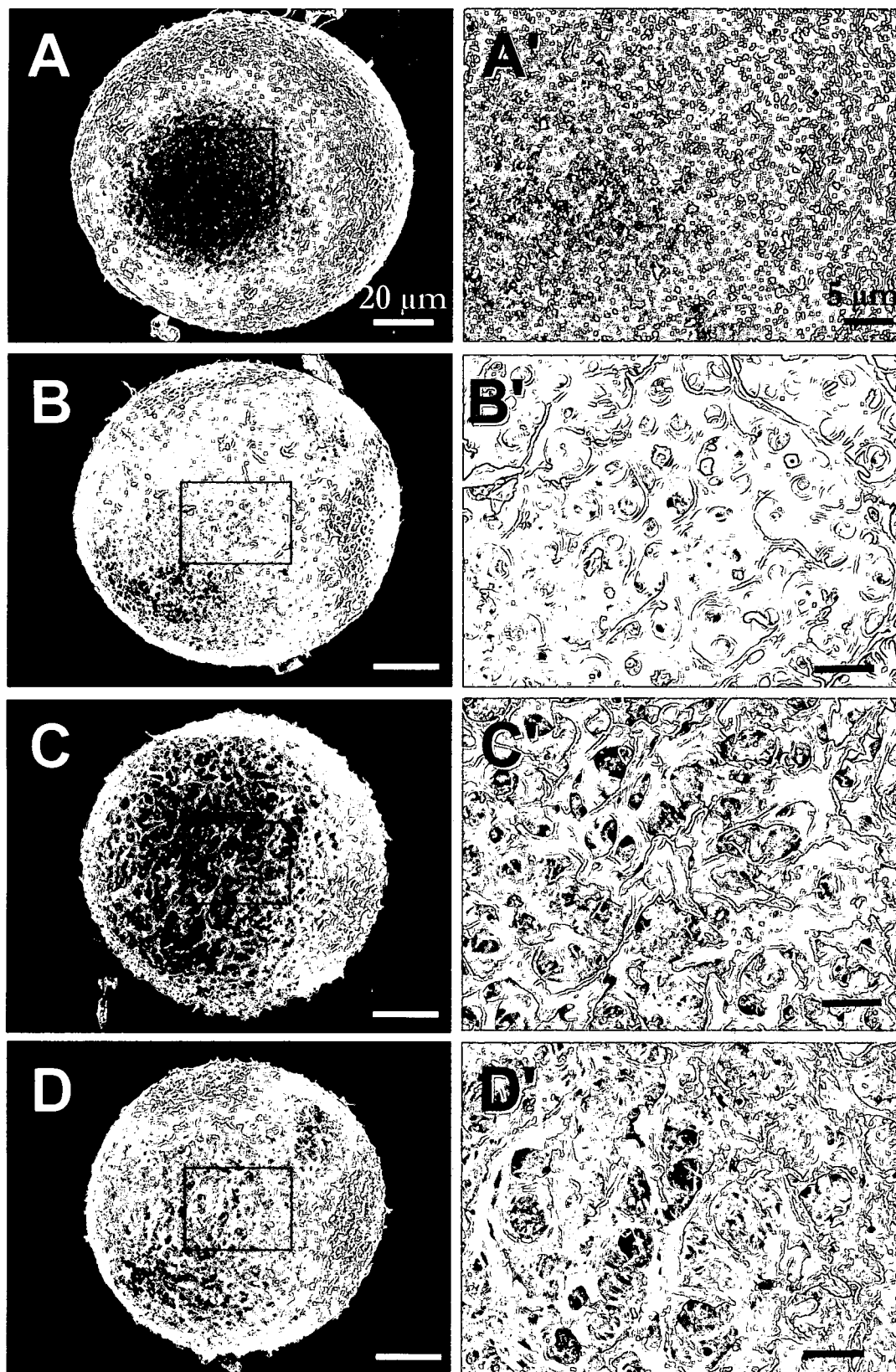


Fig. 3.16. Oocyte distribution of zona pellucida types. The pie graph shows the total number of oocytes used for this study ($n = 306$) categorized by zona pellucida type. The number of oocytes are shown for each zona pellucida type. This graph shows that the zona pellucida types are found in roughly similar percentages (29.8 to 38.3%) when type I oocytes (3.6%) are excluded.

Fig. 3.16.

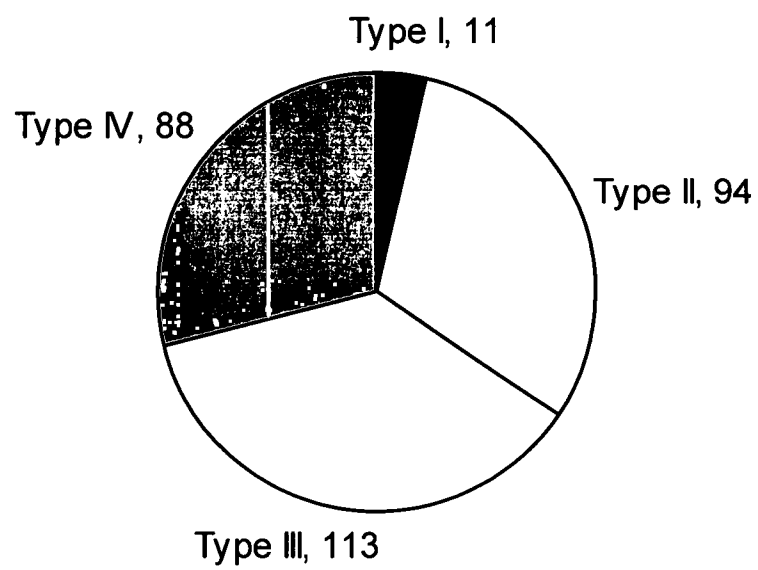


Fig. 3.17. Effect of canine donor breed on zona pellucida morphology. This bar graph shows the oocytes divided by canine breed in the columns, and within each column they are divided by zona pellucida type using different colors. The number in each color of a column indicates the number of oocytes of that zona pellucida type. Many dog breeds (46.4%) had at least three zona pellucida types, and only one breed (Medium mix) had only one zona pellucida type.

Fig. 3.17.

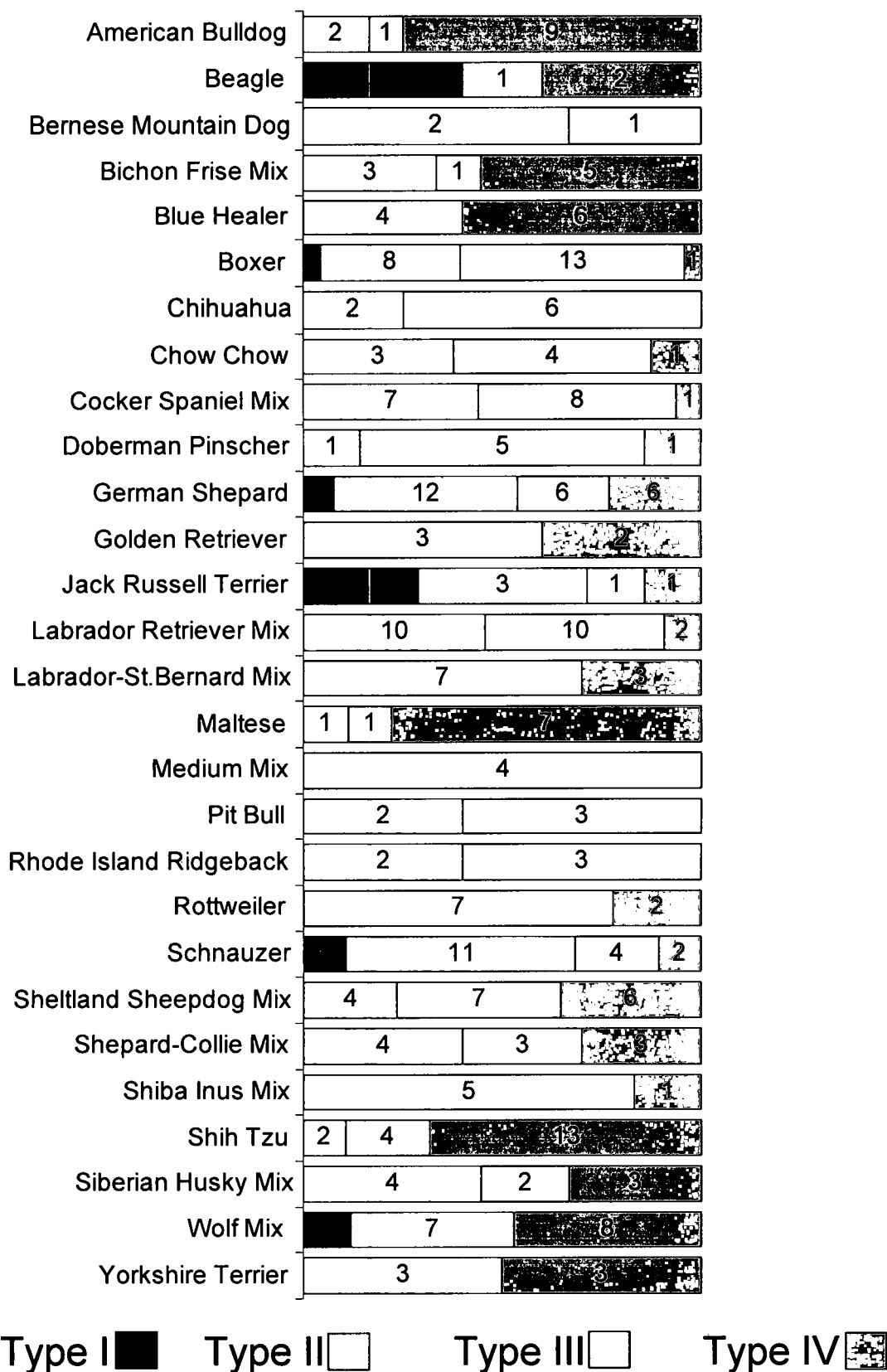


Fig. 3.18. Effect of AKC donor breed type on zona pellucida morphology. This bar graph shows the oocytes divided by American Kennel Club (AKC) canine breed type in the columns, and within each column they are divided by zona pellucida type using different colors. The number in each column color indicates the number of oocytes of that zona pellucida type. All eight of the AKC breed types had at least three of the zona pellucida types, and five breed types had all four types.

Fig. 3.18.

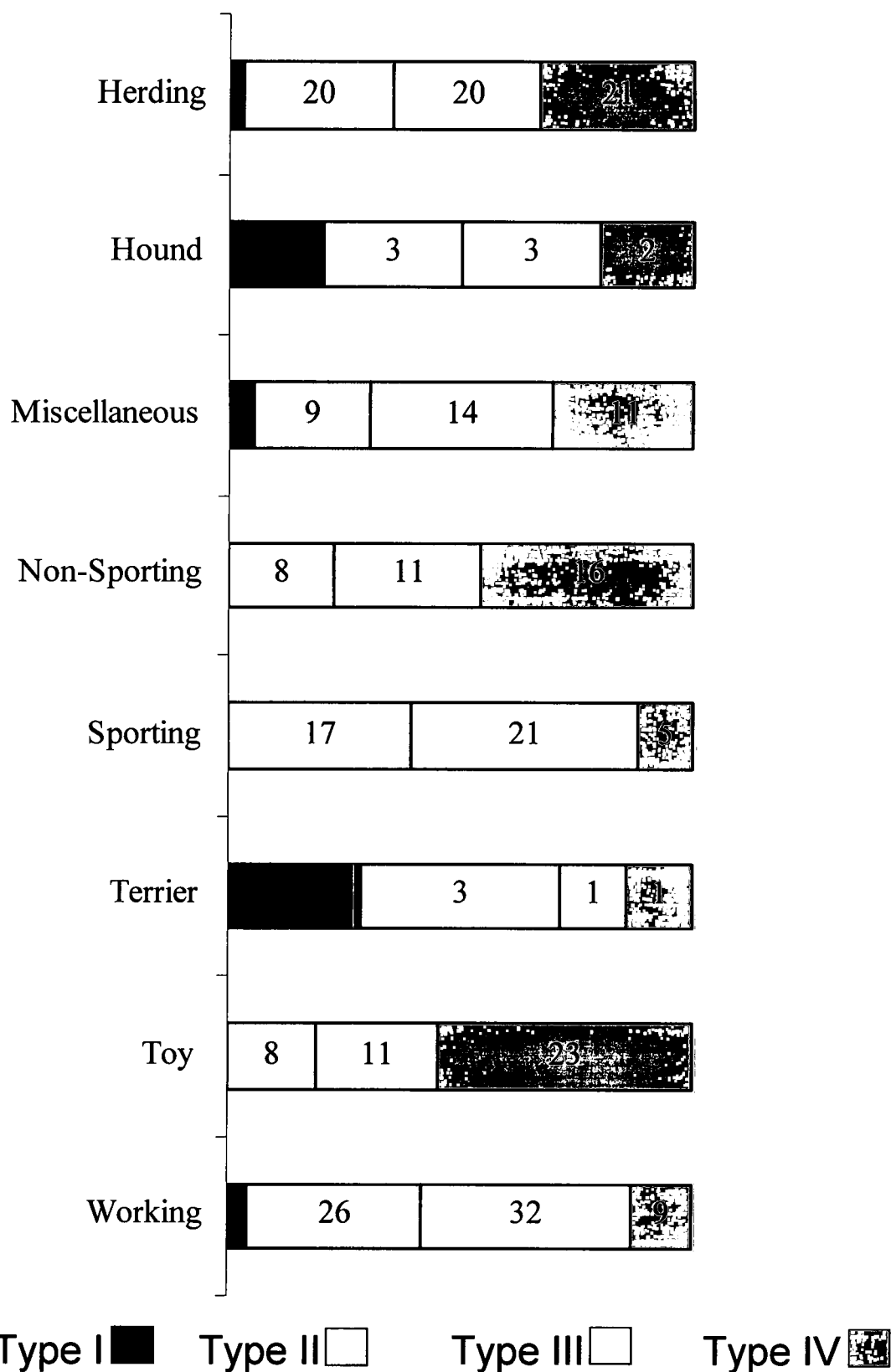


Fig. 3.19. Effect of canine donor size on zona pellucida morphology. This bar graph shows the oocytes divided by canine breed size (<13 kg small, 13 – 23 kg medium, >23 kg large) in the columns, and within each column they are divided by zona pellucida type using different colors. The number in each column color shows the number of oocytes of that zona pellucida type. All size categories had all four zona pellucida types, and Chi-square analysis showed that there is no significant effect ($P = 0.05$) of dog size on zona pellucida morphology.

Fig. 3.19.

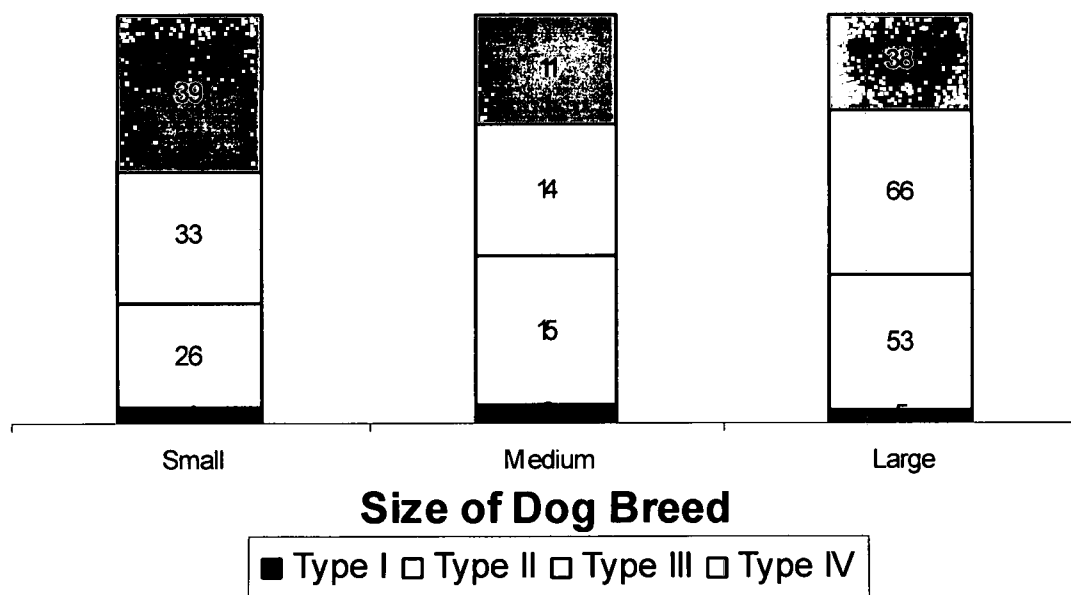


Fig. 3.20. Effect of canine donor age on zona pellucida morphology. Bar graph A shows the canine oocytes divided into age groups by columns, and within each column they are divided by zona pellucida type using different colors. The number in each column shows the number of oocytes of that zona pellucida type. Bar graph B categorizes oocytes from dogs two years and younger into smaller groups (3 months) than is shown in graph A (6 months).

Fig. 3.20A.

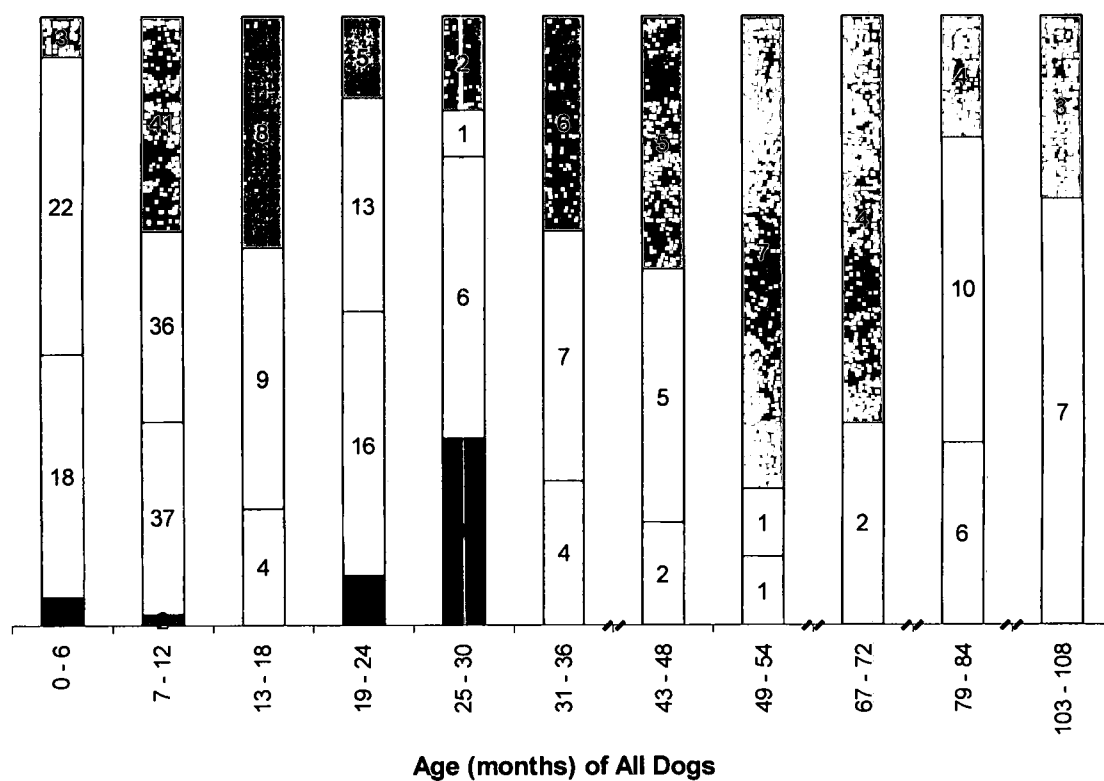


Fig. 3.20B

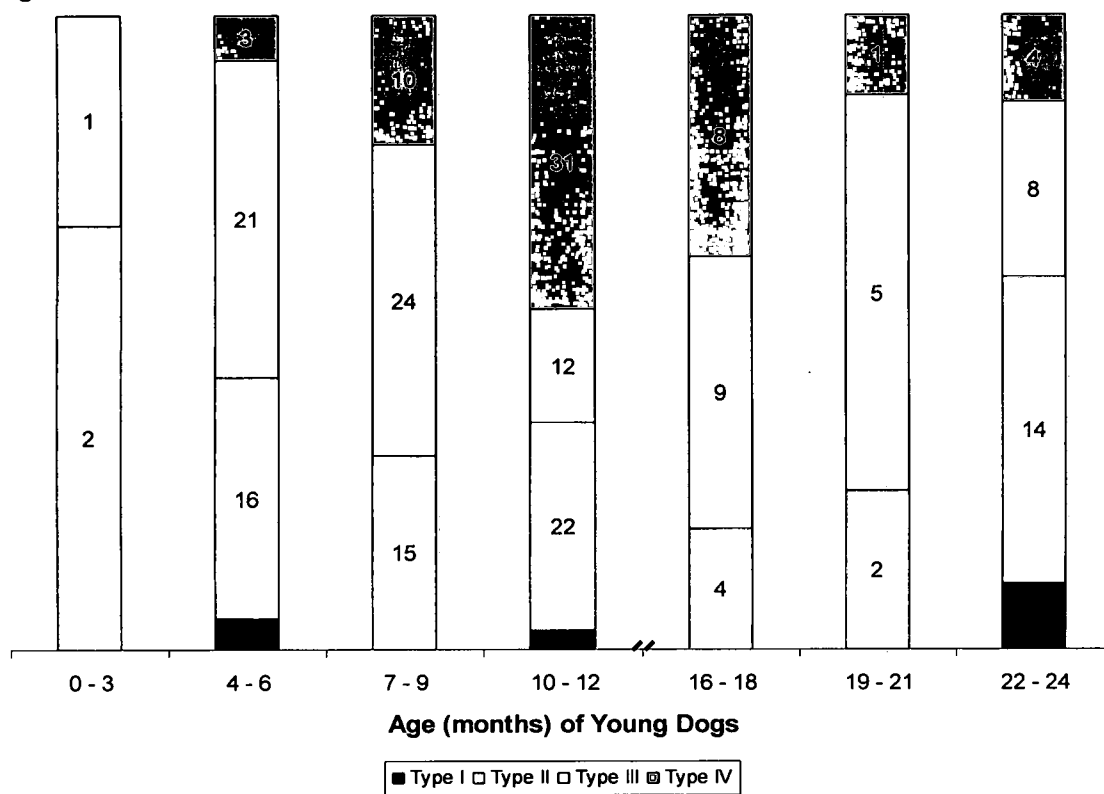


Fig. 3.21. Effect of canine reproductive maturity on zona pellucida morphology.

This bar graph shows the canine oocytes divided by age groups (prepubertal <6 months, juvenile 6 – 11 months, mature 12 – 48 months, and old >48 months) in the columns, and within each column they are divided by zona pellucida type using different colors. The number for each color of a column indicates the number of oocytes of that zona pellucida type. Three of four age groups had at least three zona pellucida types, and two had all four zona pellucida types.

Fig. 3.21.

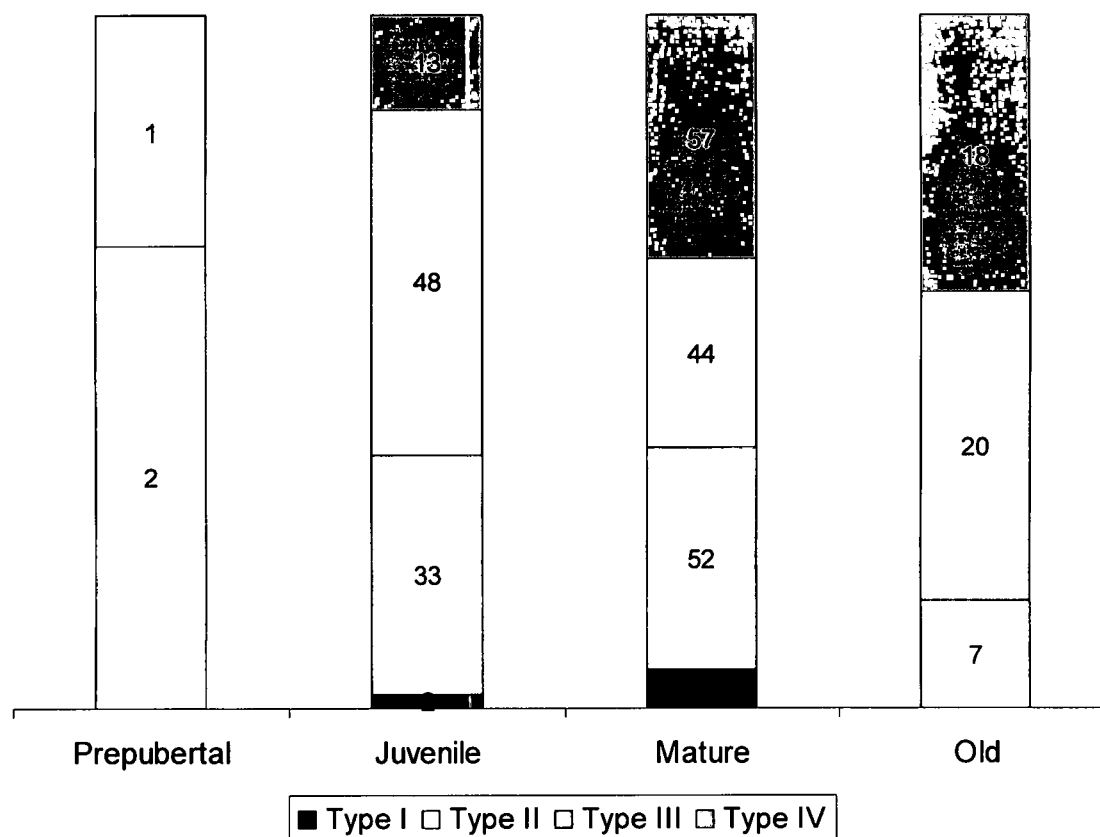
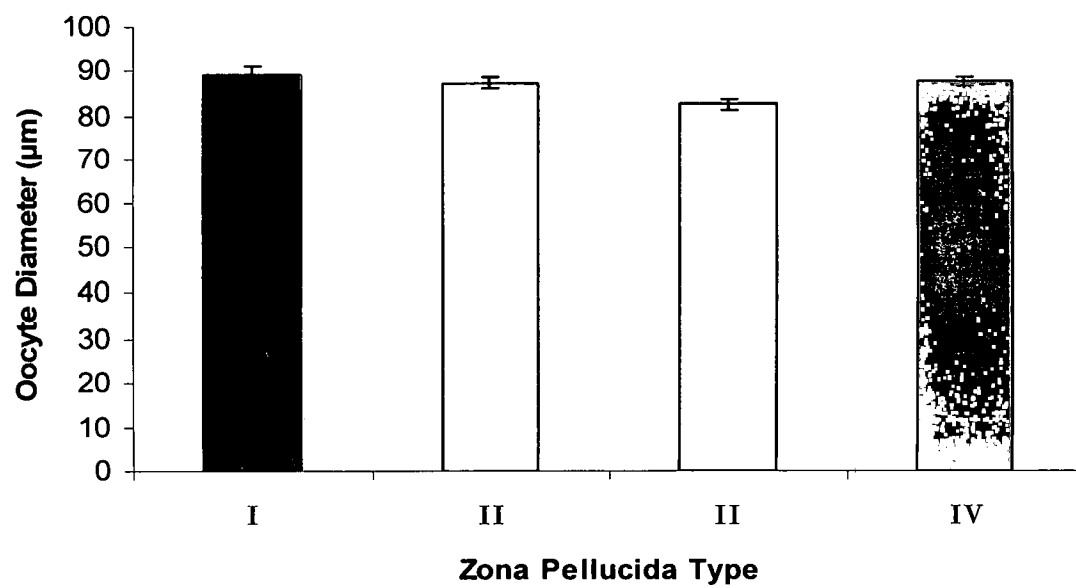


Fig. 3.22. Effect of oocyte diameter on zona pellucida morphology. Oocyte diameters are shown as the mean \pm SE for Type I ($n = 11$) $89.35 \pm 2.02 \mu\text{m}$, Type II ($n = 94$) $87.40 \pm 1.13 \mu\text{m}$, Type III ($n = 113$) $82.75 \pm 1.24 \mu\text{m}$, and Type IV ($n = 88$) $87.62 \pm 1.06 \mu\text{m}$. The average size of the oocytes for each zona pellucida type was taken and statistically compared using a one-way ANOVA and Tukey post-hoc test with a significance level of $P < 0.05$. Oocyte diameter significantly affected certain zona pellucida types in that: type III oocytes were significantly smaller than the type II and type IV oocytes. The type I oocytes were not significantly different from any of the other types.

Fig. 3.22.



CHAPTER IV

Conclusions and Future Directions

Conclusions

We initiated our study under the hypothesis that the canine zona pellucida was a porous mesh-like structure surrounding the oocyte, similar to that of other mammals. To test this hypothesis, we planned to use scanning electron microscopy. Due to the unusual reproductive physiology of the canine, our first objective was to develop methods for preparing canine oocytes to be viewed in an SEM. Because of the inability to enzymatically digest canine ovaries without harming the zona pellucida, we had to mechanically isolate follicles and COCs by slicing, as well as mechanically denude the oocytes of cumulus cells by pipetting. We determined that affixation of the oocytes to the poly-L-lysine coated glass slides worked best during simultaneous fixation. The highest resolution images were produced when the oocytes were coated with 100 Ångstroms of gold and viewed under high vacuum conditions at 15kV with a spot size of 6 – 7, objective lens aperture of 20 µm, and at a height of 11 mm.

Once we developed optimal methods to view the canine zona pellucida in the SEM that were as good or better than other SEM studies, we pursued our second goal which was to determine the ultrastructure of the canine zona pellucida. Initially, we found that the canine zona pellucida was generally similar in structure to that of other mammals. The surface of the canine zona pellucida was a spongy and fibrous meshwork structured in multiple layers. The meshwork of the zona pellucida formed pores that were usually spherical or elliptical in shape, and decreased in diameter and/or bifurcated as they penetrated deeper into the zona pellucida. It was also observed that while the canine zona pellucida had this general structure, it also appeared to be heterogeneous with different oocytes having different zona pellucida morphologies. This is similar to reports of a heterogeneous zona pellucida in other mammals (Calafell *et al.*, 1992; Jackowski and Dumont, 1979; Magerkurth *et al.*, 1999; Suzuki *et al.*, 1994; Vanroose *et al.*, 2000). Therefore, we further hypothesized that the canine zona pellucida was heterogeneous.

To test this hypothesis, we increased the number of oocytes used in the study to 306 and observed four different types of zona pellucida morphologies in the canine. The type I zona pellucida had a smooth compact surface with only a few small pores ($<0.5\ \mu\text{m}$). The type II zona pellucida had an outer surface that appeared smooth or even at high magnification, and had many elliptical or spherical pores that were often conical and/or bifurcated going deeper into the zona pellucida towards the oolemma. The type III zona pellucida was rough with an uneven surface that had pores that were less spherical and more irregular in

shape. The type IV zona pellucida was also rough with an uneven surface, but it was covered in small fibers that often clogged the deeper pores when they were present. We conclude that the surface ultrastructure of the canine zona pellucida is heterogeneous.

To determine factors possibly affecting zona pellucida morphology, we examined the effects of the characteristics of the oocyte donor (including breed, AKC classification, breed size, donor age and maturity as well as the maturity of the oocyte using oocyte diameter as a general indication of maturity) with the type of zona pellucida observed. It was found that the AKC breed type, breed size, age and maturity of the oocyte donor did not significantly affect zona pellucida morphology; however, they did have an effect on the oocyte diameter with the larger dog breeds having larger oocytes, as well as older more mature dogs having larger oocytes. The breed of the oocyte donor had an effect on the oocyte diameter as well as its zona pellucida type. In addition, oocyte diameter had an effect on the type of zona pellucida. Oocytes with a type III zona pellucida had a significantly smaller mean diameter than those that were type II and IV suggesting that on average they were more immature. This needs to be tested directly.

Based on our data and other studies using mammalian oocytes, we propose a model for the appearance of the different zona pellucida types in the canine. First, oocytes with a type III zona pellucida would be the most immature, because of their smaller diameter. The type IV zona pellucida was similar to a zona pellucida reported by Suzuki *et al.* (1994) that had many rope-like

processes. They reported that these oocytes were maturing oocytes. They also reported that their matured oocytes lacked these rope-like fibers and had a finer zona pellucida meshwork, which is similar to our zona pellucida type II. This is similar to what Allworth and Albertini (1993) reported, the mature oocytes will lose the cytoplasmic processes through retraction or disintegration. In light of these results, the type IV zona pellucida is most likely found in maturing oocytes and the type II zona pellucida may be mature oocytes. The type I zona pellucida is similar to a type reported by various authors to be from atretic oocytes (Calafell *et al.*, 1992; Familiari *et al.*, 1988, 1989). We tried to avoid collecting atretic follicles, which could be why only a few oocytes with type I zona pellucida were found. This lower proportion is similar to what Magerkurth *et al.* (1999) reported with their smooth and compact type of human zona pellucida although they did not report them as being atretic.

To be certain that the zona pellucida types correlate with oocyte maturity, studies are needed to show nuclear morphology and zona pellucida ultrastructure for each oocyte. Also, if possible it would be useful to determine functional competence by testing the ability of oocytes to be fertilized and correlate this with zona pellucida morphology

Future Studies

This research needs to focus in several directions. While many studies have looked at the zona pellucida of *in vitro* matured oocytes in a variety of mammals, much remains undiscovered in the canine. We need to determine if

the zona pellucida changes or displays another phenotype after *in vitro* or *in vivo* maturation and fertilization, different from the other four types reported in this thesis. In the canine, *in vitro* maturation of oocytes is not as effective as in other mammals. Not all oocytes mature and even fewer are competent to be fertilized. It is not known if canine oocytes will mature as effectively *in vitro* as *in vivo*, or if the optimal medium has yet to be found for IVF. If zona pellucida type was able to be correlated to oocyte maturity, we could test oocytes cultured in different *in vitro* maturation media to determine which medium was most effective at maturing the oocytes. This would be highly beneficial for IVF and other studies in the canine, but it could be most beneficial for endangered canids. Their precious few oocytes would not be wasted in determining the optimal *in vitro* maturation medium, but could be used for IVF aimed at restoring their population.

If the surface morphology of the canine zona pellucida changes after *in vitro* or *in vivo* maturation and fertilization; this would be important for research developing an immunocontraceptive vaccine. It would be possible that the antibodies blocking sperm-zona binding would not bind properly to all zona pellucida types. If *in vitro* matured oocytes are more similar to the oocytes being fertilized *in vivo*, it is important that this is known so the different antibodies can be developed if necessary.

To aid in the process of developing an immunocontraceptive vaccine, it would be important to determine which zona pellucida antibodies work most effectively to block sperm-zona binding. Antibodies could be generated to synthetic zona pellucida proteins or those expressed by *Escherichia coli*

transformed with a recombinant plasmid containing a chimeric zona pellucida protein. By using a variety of antibodies specific for the canine zona pellucida, we need to determine if specific antibodies inhibit sperm-zona binding in the canine. It would also be important to observe the effects of these antibodies *in vivo* on the structure of the zona pellucida. Since the zona pellucida is important for folliculogenesis to occur correctly, side effects could occur in its absence creating complications in the use of zona pellucida antibodies as an immunocontraceptive vaccine. This has been seen before in the use of immunocontraception on other mammals (Fayer-Hosken *et al.*, 2000).

When the research for this thesis was started, we wanted to measure the size of the pores in the canine zona pellucida to determine whether viruses could penetrate the zona pellucida. However, due to the structural heterogeneity of the canine zona pellucida, we determined that it would not be feasible, since there are not clear pore boundaries in some zona pellucida types due to the stringy filaments (type IV) as well as irregular pore shapes (type III). To determine if the viruses could pass through the entire zona pellucida we need to use florescent microbeads (40 – 200 nm; detectable with confocal laser scanning microscopy) or dextrans (3.84 kDa – 170 kDa) to determine whether they can penetrate the zona pellucida. These experiments need to be performed to determine what precautions need to be taken when working with IVF and cloning of canines that have recently been performed. If the viruses are not able to penetrate the zona pellucida, then enzymatic digestion of the zona pellucida after IVF may destroy the viruses and protect the zygote. If viruses are able to pass through the zona

pellucida, much more stringent testing would need to be done on the sperm donor to prevent viral infection of the oocyte/embryos. This information could also be applied to *in vitro* fertilization of endangered canids.

In summary, our scanning electron microscopy methods provide a means to prepare and view canine oocytes with minimal loss and high resolution in the SEM. We conclude that canine oocytes have a heterogeneous surface ultrastructure of the zona pellucida. Canine breed, AKC breed type, size, age and reproductive maturity all affected the oocyte diameter; however, canine breed was the only donor characteristic that affected zona pellucida morphology. Oocyte diameter also affected zona pellucida morphology.

This study was significant in that it laid the ground work for looking at the canine zona pellucida for future studies, which could aid in developing an immunocotraceptive vaccine and help develop better IVF techniques in the canine. The immunocotraceptive vaccine will reduce the stress of spaying a dog for the owner and dog, as well as help reduce dangerous feral dog populations. The development of better IVF techniques will further aid in canine research as well as being able help rescue endangered canids by using IVF.

CHAPTER V

Literature Cited

Allworth, A.E. and D.F. Albertini. (1993). Meiotic maturation in cultured bovine oocytes is accompanied by remodeling of cumulus cells cytoskeleton. *Dev. Bio.* 158: 101-112.

American Kennel Club, The. (1996). *The Complete Dog Book*. Howell Book House Foster City, CA.

Andersen, A.C. and M.E. Simpson. (1973). *The Ovary and Reproductive Cycle of the Dog (Beagle)*. Geron-X Los Altos, CA.

Baarends, W.M., J.W. Hoogerbrugge, M. Post, J.A. Visser, D.G. De Rooij, M. Parvinen, A.P. Themmen, and J.A. Grootegoed. (1995). Anti-mullerian hormone and anti-mullerian hormone type II receptor messenger ribonucleic acid expression during postnatal testis development and in the adult testis of the rat. *Endocrinology*. 136: 5614-5622.

Barber M.R., S.M. Lee, W.L. Steffens, M. Ard, and R.A. Fayrer-Hosken. (2001). Immunolocalization of zona pellucida antigens in the ovarian follicle of dogs, cats, horses and elephants. *Theriogenology*. 55: 1705-1717.

Blackmore, D.G., L.R. Baillie, J.E. Holt, L. Dierkx, R.J. Aitken, and E.A.

McLaughlin. (2004). Biosynthesis of the canine zona pellucida requires the integrated participation of both oocytes and granulosa cells. *Biol. Reprod.* 71: 661-668.

Bolamba D., K.D. Borden-Russ, and B.S. Durrant. (1992). *In vitro* maturation of domestic dog oocytes cultured in advanced preantral and early antral follicles. *Theriogenology*. 49: 933-942.

Calafell, J.M., C. Nogues, M. Ponsa, J. Santalo, and J. Egozcue. (1992). Zona pellucida surface of immature and *in vitro* matured mouse oocytes: analysis by scanning electron microscopy. *J. Assist. Reprod. Genet.* 9: 365-372.

Correa, J.E. (2002). *Canine Breeding and Reproduction*. Alabama Cooperative Extension System (Alabama A&M University and Auburn University).

de Paz P., A.J. Sanchez, J. De la Fuente, C.A. Chamorro, M. Alvarez, E. Anel, and L. Anel. (2001). Ultrastructural and cytochemical comparison between calf and cow oocytes. *Theriogenology*. 55: 1107-1116.

Dudkiewicz, A.B., and W.L. Williams. (1977). Fine structural observations of the mammalian zona pellucida by scanning electron microscopy. *Scan. Elec. Microsc.* 2: 317-324.

Dunbar, B.S. and M.G. O'Rand. (1991). *A Comparative Overview of Mammalian Fertilization*. MacMillan Publishing Co., New York, NY.

- Dunbar, B.S. and D.J. Wolgemuth. (1984). Structure and function of the mammalian zona pellucida, a unique extracellular matrix. In: *Modern Cell Biology*, Satir, B.H. (ed.), Alan R. Liss, New York.
- Dunbar, B.S., S. Avery, V. Lee, S. Prasad, D. Schwahn, E. Schwoebel, S. Skinner, and B. Wilkins. (1994). The mammalian zona pellucida: its biochemistry, immunochemistry, molecular biology, and developmental expression. *Reprod. Fertil. Dev.* 6: 331-347.
- Dunbar B.S., G. Kaul, M. Prasad, and S.M. Skinner. (2002). Molecular approaches for the evaluation of immune responses to zona pellucida (ZP) and development of second-generation ZP vaccines. *Reprod. Suppl.* 60: 9-18.
- Durlinger A.L., P. Kramer, B. Karels, F.H. de Jong, J.T. Uilenbroek, J.A. Grootegoed, and A.P. Themmen. (1999). Control of primordial follicle recruitment by anti-Mullerian hormone in the mouse ovary. *Endocrinology*. 140: 5789-5796.
- Durlinger A.L., M.J. Gruijters, P. Kramer, B. Karels, H.A. Ingraham, M.W. Nachtigal, J.T. Uilenbroek, J.A. Grootegoed, and A.P. Themmen. (2002). Anti-Mullerian hormone inhibits initiation of primordial follicle growth in the mouse ovary. *Endocrinology*. 143: 1076-1084.
- Durrant, B.S., N.C. Pratt, K.D. Russ, and D. Bolamba. (1998). Isolation and characterization of canine advanced preantral and early antral follicles. *Theriogenology*. 49: 917-932.

- Eberspaecher, U., A. Becker, P. Bringmann, L. van der Merwe, and P. Donner. (2001). Immunohistochemical localization of zona pellucida proteins ZPA, ZPB and ZPC in human, cynomolgus monkey and mouse ovaries. *Cell Tissue. Res.* 303: 277-287.
- Eilts, B.E. and A.P. Davidson. Breeding management of the bitch. (2005). In: *Textbook of Veterinary Internal Medicine*. Eds. S.J. Ettinger and E.C. Feldman.
- England, G.C. *Allen's Fertility and Obstetrics in the Dog*. (1998). Blackwell Science, Oxford, England.
- Epifano, O., and J. Dean. (1994). Biology and structure of the zona pellucida: a target for immunocontraception. *Reprod. Fertil. Dev.* 6: 319-330.
- Epifano, O., L.F. Liang, M. Familiari, M.C. Moos, and J. Dean. (1995). Coordinate expression of the three zona pellucida genes during mouse oogenesis. *Development*. 121: 1947-1956.
- Eppig, J.J. (1994). Oocyte-somatic cell communication in the ovarian follicles of mammals. *Sem. Dev. Biol.* 5: 51-59.
- Fair, T. (1993). Follicular oocyte growth and acquisition of developmental competence. *Anim Reprod Sci.* 78: 203-216.
- Familiari, G., S.A. Nottola, G. Micara, C. Aragona, and P.M. Motta. (1988). Is the sperm-binding capability of the zona pellucida linked to its surface structure? A scanning electron microscopic study of human *in vitro* fertilization. *J. In Vitro Fert. Embryo Transf.* 5: 134-143.

- Familiari, G., S.A. Nottola, A. Familiari, and P.M. Motta. (1989). The three-dimensional structure of the zona pellucida in growing and atretic ovarian follicles of the mouse: scanning and transmission electron-microscopic observations using ruthenium red and detergents. *Cell Tiss. Res.* 257: 247-253.
- Familiari, G., M. Relucenti, M. Ermini, C. Verlengia, S.A. Nottola and P.M. Motta. (2001). The human zona pellucida and scanning electron microscopy. Reality or artifacts? *It. J. Anat. Embryol.* 106: 33-41.
- Fayrer-Hosken R.A., H.D. Dookwah, and C.I. Brandon. (2000). Immunocontrol in dogs. *Anim Reprod Sci.* 2: 365-373.
- Flegler, S.L., J.W. Jr. Heckman, and K.L. Klomparens. (1993). *Scanning and Transmission Electron Microscopy: An Introduction*. Oxford University Press, Oxford, NY.
- Florman, H.M., and N.L. First. (1988). The regulation of acrosomal exocytosis. I. Sperm capacitation is required for the induction of acrosome reactions by the bovine zona pellucida *in vitro*. *Dev. Biol.* 128: 453-463.
- Funahashi H., H. Ekwall, and H. Rodriguez-Martinez. (2000). Zona reaction in porcine oocytes fertilized *in vivo* and *in vitro* as seen with scanning electron microscopy. *Biol. Reprod.* 63: 1437-1442.
- Garside, W.T., J.R. Loret de Mola, J.A. Bucci, R.W. Tureck, and S. Heyner. (1997). Sequential analysis of zona thickness during *in vitro* culture of human zygotes: correlation with embryo quality, age, and implantation. *Mol. Reprod. Dev.* 47: 99-104.

- Gilbert, S.F. (2000). *Developmental Biology*. 6th ed., Sinauer Associates, Sunderland, MA.
- Goodrowe K.L., S.L. Walker, D.P. Ryckman, G.F. Mastromonaco, M.A. Hay, H.L. Bateman, and W.T. Waddell. (2000). Piecing together the puzzle of carnivore reproduction. *Anim Reprod Sci.* 2: 389-403.
- Gosden R.G., D.T. Baird, J.C. Wade, and R. Webb. (1994). Restoration of fertility to oophorectomized sheep by ovarian autografts stored at -196 degrees C. *Hum. Reprod.* 9: 597-603.
- Green, D.P. (1997). Three-dimensional structure of the zona pellucida. *Rev. Reprod.* 2: 147-156.
- Greve, J.M., and P.M. Wassarman. (1985). Mouse egg extracellular coat is a matrix of interconnected filaments possessing a structural repeat. *J. Mol. Biol.* 181: 253-264.
- Guraya, S.S. (1965) A histochemical analysis of lipid yolk deposition in the oocytes of cat and dog. *J. Exp. Zool.* 160: 123-135.
- Haenisch-Woehl, A., S. Kölle, C. Neumüller, F. Sinowatz and J. Braun. (2003). Morphology of canine cumulus-oocyte complexes in pre-pubertal bitches. *Anat. Histol. Embryol.* 32: 373-377.
- Hewitt D.A., and G.C. England. (1998). The effect of oocyte size and bitch age upon oocyte nuclear maturation *in vitro*. *Theriogenology*. 49: 957-966.
- Hinsch, E., S. Oehninger, W.B. Schill, and K.D. Hinsch. (1999). Species specificity of human and murine anti-ZP3 synthetic peptide antisera and

- use of the antibodies for localization and identification of ZP3 or ZPC domains of functional significance. *Hum. Reprod.* 14: 419-428.
- Hirobe S., W.W. He, M.M. Lee, and P.K. Donahoe. (1992). Mullerian inhibiting substance messenger ribonucleic acid expression in granulosa and Sertoli cells coincides with their mitotic activity. *Endocrinology*. 131: 854-862.
- Hoage T.R. and I.L. Cameron. (1976). DNA synthesis in the oocyte of the mature mouse: a radioautographic study. *Anat. Rec.* 186: 585-594.
- Hutt, K.J., E.A. McLaughlin, and M.K. Holland. (2006). Kit ligand and *c-Kit* have diverse roles during mammalian oogenesis and folliculogenesis. *Mol. Hum. Reprod.* 12: [Epub ahead of print]
- Jackowski S., and J.N. Dumont. (1979). Surface alterations of the mouse zona pellucida and ovum following *in vivo* fertilization: correlation with the cell cycle. *Biol. Reprod.* 20: 150-161.
- Johnson, J., J. Canning, T. Kaneko, J.K. Pru, and J.L. Tilly. (2004). Germline stem cells and follicular renewal in the postnatal mammalian ovary. *Nature*. 428: 145-150.
- Jovine, L., C.C. Darie, E.S. Litscher, and P.M. Wassarman. (2005). Zona pellucida domain proteins. *Annu. Rev. Biochem.* 74: 83-114.
- Lee B.C., M.K. Kim, G. Jang, H.J. Oh, F. Yuda, H.J. Kim, M.H. Shamim, J.J. Kim, S.K. Kang, G. Schatten, and W.S. Hwang. (2005). Dogs cloned from adult somatic cells. *Nature*. 436: 641.

Lee V.H. and B.S. Dunbar. (1993). Developmental expression of the rabbit 55-kDa zona pellucida protein and messenger RNA in ovarian follicles. *Dev. Biol.* 155: 371-382.

Lindblad-Toh, K., C.M. Wade, T.S. Mikkelsen, E.K. Karlsson, D.B. Jaffe, M.

Kamal, M. Clamp, J.L. Chang, E.J. 3rd Kulbokas, M.C. Zody, E. Mauceli, X. Xie, M. Breen, R.K. Wayne, E.A. Ostrander, C.P. Ponting, F. Galibert, D.R. Smith, P.J. DeJong, E. Kirkness, P. Alvarez, T. Biagi, W. Brockman, J. Butler, C.W. Chin, A. Cook, J. Cuff, M.J. Daly, D. DeCaprio, S. Gnerre, M. Grabherr, M. Kellis, M. Kleber, C. Bardeleben, L. Goodstadt, A. Heger, C. Hitte, L. Kim, K.P. Koepfli, H.G. Parker, J.P. Pollinger, S.M. Searle, N.B. Sutter, R. Thomas, C. Webber, J. Baldwin, A. Abebe, A. Abouelleil, L. Aftuck, M. Ait-Zahra, T. Aldredge, N. Allen, P. An, S. Anderson, C. Antoine, H. Arachchi, A. Aslam, L. Ayotte, P. Bachantsang, A. Barry, T. Bayul, M. Benamara, A. Berlin, D. Bessette, B. Blitshteyn, T. Bloom, J. Blye, L. Boguslavskiy, C. Bonnet, B. Boukhgalter, A. Brown, P. Cahill, N. Calixte, J. Camarata, Y. Cheshatsang, J. Chu, M. Citroen, A. Collymore, P. Cooke, T. Dawoe, R. Daza, K. Decktor, S. DeGray, N. Dhargay, K. Dooley, K. Dooley, P. Dorje, K. Dorjee, L. Dorris, N. Duffey, A. Dupes, O. Egbiremolen, R. Elong, J. Falk, A. Farina, S. Faro, D. Ferguson, P. Ferreira, S. Fisher, M. FitzGerald, K. Foley, C. Foley, A. Franke, D. Friedrich, D. Gage, M. Garber, G. Gearin, G. Giannoukos, T. Goode, A. Goyette, J. Graham, E. Grandbois, K. Gyaltsen, N. Hafez, D. Hagopian, B. Hagos, J. Hall, C. Healy, R. Hegarty, T. Honan, A. Horn, N. Houde, L.

Hughes, L. Hunnicutt, M. Husby, B. Jester, C. Jones, A. Kamat, B. Kanga, C. Kells, D. Khazanovich, A.C. Kieu, P. Kisner, M. Kumar, K. Lance, T. Landers, M. Lara, W. Lee, J.P. Leger, N. Lennon, L. Leuper, S. LeVine, J. Liu, X. Liu, Y. Lokyitsang, T. Lokyitsang, A. Lui, J. Macdonald, J. Major, R. Marabella, K. Maru, C. Matthews, S. McDonough, T. Mehta, J. Meldrim, A. Melnikov, L. Meneus, A. Mihalev, T. Mihova, K. Miller, R. Mittelman, V. Mlenga, L. Mulrain, G. Munson, A. Navidi, J. Naylor, T. Nguyen, N. Nguyen, C. Nguyen, T. Nguyen, R. Nicol, N. Norbu, C. Norbu, N. Novod, T. Nyima, P. Olandt, B. O'Neill, K. O'Neill, S. Osman, L. Oyono, C. Patti, D. Perrin, P. Phunkhang, F. Pierre, M. Priest, A. Rachupka, S. Raghuraman, R. Rameau, V. Ray, C. Raymond, F. Rege, C. Rise, J. Rogers, P. Rogov, J. Sahalie, S. Settipalli, T. Sharpe, T. Shea, M. Sheehan, N. Sherpa, J. Shi, D. Shih, J. Sloan, C. Smith, T. Sparrow, J. Stalker, N. Stange-Thomann, S. Stavropoulos, C. Stone, S. Stone, S. Sykes, P. Tchuinga, P. Tenzing, S. Tesfaye, D. Thoulutsang, Y. Thoulutsang, K. Topham, I. Topping, T. Tsamla, H. Vassiliev, V. Venkataraman, A. Vo, T. Wangchuk, T. Wangdi, M. Weiland, J. Wilkinson, A. Wilson, S. Yadav, S. Yang, X. Yang, G. Young, Q. Yu, J. Zainoun, L. Zembek, A. Zimmer, and E.S. Lander. (2005). Genome sequence, comparative analysis and haplotype structure of the domestic dog. *Nature*. 438: 803-819.

Liu C., E.S. Litscher, S. Mortillo, Y. Sakai, R.A. Kinloch C.L. Stewart and P.M. Wassarman. (1996). Targeted disruption of the *mZP3* gene resulting in

- production of eggs lacking a zona pellucida and infertility in female mice.
Proc. Natl. Acad. Sci. 93: 4121-4131.
- Lussier J.G., P. Matton, and J.J. Dufour. (1987). Growth rates of follicles in the ovary of the cow. *J. Reprod. Fertil.* 81: 301-307.
- Luvoni G.C., S. Chigioni, E. Allievi, and D. Macis. (2005). Factors involved *in vivo* and *in vitro* maturation of canine oocytes. *Theriogenology*. 63: 41-59.
- Magerkurth, C., E. Topfer-Petersen, P. Schwartz, and H.W. Michelmann. (1999). Scanning electron microscopy analysis of the human zona pellucida: influence of maturity and fertilization on morphology and sperm binding pattern. *Hum. Reprod.* 14: 1057-1066.
- Mahi, C.A. and R. Yanagimachi. (1976). Maturation and sperm penetration of canine ovarian oocytes *in vitro*. *J. Exp. Zool.* 196: 189-196.
- Mazia, D., G. Schatten, and W. Sales. (1975). Adhesion of cells to surfaces coated with polylysine: applications to electron microscopy. *J. Cell. Biol.* 66: 198-200.
- McDougall K., M.A. Hay, K.L. Goodrowe, C.J. Gartley, and W.A. King. (1997). Changes in the number of follicles and of oocytes in ovaries of prepubertal, peripubertal and mature bitches. *J. Reprod. Fertil. Suppl.* 51: 25-31.
- McGee E.A., R. Smith, N. Spears, M.W. Nachtigal, H. Ingraham, and A.J. Hsueh. (2001). Mullerian inhibitory substance induces growth of rat preantral ovarian follicles. *Biol. Reprod.* 64: 293-298.

Michelmann H.W., E. Topfer-Petersen, P. Schwartz, G. Gratz, and C.

Magerkurth. (2001). Use of microbeads for the detection of binding sites on the human zona pellucida: a scanning electron microscopy (SEM) assay. *Andrologia*. 33: 266-271.

Miller, D.J., and B.D. Shur. (1994). Molecular basis of fertilization in the mouse. *Sem. Dev. Biol.* 5: 255-264.

Mizunuma H., X. Liu, K. Andoh, Y. Abe, J. Kobayashi, K. Yamada, H. Yokota, Y. Ibuki, and Y. Hasegawa. (1999). Activin from secondary follicles causes small preantral follicles to remain dormant at the resting stage. *Endocrinology*. 140: 37-42.

Moller, C.C., J.D. Bleil, R.A. Kinloch, and P.M. Wassarman. (1990). Structural and functional relationships between mouse and hamster zona pellucida glycoproteins. *Dev. Biol.* 137: 276-286.

Motro, B., and A. Bernstein. (1993). Dynamic changes in ovarian *c-kit* and *Steel* expression during the estrous reproductive cycle. *Dev Dyn.* 197: 69-79.

Nikas, G., T. Paraschos, A. Psychoyos, and A.H. Handyside. (1994). The zona reaction in human oocytes as seen with scanning electron microscopy. *Hum. Reprod.* 9: 2135-2138.

Otoi, T., M. Fujii, M. Tanaka, A. Ooka, and T. Suzuki. (2000). Oocyte diameter in relation to meiotic competence and sperm penetration. *Theriogenology*. 54: 535-542.

- Otoi T., T. Shin, D.C. Kraemer, and M.E. Westhusin. (2004). Influence of maturation culture period on the development of canine oocytes after *in vitro* maturation and fertilization. *Reprod. Nutr. Dev.* 44: 631-637.
- Ostrander, E.A., F. Galibert, and D.F. Patterson. (2000). Canine genetics comes of age. *Trends Genet.* 16: 117-124.
- Parillo F., R. Zelli, A. Verini Supplizi, O. Fagioli, and A.M. Gargiulo. (2005). Topographical localisation of glucidic residues and their variations in the canine zona pellucida during folliculogenesis. *J. Mol. Histol.* 36: 131-137.
- Parker H.G., L.V. Kim, N.B. Sutter, S. Carlson, T.D. Lorentzen, T.B. Malek, G.S. Johnson, H.B. DeFrance, E.A. Ostrander, and L. Kruglyak. (2004). Genetic structure of the purebred domestic dog. *Science.* 304: 1160-1164.
- Patterson, D.F. (2000). Companion animal medicine in the age of medical genetics. *J. Vet. Intern. Med.* 14: 1-9.
- Phillips, D.M. and R.M. Shalgi. (1980). Surface properties of the zona pellucida. *J. Exp. Zool.* 213: 1-8.
- Prasad, S.V., and B.S. Dunbar. (2000). Human sperm-oocyte recognition and infertility. *Semin. Reprod. Med.* 18: 141-149.
- Prasad, S.V., B. Wilkins, S.M. Skinner, B.S. and Dunbar. (1996). Evaluating zona pellucida structure and function using antibodies to rabbit 55 kDa ZP protein expressed in baculovirus expression system. *Mol. Reprod. Dev.* 43: 519-529.

Prasad S.V., S.M. Skinner, C. Carino, N. Wang, J. Cartwright, and B.S. Dunbar.

(2000). Structure and function of the proteins of the mammalian Zona pellucida. *Cells Tissues Organs*. 166: 148-164.

Rankin, T., M. Familari, E. Lee, A.M. Ginsberg, N. Dwyer, J. Blanchette-Mackie,

J. Drago, H. Westphal, and J. Dean. (1996). Mice homozygous for an insertional mutation on the *Zp3* gene lack a zona pellucida and are infertile. *Development*. 122: 2903-2910.

Rankin, T., S. Soyal, and J. Dean. (2000). The mouse zona pellucida:

folliculogenesis, fertility and pre-implantation development. *Mol Cell Endocrinol*. 163: 21-25.

Rankin T.L., M. O'Brien, E. Lee, K. Wigglesworth, J. Eppig, and J. Dean. (2001).

Defective zonae pellucidae in *Zp2*-null mice disrupt folliculogenesis, fertility and development. *Development*. 128: 1119-1126.

Rutberg, A.T., R.E. Naugle, L.A. Thiele, and I.K.M. Liu. (2004). Effects of

immunocontraception on a suburban population of white-tailed deer *Odocoileus virginianus*. *Bio. Con*. 116: 243-250.

Saetre P., J. Lindberg, J.A. Leonard, K. Olsson, U. Pettersson, H. Ellegren, T.F.

Bergstrom, C. Vila, and E. Jazin. (2004). From wild wolf to domestic dog: gene expression changes in the brain. *Brain Res Mol Brain Res*. 126: 198-206.

Schwartz, P., C. Magerkurth, and H.W. Michelmann. (1996). Scanning electron

microscopy of the zona pellucida of human oocytes during intracytoplasmic sperm injection (ICSI). *Hum. Reprod*. 11: 2693-2696.

- Shivers C.A. and B.S Dunbar. (1977). Autoantibodies to zona pellucida: a possible cause for infertility in women. *Science*. 197: 1082-1084.
- Silva C.P., V. Silva, K. Kommineni, and D. Keefe. (1997). Effect of *in vitro* culture of mammalian embryos on the architecture of the zona pellucida. *Biol. Bull.* 193: 235-236.
- Silverthorn D.U., W.C. Ober, C.W. Garrison, A.C., Silverthorn, and B.R. Johnson. (2004). *Human Physiology: An Integrated Approach with Interactive Physiology*. Benjamin-Cummings Publishing Company. San Francisco City, CA
- Sinowatz, F., W. Amselgruber, E. Topfer-Petersen, I. Totzauer, J. Calvete, and J. Plendl. (1995). Immunocytochemical characterization of porcine zona pellucida during follicular development. *Anat. Embryol. (Berl)*. 191: 41-46.
- Sinowatz, F., E. Topfer-Petersen, S. Kolle, and G. Palma. (2001). Functional morphology of the zona pellucida. *Anat. Histol. Embryol.* 30: 257-263.
- Snustad, D.P., and M.J. Simmons. (2000). *Principles of Genetics*. 4th ed., John Wiley & Sons, Hoboken, NJ.
- Spears N., S. Baker, V. Srsen, R. Lapping, J. Mullan, R. Nelson, and V. Allison. (2002). Mouse ovarian follicles secrete factors affecting the growth and development of like-sized ovarian follicles *in vitro*. *Biol. Reprod.* 67: 1726-1733.
- Stokes, D.J. (2003). Recent advances in electron imaging, image interpretation and applications: environmental scanning electron microscopy. *Philos. Transact. A Math Phys. Eng. Sci.* 361: 2771-2787.

- Ström Holst, B., B. Larsson, C. Linde-Forsberg, and H. Rodriguez-Martinez. (2000). Sperm binding capacity and ultrastructure of the zona pellucida of stored canine oocytes. *J. Reprod. Fertil.* 119: 77-83.
- Ström Holst, B., B. Larsson, H. Rodriguez-Martinez, A.S. Lagerstedt, and C. Linde-Forsberg. (2001). Prediction of the oocyte recovery rate in the bitch. *J. Vet. Med. A Physiol. Pathol. Clin. Med.* 48: 587-592.
- Suzuki, H., X. Yang, and R.H. Foote. (1994). Surface alterations of the bovine oocyte and its investments during and after maturation and fertilization *in vitro*. *Mol. Reprod. Dev.* 38: 421-430.
- Suzuki, H., B.S. Jeong, and X. Yang. (2000). Dynamic changes of cumulus-oocyte cell communication during *in vitro* maturation of porcine oocytes. *Biol. Reprod.* 63: 723-729.
- Telfer E.E., J.P. Binnie, F.H. McCaffery, and B.K. Campbell. (2000). *In vitro* development of oocytes from porcine and bovine primary follicles. *Mol. Cell Endocrinology.* 163: 117-123.
- Telfer E.E., R.G. Gosden, A.G. Byskov, N. Spears, D. Albertini, C.Y. Andersen, R. Anderson, R. Braw-Tal, H. Clarke, A. Gougeon, E. McLaughlin, A. McLaren, K. McNatty, G. Schatten, S. Silber, and A. Tsafiriri. (2005). On regenerating the ovary and generating controversy. *Cell.* 122: 821-822.
- Tengowski, M.W., and G. Schatten. (1997). Low-voltage scanning electron microscopy of mammalian fertilization *in vitro*: preparation of oocytes. *Microsc. Microanal.* 3: 193-202.

- Tengowski, M.W., M.J. Wassler, B.D. Shur, and G. Schatten. (2001). Subcellular localization of beta1,4-galactosyltransferase on bull sperm and its function during sperm-egg interactions. *Mol. Reprod. Dev.* 58: 236-244.
- Tesoriero J.V. (1981). Early ultrastructural changes of developing oocytes in the dog. *J. Morphol.* 168: 171-179.
- Thomas F.H., K.A. Walters, and E.E. Telfer. (2003). How to make a good oocyte: an update on *in vitro* models to study follicle regulation. *Hum. Reprod. Update.* 9: 541-555.
- Tulsiani, D. (2003). *Introduction to Mammalian Reproduction*. Kluwer Academic Publishers, Boston, MA.
- Vanroose, G., H. Nauwynck, A.V. Soom, M.T. Ysebaert, G. Charlier, P.V. Oostveldt, and A. de Kruif. (2000). Structural aspects of the zona pellucida of *in vitro*-produced bovine embryos: a scanning electron and confocal laser scanning microscopic study. *Biol. Reprod.* 62: 463-469.
- Verginelli F., C. Capelli, V. Coia, M. Musiani, M. Falchetti, L. Ottini, R. Palmirotta, A. Tagliacozzo, I. De Grossi Mazzorin, and R. Mariani-Costantini. (2005). Mitochondrial DNA from prehistoric canids highlights relationships between dogs and South-East European wolves. *Mol. Biol. Evol.* 22: 2541-2551.
- Vila C., C. Walker, A.K. Sundqvist, O. Flagstad, Z. Andersone, A. Casulli, I. Kojola, H. Valdmann, J. Halverson, and H. Ellegren. (2003). Combined use of maternal, paternal and bi-parental genetic markers for the identification of wolf-dog hybrids. *Heredity.* 90: 17-24.

- Wassarman, P.M. (1990). Regulation of mammalian fertilization by zona pellucida glycoproteins. *J. Reprod. Fertil. Suppl.* 42: 79-87.
- Wassarman P.M. and R.A. Kinloch. (1992). Gene expression during oogenesis in mice. *Mutat. Res.* 296: 3-15.
- Wayne R.K. (1993). Molecular evolution of the dog family. *Trends Genet.* 9: 218-224.
- Wayne, R.K., and E.A. Ostrander. (1999). Origin, genetic diversity, and genome structure of the domestic dog. *Bioessays.* 21: 247-257.
- Wright, S.J. (2005). *A Photographic Atlas of Developmental Biology*. Morton Publishing Company.
- Xia P., Z. Wang, Z. Yang, J. Tan, and P. Qin. (2001). Ultrastructural study of polyspermy during early embryo development in pigs, observed by scanning electron microscope and transmission electron microscope. *Cell Tissue Res.* 303: 271-275.
- Zuckerman, Sir. S., A.M. Mandl, and P. Eckstein. (1962). *The Ovary*. Academic Press, New York, NY.

R00 2522057

The HF Group

Indiana Plant

T 047082 M 37 00



5/11/2006